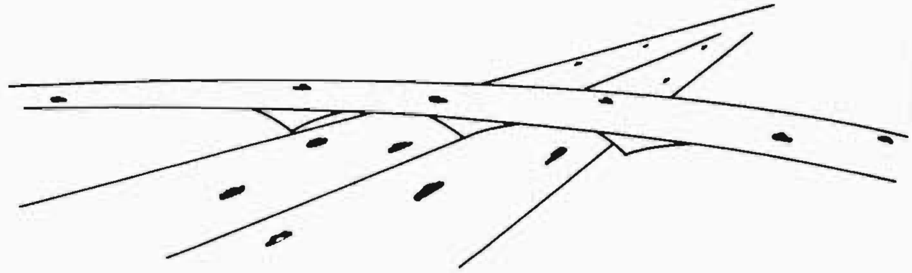

DEPARTMENTAL RESEARCH

Report Number SS 1.2

SENSITIVITY STUDY OF A DESIGN SYSTEM FOR DETERMINING THICKNESS OF ASPHALTIC CONCRETE OVERLAY ON RIGID HIGHWAY PAVEMENT

TEXAS HIGHWAY DEPARTMENT

SENSITIVITY STUDY OF A DESIGN SYSTEM FOR DETERMINING THICKNESS OF ASPHALTIC CONCRETE OVERLAY ON RIGID HIGHWAY PAVEMENT

by

Larry Jack Buttler
Senior Designing Research Engineer

Special Study 1.2

Research Section-Highway Design Division

TEXAS HIGHWAY DEPARTMENT

January 1971

ACKNOWLEDGEMENTS

The author wished to acknowledge the many hours of counsel given by Dr. B. F. McCullough during the development of this study and in the writing of this report. Acknowledgement is also given to Dr. W. R. Hudson for reading the manuscript and for the encouragement and help which he extended.

Acknowledgement is given to Mr. R. L. Lewis, Mr. J. F. Nixon, and other members of the Texas Highway Department for their help and interest. Thanks are due to Mr. J. L. Brown for the formulation of ideas during the initial stages of the study. A special thanks is given to Mr. P. S. Fisher for work on computer programming and suggestions made during the writing of this report.

ABSTRACT

This report analyzes the sensitivity of variables input into "A Pavement Overlay Design System Considering Wheel Loads, Temperature Changes, and Performance", developed by Dr. B. F. McCullough, in 1969, and reported in his Dissertation at the University of California, Berkeley. This sensitivity study pertains to asphaltic concrete overlays of rigid highway pavements. Included is an analysis of only those variables that affect the wheel load stress and fatigue life of the concrete pavement. Volume change stresses caused by variations in temperature are not analyzed in this study.

The report first introduces and describes the design system and the procedure for studying the input variables is explained. The results of the study are then presented and an analysis is made. From this analysis, revisions to the system are recommended. In the last chapter, recommendations are given as to which variables are more important and where more time should be spent to effectively develop inputs to the design system.

TABLE OF CONTENTS

	Page
ACKNOWLEDGMENTS	iv
ABSTRACT	v
LIST OF FIGURES	viii
LIST OF TABLES	xii
CHAPTER	
1. INTRODUCTION	1
Background	1
Objectives	2
Scope	2
2. DESIGN SYSTEM	3
Field Work and Analysis	3
Computations on Existing Pavement	8
Computations on Overlaid Pavement	11
LAYER Program	12
POTS Program	12
PROFILE ANALYSIS Program	15
3. GENERAL APPROACH AND SELECTION OF DESIGN VARIABLE VARIATIONS	20
Introduction	20
General Approach to Analysis	20
Selection of Design Variables	21
Specific Approach to Analysis	28
4. PRESENTATION OF RESULTS	30
Subsystems for Existing Pavement	30
Subsystems for Overlaid Pavement	60
Summary	73
5. ANALYSIS OF RESULTS	74
Subsystems for Existing Pavement	74
Subsystems for Overlaid Pavement	79
Summary	81

6. REVISED SYSTEM 85

Use of Dynaflect 85
Revised Computer Programs. 86
Desired Revisions to System. 87
Summary. 90

7. CONCLUSIONS AND RECOMMENDATIONS. 92

Conclusions. 92
Recommendations. 93
Weak versus Strong Points of the Overlay Design System 94

APPENDIX A. Using a Curve to Approximate Tangential Stress Leading to the Calculation of Cumulative Damage. . . 96

APPENDIX B. Dynaflect Deflection Basins. 115

APPENDIX C. Computer Program to Determine the Significant Difference Between Design Sections and a Sample Output of Program-Profile Analysis 129

APPENDIX D. Computer Program to Approximate Tangential Stress and Determine the Cumulative Damage of an In-Service Pavement and a Sample Output of the Program. 138

REFERENCES. 147

LIST OF FIGURES

Figure No.		Page
2.1	General Work Flow Diagram.	4
2.2	Detailed Work Flow Diagram for Each Subsystem.	5
2.3	Dynaflect Load Wheels.	9
2.4	Location of Wheel Loads.	10
2.5	Pavement Structure for LAYER Program	13
2.6	Profile of Deflections	16
2.7	Breakpoints Chosen for Design Sections in Profile of Deflections.	17
2.8	Statistically Different Design Sections in Profile of Deflections	19
3.1	Typical Pavement Structure	22
3.2	Sequence of Sensitivity Calculations	29
4.1	Tangential Stress versus Wheel Loads for Single Axle .	32
4.2	Tangential Stress versus Wheel Loads for Tandem Axle .	33
4.3	Percent change in Tangential Stress versus Wheel Load for Unit Variable Changes	38
4.4	Percent Change in Tangential Stress versus Wheel Load for Unit Variable Changes	39
4.5	Summary of Percent Change in Tangential Stress for the Normal Stiffness Pavement (Single Axle). . . .	41
4.6	Summary of Percent Change in Tangential Stress for the Normal Stiffness Pavement (Tandem Axle). . . .	42
4.7	Summary of Percent Change in Tangential Stress for the Walker County Pavement (Single Axle)	43
4.8	Summary of Percent Change in Tangential Stress for the Walker County Pavement (Tandem Axle)	44

Figure No. Page

4.9 Summary of Percent Change in Tangential Stress for the Low Stiffness Pavement 46
(Both Single and Tandem Axle)

4.10 Summary of Percent Change in Tangential Stress for the High Stiffness Pavement. 47
(Both Single and Tandem Axle)

4.11 Deflection versus Subgrade Modulus (E_4). 48

4.12 Concrete Fatigue Equation for Cumulative Damage Equal to 1.0 50

4.13 Conceptual Diagram Illustrating the Log-normal Distributions of Axle Applications for a given Flexural Strength. 52

4.14 Standard Error in Flexural Strength versus Pavement Failures 53

4.15 Cumulative Damage versus Tangential Stress 55

4.16 Cumulative Damage versus Tangential Stress 55

4.17 Percent Change in Cumulative Damage for the Four Estimates of Traffic Distributions given in Table 4.3. 58

4.18 Flexural Strength versus Cumulative Damage 59

4.19 Cumulative Damage versus Wheel Load for Various Values of Slope in the Fatigue Equation. . . . 61

4.20 Tangential Stress versus Overlay Thickness for Single Axle 62

4.21 Tangential Stress versus Overlay Thickness for Tandem Axle 63

4.22 Summary of Percent Change in Tangential Stress for Overlaid Pavement (Single Axle) 65

4.23 Summary of Percent Change in Tangential Stress for Overlaid Pavement (Tandem Axle) 66

4.24 Overlay versus Damage for Normal Stiffness Pavement. 68

Figure No.		Page
4.25	Overlay versus Damage for Low Stiffness Pavement	69
4.26	Overlay versus Damage for High Stiffness Pavement	70
4.27	Overlay versus Damage for Walker County Pavement	71
4.28	Overlay versus Damage for Normal Stiffness Pavement	72
6.1	Tangential Stress Before and After Overlay	89
A.1	Tangential Stress versus Wheel Load for Tandem Axle	100
A.2	Coordinates for Circular Curve Approximation of Tangential Stress	101
B.1	Location of Walker County Project	120
B.2	Typical Half Section for Walker County Project	121
B.3	Measured and Calculated Deflection Basins for Section No. 1 (E_1 = 5,000,000 psi)	123
B.4	Measured and Calculated Deflection Basins for Design Section No. 2 (E_1 = 5,000,000 psi)	123
B.5	Calculated Deflection Basins Showing the Effect of Varying Elastic Modulus of Layer 1	124
B.6	Measured and Calculated Deflection Basins for Design Section No. 1 (E_1 = 3,000,000)	125
B.7	Measured and Calculated Deflection Basins for Design Section No. 2 (E_1 = 3,000,000)	125
B.8	Calculated Deflection Basins Showing the Effect of varying the Elastic Modulus of Layer 2 (E_1 = 5,000,000)	126
B.9	Calculated Deflection Basins Showing the Effect of Varying the Elastic Modulus of Layer 2 (E_1 = 3,000,000)	126

Figure No.		Page

B.10 Calculated Deflection Basins Showing the Effect of Varying the Thickness of Layer 1 (E_1 = 5,000,000) . . 127

B.11 Position of Dynaflect Sensors During Testing 128

LIST OF TABLES

Table No.		Page
3.1	Material Properties Used in Computational Experiment. . . .	23
3.2	Traffic Distributions and Volumes Taken from Walker County Design	26
3.3	Factorial for Calculating Tangential Stress	27
4.1	Percent Change in Tangential Stress for Unit Variable Change to Low Values for Normal Stiffness Pavement	36
4.2	Percent Change in Tangential Stress for Unit Variable Change to High Values for Normal Stiffness Pavement	37
4.3	Estimated Traffic Volumes for Walker County Design	57
5.1	Relative Effect of Input Variables on the Tangential Stress in Concrete	82
A.1	Comparison of Tangential Stress	107
A.2	Comparison of Cumulative Damage	108
A.3	Comparison of Tangential Stress	109
A.4	Comparison of Cumulative Damage	110
A.5	Comparison of Tangential Stress	111
A.6	Comparison of Cumulative Damage	112
A.7	Comparison of Tangential Stress	113
A.8	Comparison of Cumulative Stress	114
B.1	Layer Depth and Elastic Properties.	122

CHAPTER 1. INTRODUCTION

Background.

In the past, asphaltic concrete overlays of rigid highway pavements, for the most part, have been designed by empirical equations or by engineering judgment based on experience. Few pavement overlays have been designed using a sound rational approach. A comprehensive study of existing design procedures was made by Dr. B. F. McCullough in 1969. As a result of the study, a new design procedure was developed and reported by Dr. McCullough in Reference 15.

This new design system consists of two parts. One part is the design for wheel load stresses, and the second part is the design for temperature volume stresses. The first part consists of three phases of operations, namely: (1) Collation of material properties using field deflection and laboratory measurements; (2) Estimation of remaining life of the pavement considering the past history of wheel loads during the life of the pavement; and (3) Estimation of the cumulative stress damage from future wheel loads on the overlaid pavement. In the third phase, a thickness of overlay is selected to make the pavement last the length of the design period.

The second part of the design system, establishes the minumum thickness of overlay required to reduce the computed volume change stresses in the overlay to an acceptable level. The volume change stresses are induced by both the changes in volumes within the overlay and the volume changes of the existing pavement.

One application of this design system is to choose the thicknesses for an asphaltic concrete overlay of a rigid highway pavement. In this capacity, the design system was first used by the Texas Highway Department in the design of the thickness of an asphaltic concrete overlay of a continuously reinforced concrete pavement for Project I45-2(33)102, of Interstate Highway 45, in Walker County (Ref 15). During the design analysis, it became apparent that the design engineer needs a working knowledge of how each input affects the design system before the designer will have adequate confidence in the system's answers.

Objectives.

The objectives of this study are to determine the sensitivity of the design system with respect to its input variables, to give information to the designer as to which variables are most important, and where more time should be spent to effectively develop inputs for the system. An additional objective is to recommend revisions to the system, where desirable, and to enumerate the advantages and disadvantages of using the system.

Scope.

This study will include an analysis of only those variables that affect the wheel load stresses and fatigue life of the concrete pavement and will not cover the volume change stresses caused by variations in temperature. The volume change calculations are straightforward and should be analyzed in detail for each pavement section by the desgin engineer.

CHAPTER 2. DESIGN SYSTEM

This chapter describes the order in which work occurs on the typical problem of designing the thickness of an asphaltic concrete overlay on a rigid highway pavement. Three computer programs, PROFILE ANALYSIS, LAYER, AND POTS, were used in this design strategy. These will be introduced here and discussed in more detail in the latter part of the chapter.

The program PROFILE ANALYSIS (Ref 3) is a tool used to check statistically the designer's choice of a design section. In this design system the sections chosen are based on deflections or pavement failure measurements. Program LAYER (Ref 25) uses the linear elastic layer theory to compute the state-of-stress and strain in a pavement structure: The program POTS (Ref 15) calculates fatigue damage to the pavement structure by utilizing inputs of past or predicted traffic and stress or strain.

This system works in three major sections as illustrated in Figure 2.1. These three sections, "Field Work and Analysis", "Computations for Existing Pavements", and "Computations for Overlaid Pavements", have the working part of each section shown in more detail in Figure 2.2. The work outlined in these two figures will be discussed in the following paragraphs.

Field Work and Analysis

The field work and analysis are done in three steps as shown in Figure 2.1. Each step is discussed in detail as follows:

Determine Design Deflection. Deflections are taken along the

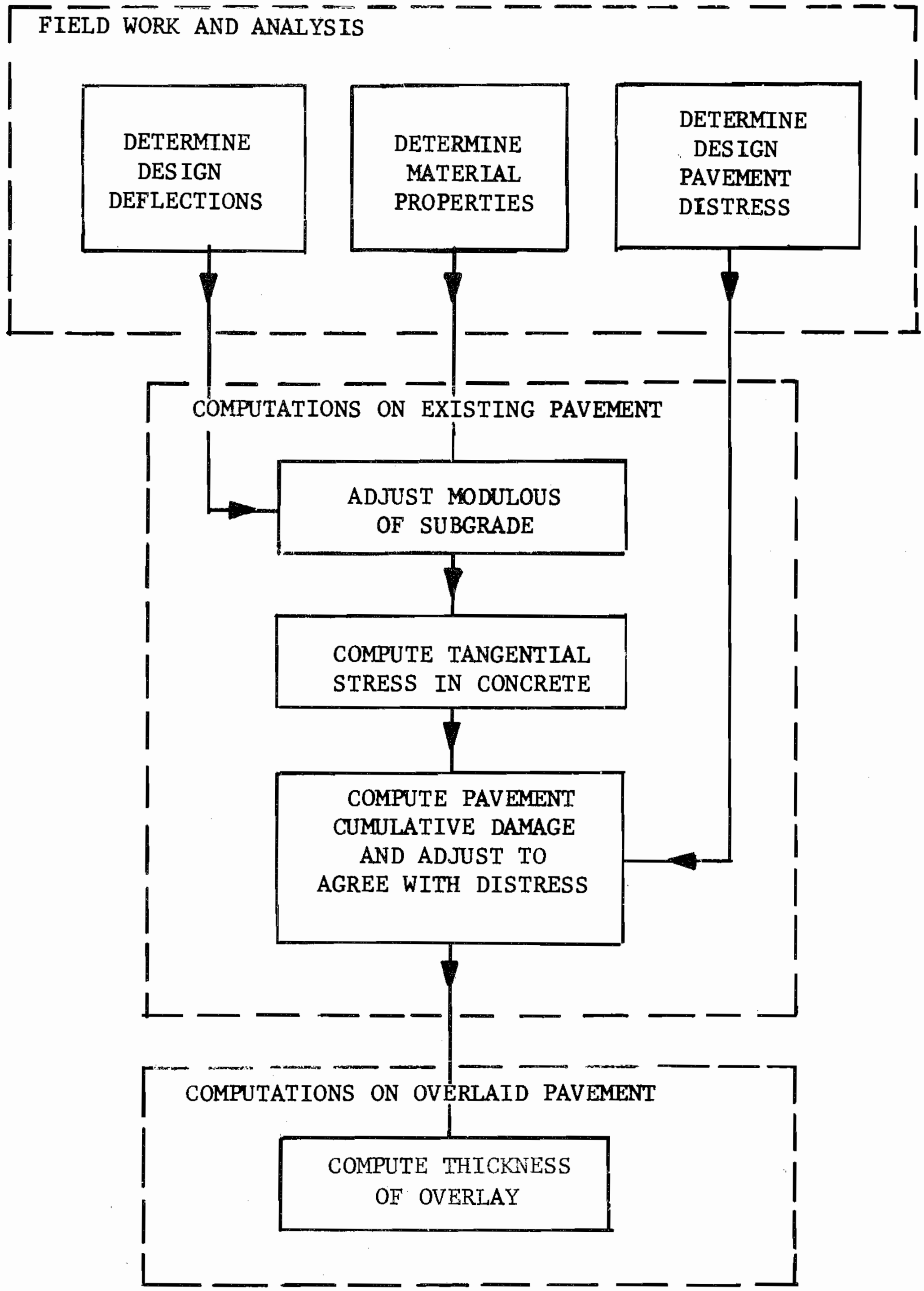

Figure 2.1. General Work Flow Diagram

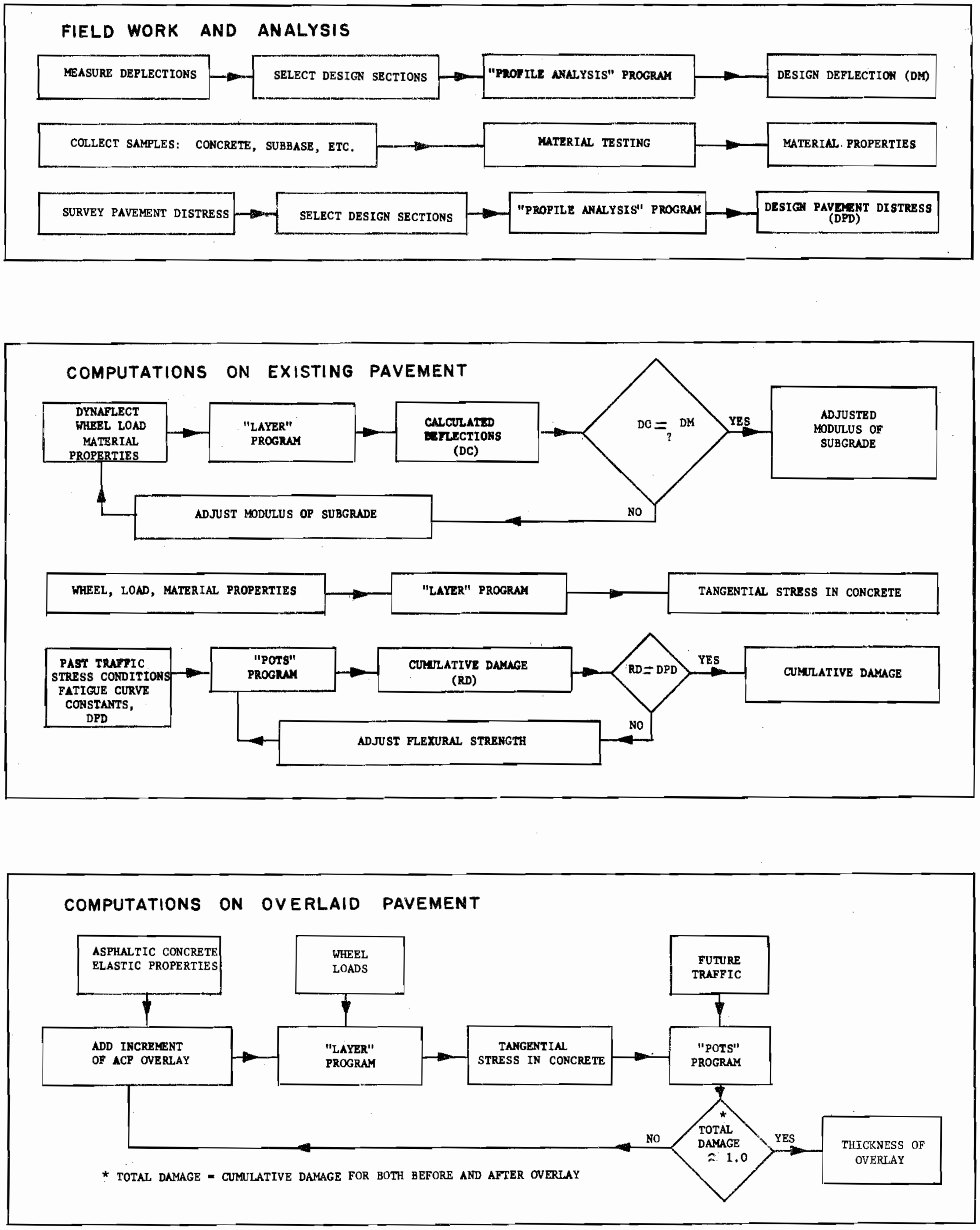

Fig 2.2. Detailed Work Flow Diagram For Each Subsystem

roadway at uniform intervals. The designer, usually with the aid of a profile plot of these deflections, chooses design sections based on apparent changes in the deflection pattern. The program PROFILE ANALYSIS is used to check the choice of sections statistically. The statistical test now incoporated in the program is analysis of variance (Ref 2). This statistical test determines whether or not the means of the measurements in adjacent design sections differ significantly. The output of the program gives the average and standard deviation for the deflection sections of significant difference. The designer then chooses design deflection values for each section based on the desired confidence level.

Determine Material Properties. Method for determining material properties falls into two general categories of nondestructive and destructive testing. The most desirable of the two is, obviously, nondestructive testing. Unfortunately, the state-of-the-art, has not developed to where a complete evaluation of a pavement is feasible at this time. This section will relate the destructive type sampling use to obtain samples and lab testing. In later sub-headings, Adjust Modulus of Subgrade" and "Compute Tangential Stress in Concrete", the adjustment of material properties determined in the lab using non-destructive testing and observations will be discussed.

The measurement of material properties is an expensive process relative to the cost of obtaining deflection measurements. Therefore, it is more economical to first establish design sections as described under the previous subheading "Determine Design Deflection"; then, a sampling plan can be programmed to utilize the more expensive material tests to the best advantage.

The basic information required are elastic modulus, Poisson's ratio, and the thickness of each layer. The strength of each material is also necessary. To establish these material properties, it first is necessary to core the existing pavement for sample of the subbases and subgrade. If beams cannot be cut from the existing concrete pavement slab, then pavement cores can be used in an indirect tensile test (ref 6) to approximate flexural strength and the elastic properties of the concrete. The beam test for determining the properties of concrete is discribed in reference 15.

For granular base, fine grained materials, and stabilized materials, a dynamic modulus can be determined by the Resilient Modulus Test (Ref 19). Since undistributed samples cannot be obtained in coring, these tests may be performed on the remolded specimens. This test is also described in McCullough's dissertation (Ref 15).

For asphalt concrete, the quasi-elastic modulus, termed stiffness, may be obtained using the procedure developed by Heukelom and Klomp (Ref 21). This procedure basically used the penetration test for asphalt at 77^{o}F, the Ring and Ball softening point of asphalt, the volume concentration of the aggregate, and the air voids in the compacted mix. Again, details of the procedures are also described in McCullough's dissertation.

Determine Pavement Distress. The length of the area of pavement distresses or failures in each wheel path of the pavement is measured and referenced to the deflections by stations (Ref 4). For this system, distress is defined as the length of structural failures visible in the concrete pavement surface. The percent failures are the longitudinal length of failures per length of the design section studied. The percent failures are calculated for the design wheel path, and design sections are chosen in a way similar to the method used for design deflection.

Computation for Existing Pavement.

Computations are made in three steps, as shown in Figures 2.1 and 2.2. Each step is discussed in detail as follows:

Adjust Modulous of Subgrade. Elastic properties as determined in the lab analysis are used as inputs for the program LAYER. In the program, the Dynaflect (Ref 18) loads are simulated by two static 500 pound wheel loads placed 20 inches apart as shown in Figure 2.3. A deflection is computed in the LAYER Program at a radius of 10 inches (Point D_p) for one wheel load. This deflection is doubled to account for the effect of both wheel loads using the prin- of superposition. While holding all other variable constant, the modulus of elasticity of the subgrade (E_4) is varied until the computed deflections at Point "D_p" are equivalent to the measured values. Adjusted E_4 values are thus established for the design. The measured E_4 values as determined in the lab from field samples are used as checks of reasonableness for values for computations. If adjusted E_4 values are determined not reasonable, then a re-evaluation of all input values will be necessary to determine what error is occurring.

Compute Tangential Stress of Concrete. The LAYER program was used to compute tangential stress in the bottom of the concrete. This stress was computed for both single and tandem axles for a range of desired wheel loads. Considering single axle loads, the tangential stress caused by load wheel was computed at Point "P" in Figure 2.4. For the tandem axle loads, tangential stress caused by both load wheels

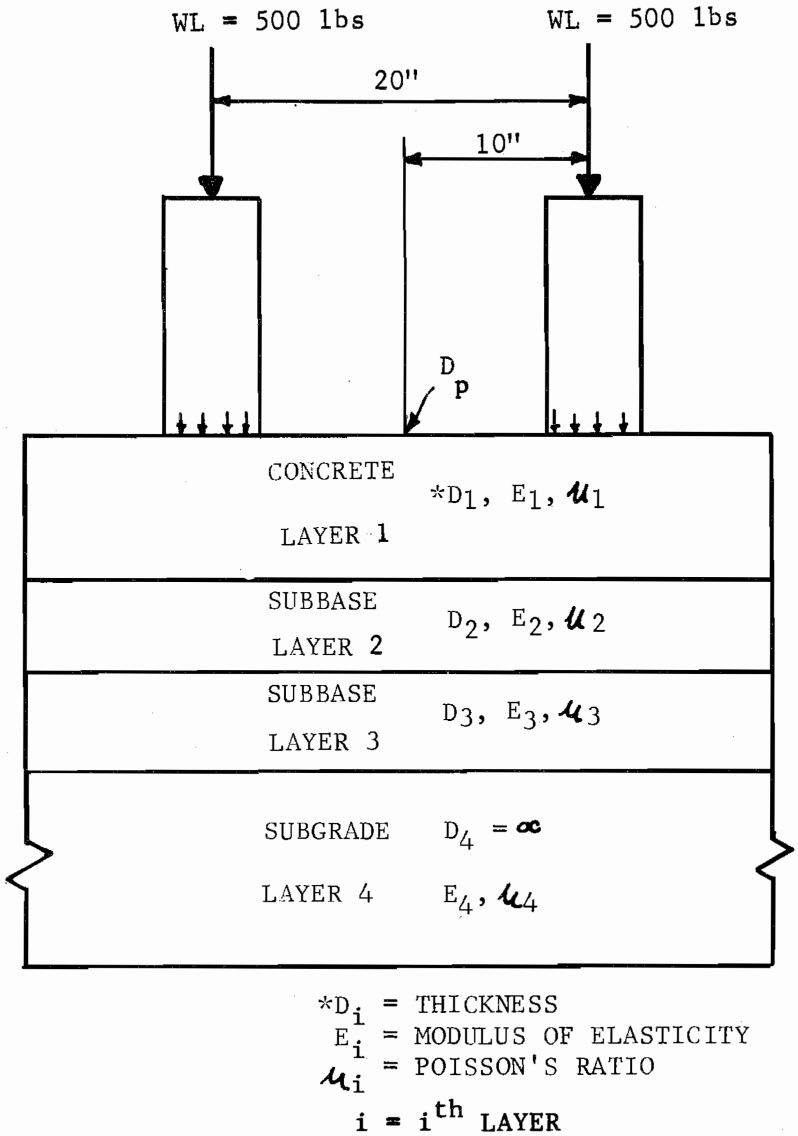

Fig 2.3. Dynaflect Load Wheels

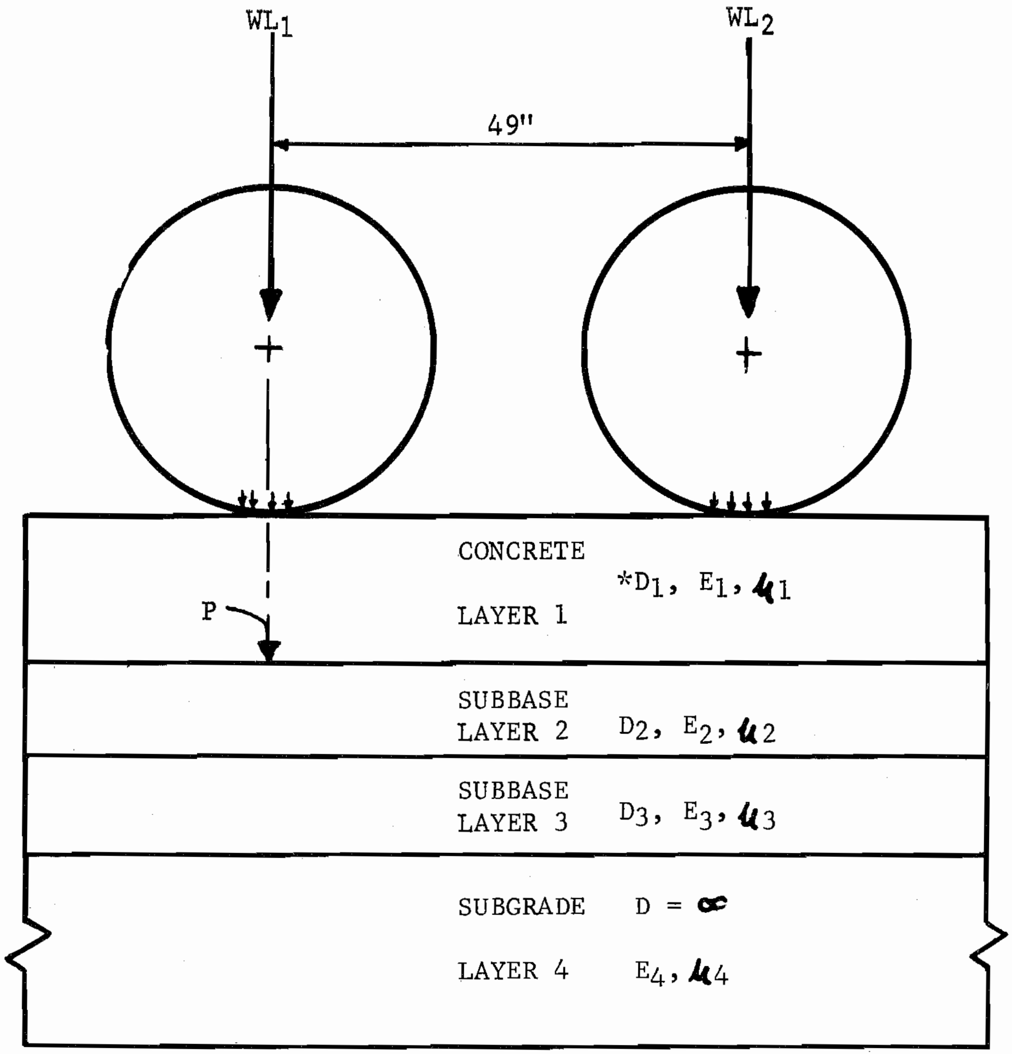

$^*D_i$ = THICKNESS
E_i = MODULUS OF ELASTICITY
μ_i = POISSON'S RATIO
$i = i^{th}$ LAYER

Fig 2.4. Location of Load Wheels

was computed at point "P". The stresses caused by each wheel load were added according to the principle of superposition.

For the four different types of pavements investigated in this study, tangential stress of the concrete was found to be the critial stress. The compressive stress in all cases did not approach the strength of any layer. It must be recognized that cases could exist where other stresses or strains could be critical in the design. One example might be a very soft and weak layer placed between the concrete pavement and another relatively stiff layer.

Compute Pavement Cumulative Damage. The stresses calculated and past traffic distributions and volumes are input in the program "POTS" to compute cumulative damage ($\overline{RD}$) of the concrete pavement. The calculated $\overline{RD}$ is checked against the distress measured in the field (Ref. 4). If these values are not in agreement, the flexural strength of the concrete pavement is adjusted to make the calculated damage agree with the measured damage. Design values for cumulative damage and flexural strength are thus determined.

Computations for Overlaid Pavement.

This sections output is the design depth of asphaltic concrete overlay. The tangential stress in the concrete for a one inch depth of overlay is calculated with the program LAYER. Future cumulative damage ($\overline{RD}_o$) for the overlaid pavement is computed in the POTS program using the stresses mentioned above and the future traffic. The above procedure is then repeated adding one inch of overlays if necessary, until total cumulative damage, for both before and after overlaying, is approximately 1.0. Cumulative damage after overlaying can be interpolated if plots are made of damage versus inches of asphalt.

LAYER Program.

The Chevron research Corporation recently developed a multi-layer program which allows the designer to calculate the complete state-of-stress or strain at any point in a pavement structure of up to fifteen layers (Ref 25). This program uses the linear elastic theory with full continuity between layers. To save computer storage and time, a five layer version was used in designing this system. The program allows the modulus of elasticity, Poisson's Ratio, and thickness, for each layer, to be treated as input variables. The wheel load size and tire contact pressure are used to define the type of load. The program assumes a circular load to be placed on the center of circular layers of infinite radii as shown in Figure 2.5.

POTS Program.

This program calculates the cumulative damage of the pavement. To obtain cumulative damage, the number of cycles to failure, N_j, must first be calculated by equation 2.1.

$$N_j = C \left(\frac{f_c}{\overline{TS}_j}\right)^K \quad \text{. . . . . (2.1)}$$

Where:

N_j = number of cycles to failure for the j^{th} wheel load group.

f_c = static flexural strength of concrete; psi.

$\overline{TS}_j$ = stress in the concrete for the j^{th} wheel load group, psi.

C, K = constants derived from laboratory data.

In the design of rigid highway pavements, the analysis

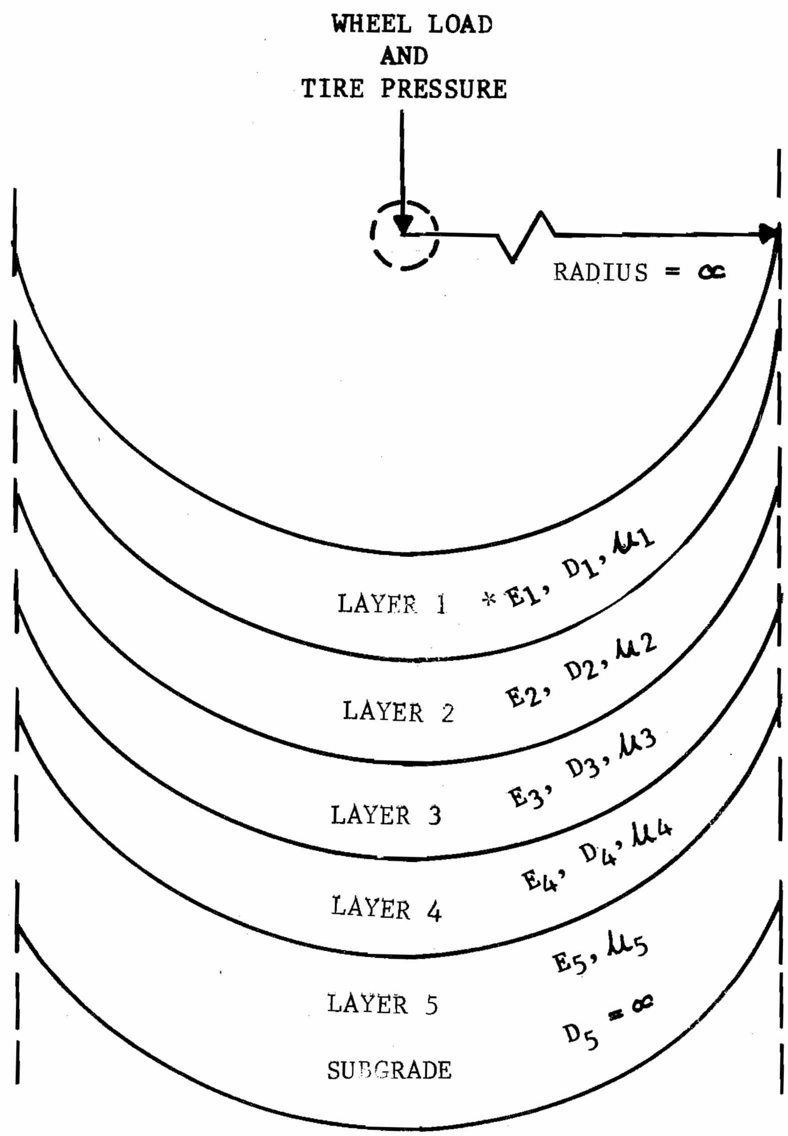

$*E_i$ = ELASTIC MODULUS

D_i = THICKNESS OF LAYER

μ_i = POISSON'S RATIO

i = i^{th} LAYER

Fig 2.5. Pavement Structure for LAYER Program verified that the pavement should be designed to withstand the tangential stress at the bottom of the concrete layer. Using the constants developed for concrete, equation 2.1 takes the following form:

$$N_j = 0.5274 \left(\frac{f_c}{TS_j}\right)^{34.25} \quad \ldots\ldots\ldots\ldots\ldots (2.2)$$

Then, the cumulative damage for the average condition is then determined by Equation 2.3.

$$\overline{RD} = \sum_{j=1}^{j=m} \frac{n_j}{N_j} \quad \ldots\ldots\ldots\ldots\ldots\ldots\ldots (2.3)$$

Where:

$\overline{RD}$ = cumulative damage.

n_j = number of repetitions for the j^{th} wheel load group.

m = number of wheel load groups.

In the program, cumulative damage is computed for any confidence level specified by using the standard error of the number of cycles. In some intances, this value is not available; therefore, it may be computed by using the following transformation which represents the standard error of cycles to failure as a logarithm for input into the program. These are hand calculated as follows:

$$\sigma_N = \text{Log}\ .5274 + 34.25\ \text{Log}\ \left(\frac{f_c}{f_c - \sigma_{f_c}}\right) \quad \ldots\ldots (2.4)$$

Where:

σ_N = log of the standard error of the number of cycles to failure.

σ_{f_c} = standard error in flexural strength; psi.

The cycles to failure for a given confidence level are calculated in the program as follows:

$$N_c = \text{Antilog}\ (\text{Log}\ N_j - t\ (\sigma_N)) \quad \ldots\ldots\ldots\ldots\ldots \quad (2.5)$$

Where:

t = contant from the normal curve tables for desired confidence. level.

N_c = number of cycles to failure at a given level of confidence.

Then, in equation 2.3, N_j is replaced by N_c and the remaining life in the pavement is calculated as follows:

$$\overline{RL} = 1.0 - \overline{RD} \quad \ldots\ldots\ldots\ldots\ldots\ldots\ldots\ldots \quad (2.6)$$

This program was written for the general case, where an asphaltic concrete overlay is placed. The stress conditions may be input for various elastic modulii which change with temperature, and the damage is calculated for each month. The sum of these damages is also obtained as defined in equation 2.3.

PROFILE ANALYSIS Program

This program (Ref 3) was developed to check the Engineer's selection of design sections statistically chosen from a series or profile of measurements. For example, on a design project, a profile of deflection measurements is taken (Figure 2.6), and the deflections are plotted. From this plot, the Engineer visually separates sections that appear to have distinct changes in the deflection pattern. The section divisions are referred to as "break points". Figure 2.7 outlines the manner in

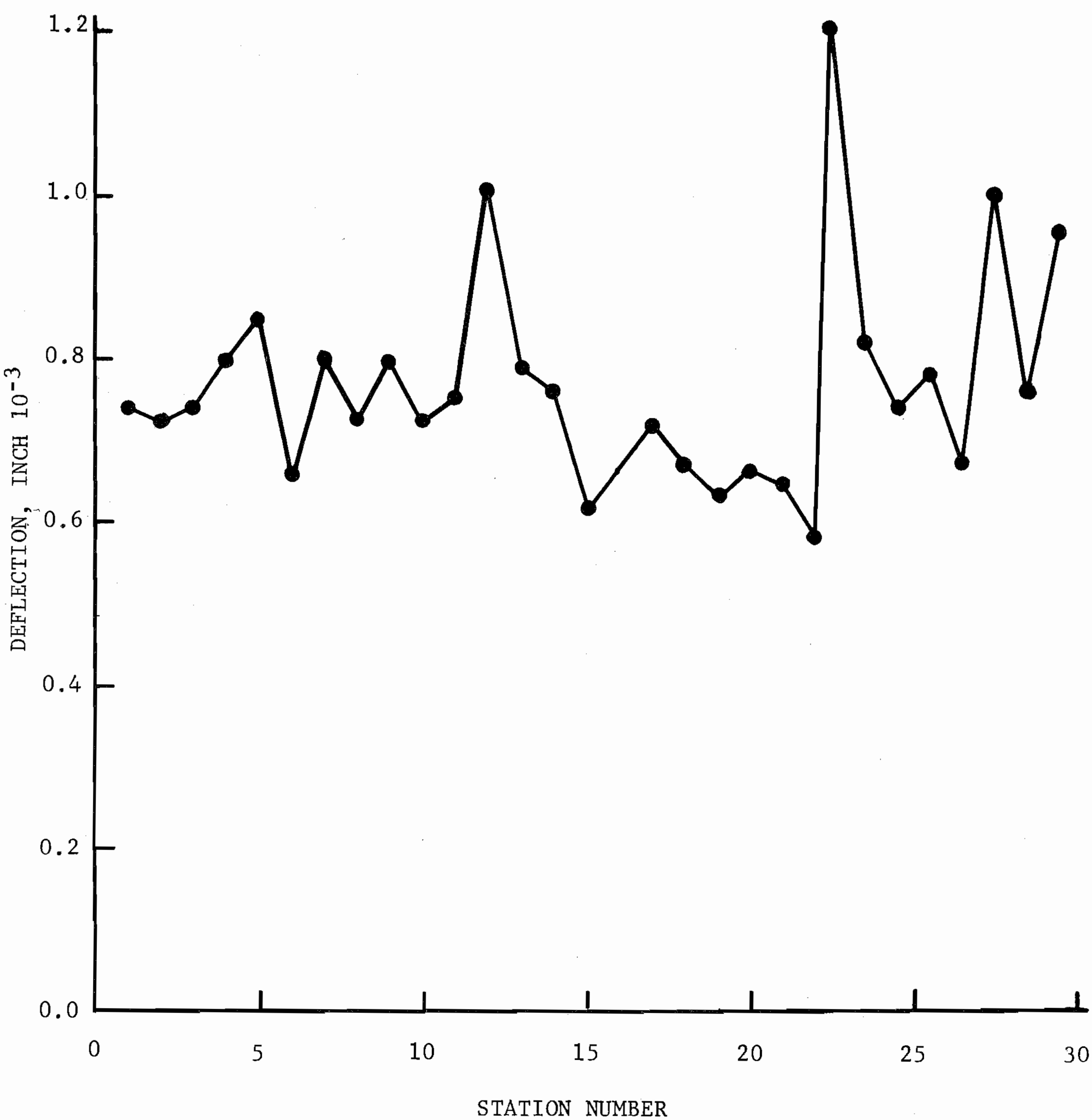

Fig 2.6. Profile of Deflections

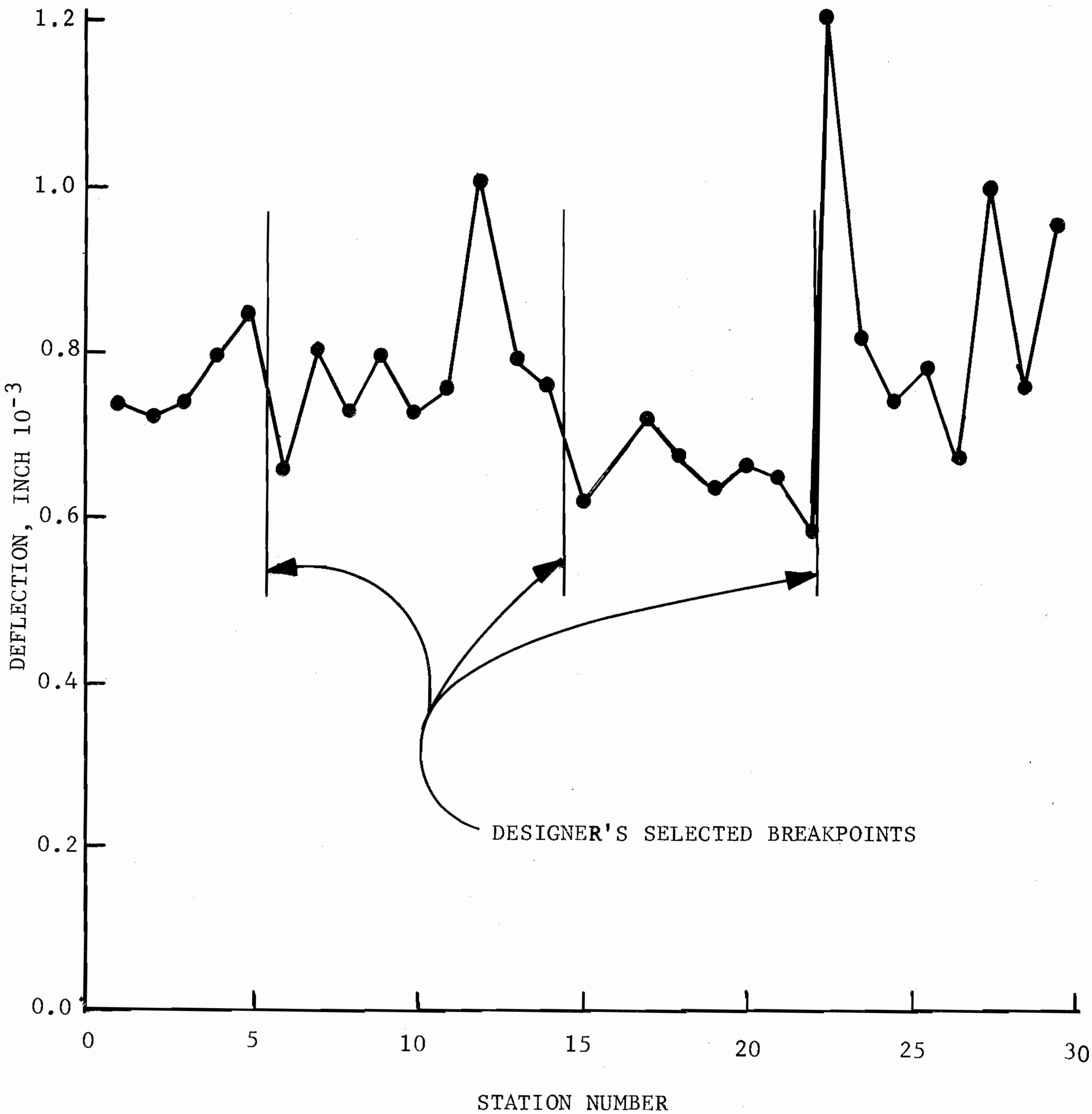

Fig 2.7. Breakpoints Choosen for Design Sections in Profile of Deflections

which the Engineer might choose input breakpoints. These breakpoints are then input into the program PROFILE ANALYSIS. After analyzation within the program, it was found that the two left-most sections do not differ significantly. Figure 2.8 illustrates the four remaining statistically different sections with the average line plus and minus one standard error as calculated by the program PROFILE ANALYSIS. A sample output for the program is shown in Appendix C.

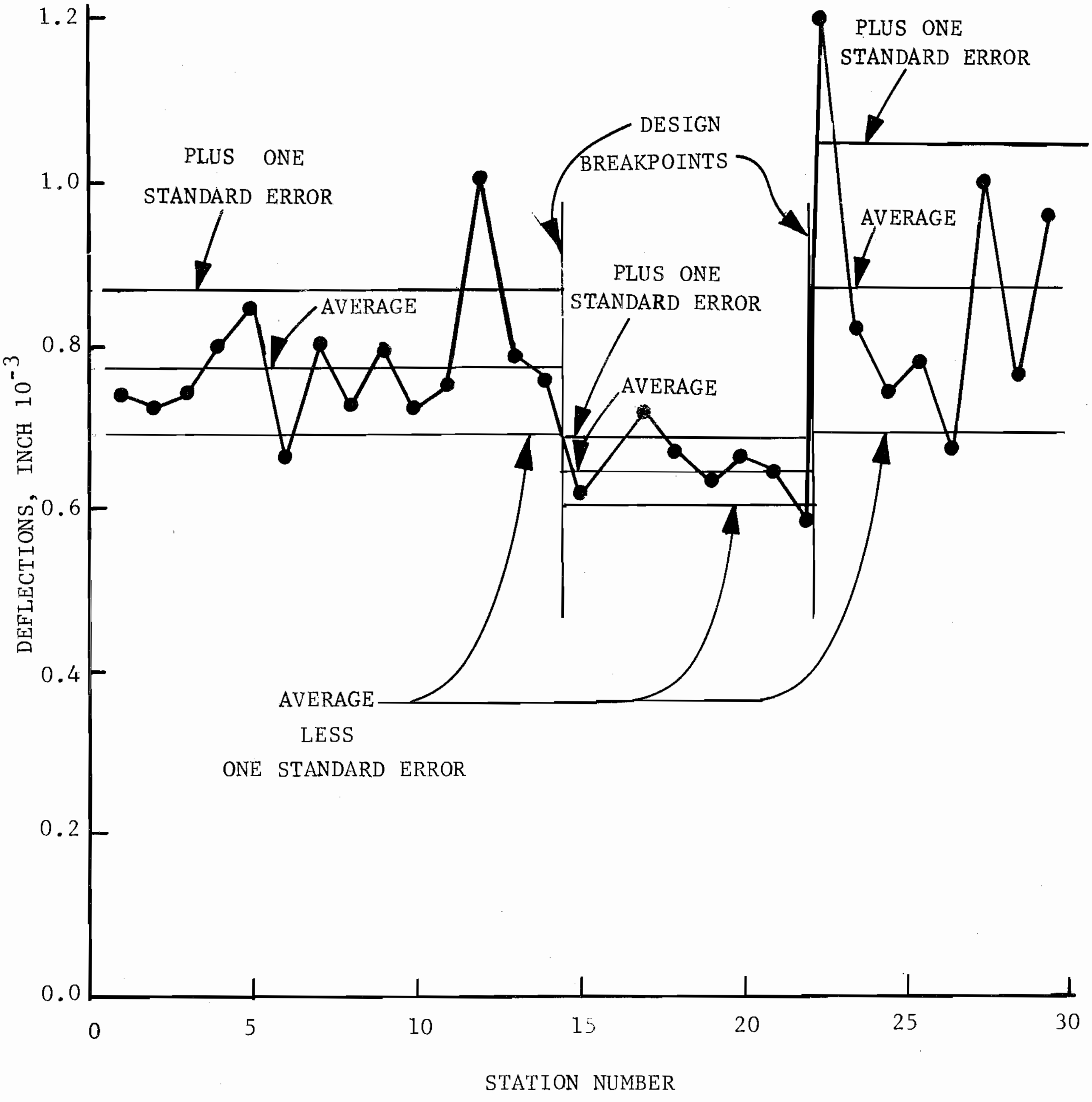

Fig 2.8. Statistically Different Design Sections in Profile of Deflections

CHAPTER 3. GENERAL APPROACH AND SELECTION OF DESIGN VARIABLE VARIATIONS

Introduction.

This chapter first presents the general approach taken to determine the sensitivity of the system with respect to input variables. Second, the selection of design variables is presented and discussed. The last part of this chapter presents the specific breakdown of the subsystems to be studied.

General Approach to Analysis.

A sensitivity analysis of a system is a procedure to determine the change in a dependent variable caused by a unit change in an independent variable. For an analysis, it would be desirable to determine how the variation of each input variable affects the final results. This type investigation of the "Overlay Design System" would necessitate thousands of computer solutions. In order to present these solutions in a complete form, hundreds of charts, graphs, and tables would be needed.

A more practical route for analysis was chosen for this study. The design system was broken into smaller subsystems, each being studied separately. The effect of a single variable on an individual subsystem was first studied; then, the effect of each subsystem on the entire design system was analyzed. As the investigation continued, it became apparent that a unit change in certain variables had no significant effect on the system. When these variables were identified, they were deleted from further study. Therefore, this sensitivity analysis will be a correct and meaningful representation of the design system.

Selection of Design Variables.

The pavement structure may be multiple-layer, which could be best modeled by anything from a two to ten layer design. In this analysis, a four layer pavement was selected to represent a typical rigid highway pavement. Figure 3.1 shows the typical pavement structure that was analyzed. It is realized that numerous two and three layer rigid pavements are now in existence today and will need overlays designed in the forseeable future. Most of the rigid pavements designed after the completion of th AASHO Road Test (Refs 1, 20, and 21) have had a minimum of one stabilized subbase below the concrete. Many rigid pavements have been built with more than one stabilized layer to guard against the pumping action of the concrete slab.

A pavement design of more than four layers was not chosen for analysis in this study. The reason for this is that rigid highway pavement designs of more than four layers are rarely built. The four layer design was chosen over the two and three layer design so that a more complex complex design could be studied. Also, after the completion of the four layer study it is anticipated that a sensitivity study of the two and three layer structure will be relatively easy.

Elastic Properties and Layer Thicknesses of Existing Pavement. Choosing the elastic properties and thicknesses is based on a feasible range of material property values that could occur on an existing rigid pavement built originally to the specifications of an 8-inch concrete slab with five sacks of cement per cubic yard (Ref 13).

The range for each individual variable in Table 3.1 is chosen based on the Engineer's ability to estimate material properties in an existing pavement using the present state-of-the-art. For example, in

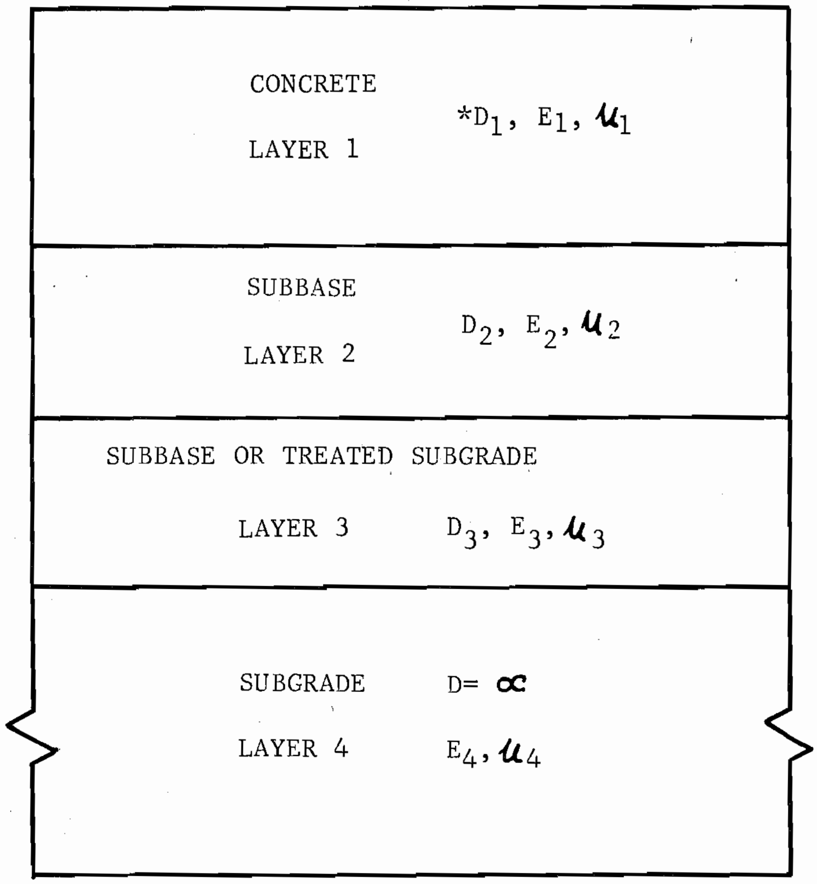

$^*D_i$ = THICKNESS
E_i = MODULUS OF ELASTICITY
μ_i = POISSON'S RATIO
$i = i^{th}$ LAYER

Fig 3.1. Typical Pavement Structure

MATERIAL	INPUT VARIABLE*	PAVEMENT STIFFNESS			
		LOW	NORMAL	HIGH	WALKER COUNTY
CONCRETE	E_1	4,500,000	5,000,000	5,500,000	5,000,000
	μ_1	.20	.15	.12	.20
	D_1	7.0	7.5	8.0	7.5
SUBBASE #1	E_2	10,000	100,000	300,000	10,000,00
	μ_2	.50	.40	.35	.40
	D_2	4.0	6.0	8.0	6.0
SUBBASE #2	E_3	10,000	80,000	100,000	80,000
	μ_3	.50	.40	.35	.35
	D_3	4.0	6.0	8.0	6.0
SUBGRADE	E_4	4,100	13,000	20,000	8,200
	μ_4	.50	.45	.35	.45

* See Figure 3.1 for explanation of symbols.

Table 3.1. Material Properties Used In Computational Experiment

Table 3.1 the range of input variables defging material properties for concrete is relatively small compared to the ranges shown for both subbase materials. The reason for this is two-fold: (1) the specifications for materials and construction of concrete are better controlled, therefore giving the Engineer a better chance of estimating the concrete properties and (2) there has been more experience in testing and building of concrete pavements than any specific subbase material, which again gives the Engineer a better estimate of the material properties. The range of material property values for the subgrade is based on experience obtained from Reference 15 and computations made in Appendix B.

Before final selection of the variables in Table 3.1, the range of material properties were compared with values obtained by Treybig in a "Sensitivity Analysis of the Extended AASHO Rigid Pavement Design Equation" (Ref 23). Additional information concerning elastic properties of subbase materials was obtained from Research Project 3-8-66-98, "Evaluation of Tensile Properties of Subbases for Use in New Pavement Design", which is now being conducted at the University of Texas (Refs 7, 8, 9, 12, 16, 17, and 24).

The next step in the study of material properties is the selection of a variety of pavement designs which would vary the stiffness or rigidity of the entire pavement. All the low stiffness values chosen for each individual material were selected together to represent a very flexible rigid-pavement. These are the values listed in the first column of Table 3.1 and hereafter in this report will be referred to as "Low Stiffness" pavement. Likewise, the high values chosen were selected to represent a very stiff pavement and the normal values were selected to represent a medium stiffness pavement. These two pavement designs will be referred to in the following text as "High Stiffness" and "Normal Stiffness" pavements, respectively.

The "Walker County" pavement properties, given in the last column of Table 3.1, are values used in the first project designed by this system (Ref 15). Using these values in the sensitivity analysis allows the Engineer to compare the "Walker County" design values with the other design values in Table 3.1. A comparison can also be made between design calculations made in this study and previous calculations made in Reference 15.

Traffic Distributions and Volumes. The traffic distributions and volumes used on the Walker County Design project were used in all of the basic runs for calculating fatigue damage to the pavement. Table 3.2 shows the distribution and volumes. Changes in damage caused by variations in traffic volumes and distributions will be discussed in Chapters 4 and 5.

Elastic Properties and Layer Thickness or ACP Overlay. The range of values in Table 3.3 were taken directly from values used in the Walker County Design. The elastic modulii selected were chosen to account for the effect of seasonal temperatures on the stiffness of the asphalt concrete overlay. In that study, no direct attempt was made to account for stiffness variations caused by the design of the asphaltic concrete mix. However,the range of the elastic modulii chosen provided a good range to study the variations in the ACP mix design.

Various Inputs. Inputs such as flexural strength of the concrete, the K-constant for the fatigue equation, lane and directional

Axle Group* Kips	Average Wheel Load Kips	Total Applications 1961 - 1969 Past	1969 - 1981 Predicted
2 - 6 (SA)	2.6	841,090	2,380,100
7 - 11 (SA)	4.5	3,269,000	9,290,000
12 - 16 (SA)	7.2	696,000	1,971,000
17 - 18 (SA)	8.7	110,600	313,000
19 - 20 (SA)	9.6	39,800	112,600
21 - 22 (SA)	10.7	14,550	41,200
4 - 13 (TA)	2.6	1,443,340	4,086,630
14 - 25 (TA)	4.5	1,384,600	3,928,000
26 - 32 (TA)	7.2	1,639,000	4,639,000
33 - 36 (TA)	8.7	183,500	518,900
37 - 40 (TA)	9.6	40,740	115,300
41 - 44 (TA)	10.7	20,370	57,090
50 (TA)	12.5	1,940	5,490

*SA - Single Axle
TA - Tandem Axle

Table 3.2. Traffic Distributions and Volumes Taken From Walker County Design

TYPE AXLE	WHEEL LOAD, KIPS	OVERLAY THICKNESS, INCHES	ELASTIC MODULUS OF OVERLAY, psi		
			250,000	750,000	1,300,000
SINGLE	2	4.5			
		10.7			
	4	4.5			
		10.7			
	6	4.5			
		10.7			
	8	4.5			
		10.7			
TANDEM	2	4.5			
		10.7			
	4	4.5			
		10.7			
	6	4.5			
		10.7			
	8	4.5			
		10.7			

Table 3.3. Factorial for Calculating Tangential Stress

distribution of traffic and various statistical confidence levels are basically the same values used for the Walker County Design Project. The size and variation of these values are discussed in Chapter 4 and 5.

Specific Approach to Analysis.

For this study, the computations for analysis were divided into two sections, (1) Computations on existing pavement and (2) Computations on overlaid pavement. Figure 3.2 briefly outlines the computations made in the two sections. A brief review of Figures 2.1 and 2.2 may also be benifical in the understanding of these computations. Each of the two sections are broken in smaller subsections for specific calculations. The individual computations made with each variable shown in Figure 3.2 will be presented in Chapter 4 along with the results obtained.

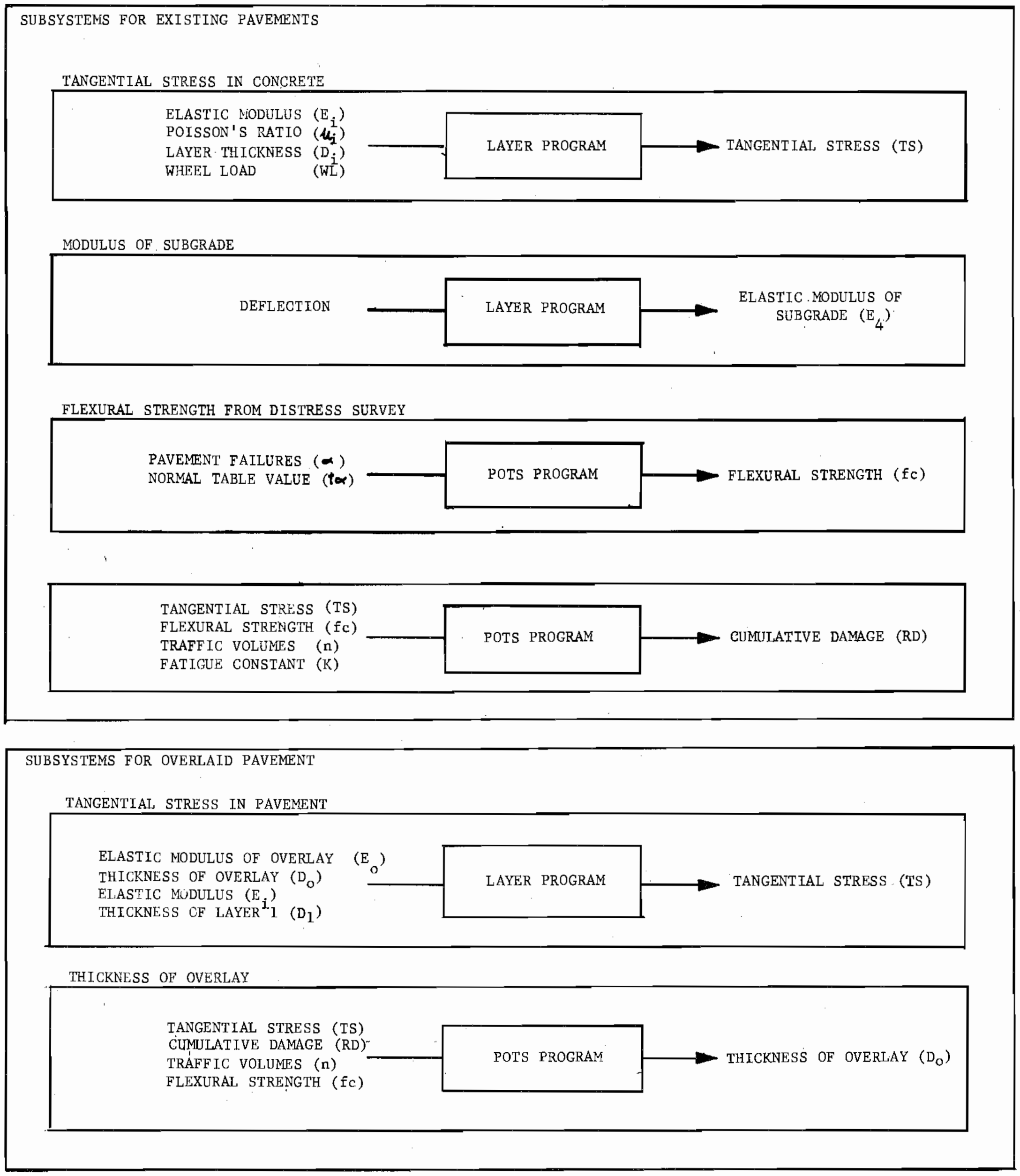

Fig 3.2. Subsystems for Analysis

CHAPTER 4. PRESENTATION OF RESULTS

The presentation of results is divided into two sections: (1) Computation on Existing Pavement and (2) Computation on Overlaid Pavement. The discussion of each section is divided into subsections as listed in Figure 3.2. In each subsection, where applicable, a brief review of the calculations made is presented; and, the results are displayed in graphical or tabular form.

Subsystems for Existing Pavement.

This section is broken into four subsystems: (1) Tangential Stress in Concrete, (2) Modulus of Subgrade, (3) Flexural Strength and (4) Cumulative Damage. The last subsystem "Cumulative Damage" is basically the whole "Subsystem for Existing Pavement". The output of the first three subsystems will be studied to determine the effect on the last "Cumulative Damage".

Tangential Stress In Concrete. Computations of tangential stress in a typical problem require calculating the stress for a pavement of given material properties and layer thicknesses. The calculations must be made for each of the different wheel loads under consideration. The subsystem, as used in the first design problem, calculated the tangential stresses for a total of thirteen different wheel loads.

In this sensitivity analysis, the number of computer runs for calculating tangential stress would multiply the work of the original problem by 88 or an additional 1144 computer runs on the LAYER program. The multipler of 88 comes from the fact that there are four different pavement stiffness conditions to be analyzed, (See Table 3.1), each having eleven variables to be run at two different levels of stiffness. The large number of computer runs presents a two-fold problem, (1) the cost in time or money to make these runs, and (2) the volume of charts or graphs necessary to make a meaningful presentation of the results. Thus, a short-cut to making these calculations was sought, along with a abbreviated way of presenting the results. In this section, the approximations made will first be discussed, then a disscussion of why the presentation of certain results was deleted. Last, a summary of the results are given.

Approximate Calculations.- After ovserving past calculations, it was determined that a change in stress, caused by an increase in wheel load size, could be accurately approximated by the equation of a circle. Figures 4.1 and 4.2 show the circular approximations made for the four pavement stiffness conditions in Table 3.1 for the single and tandem axle wheel loads. For these four pavement conditions, the approximating circle of stress was forced through the known tangential stresses for the 4.5 Kip and 10.7 Kip wheel loads. In this presentation, "force points" will be defined as the two points through which the circle for approximating the tangential stresses was forced. That is, in this case, the tangential stresses calculated by the LAYER program using the 4.5 Kip and 10.7 Kip wheel loads, respectively. A graphical representation of these "force points" is given in Appendix A. The actual stresses calculated for the "Normal Stiffness" and "Walker County" pavements are shown in Figures 4.1 and 4.2. The approximation errors are too small to be seen in these plots. As discussed in Appendix A, the errors in approximateing tangential stress are well below one percent. The choice of the 4.5 Kip and

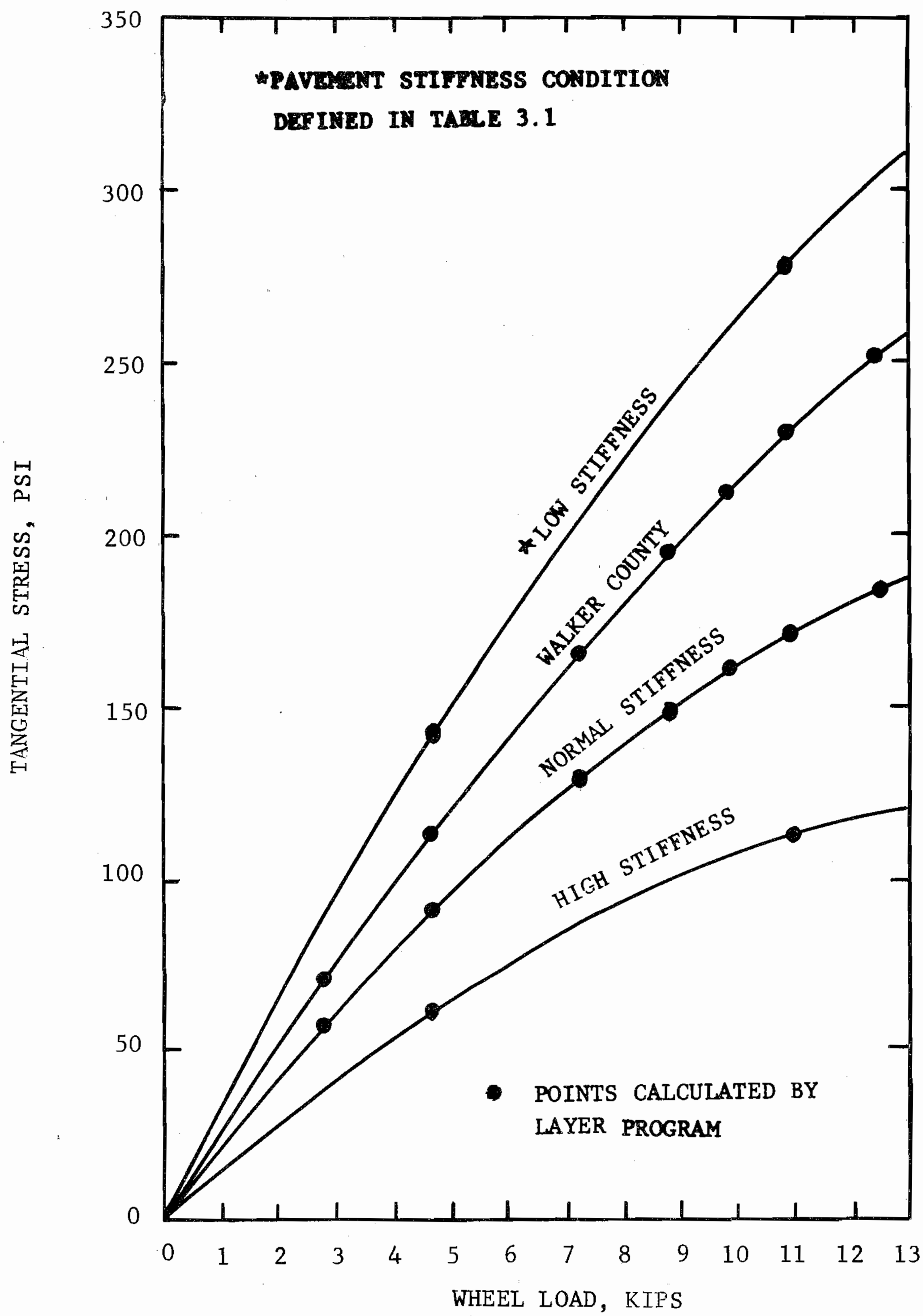

Fig 4.1. Tangential Stress versus Wheel Load for Single Axle

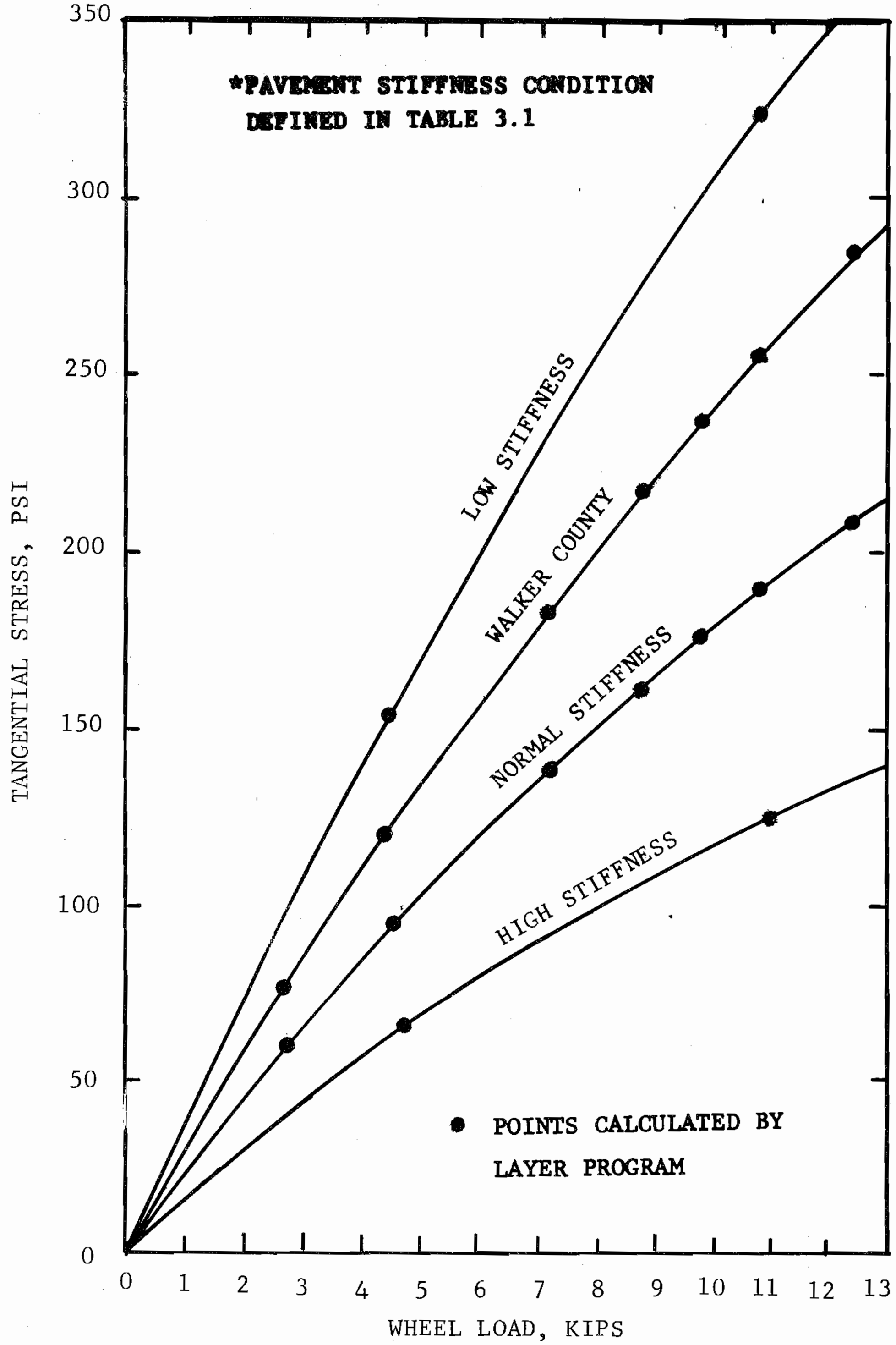

Fig 4.2. Tangential Stress versus Wheel Load for Tandem Axle

10.7 Kip wheel loads as "force points" was to give the best picture of the range of tangential stresses under consideration. If wheel loads are needed larger than the maximum of 12.5 Kip used in this study, the "force points" should be increased in size to prevent extrapolation errors.

Deletion of Certain Results.- For each of the four pavement stiffness conditions in Table 3.1, tangential stresses were calculated at two additional levels of pavement stiffness. For the "Normal Stiffness" pavement, tangential stress was computed while each variable was changed one at a time. First, it placed each variable at the "Low Stiffness" value, then at the "High Stiffness" value. Hence, calculations were made holding all other variables in the particular pavement stiffness condition at the original values and changing only the variable of interest.

The above type procedure was repeated for the remaining three pavement stiffness conditions. The "Walker County" pavement was run at the low and high levels. Then the "Low Stiffness" pavement was run at the normal and high levels. Last, the "High Stiffness" pavement was run at the low and normal levels. The total of computer runs using the LAYER program and circular approximate program represents 1196 different tangential stresses that could be presented at this time. This includes the original stresses calculated for the four basic pavements in Table 3.1 plus the 1144 created by this sensitivity study. After viewing the massive group of tangential stress data, it was decided to define the change in stress caused by a unit variable change in terms of a percentage of the original tangential stress calculated for the particular pavement stiffness condition as shown in the following equation:

$$\overline{PC} = 100(\overline{TS}_c - \overline{TS}_o)/\overline{TS}_o \quad \ldots \quad (4.1)$$

Where:

$\overline{PC}$ = Percent change from original tangential stress.

$\overline{TS}_c$ = Tangential Stress after variable change; psi.

$\overline{TS}_o$ = Tangential Stress of original pavement stiffness condition; psi.

Tables 4.1 and 4.2 show a list of percent changes calculated for the "Normal Stiffness" pavement. As can be seen, each table consists of 143 values, one for each of 11 variables changed and one for each of the 13 wheel loads. Since these tables are hard to interpret, additional tables for the "Low Stiffness", "High Stiffness", and "Walker County" pavements were deleted. A study of these tables was made to determine if a trend in the percent change values existed. For unit changes in Poisson's Ratio (μ), it can be seen that the percent change in stress remains approximately constant as the loads are increased for both the single axle and the tandem axle wheel loads. For unit changes in the thickness of layers 2 and 3, the percent change does not remain constant with wheel load size. The total percent change in stress created by unit changes in the thickness of layer 2 and 3, is relatively low, which leads to the conclusion that a study of how it varies with the wheel load size is not necessary. For the most part, it appears that the remaining variables from Table 3.1(E_1, E_2, E_3, E_4 and D_1) do have significant variations in the percent change value as wheel load is increased. Figures 4.3 and

		VARIABLE										
		E_1	U_1	D_1	E_2	U_2	D_2	E_3	U_3	D_3	E_4	U_4
SINGLE AXLE WHEEL LOAD	2.65	-2.5	4.7	11.9	14.5	- .5	2.0	5.8	0	1.4	15.3	0
	4.5	-2.8	4.7	10.8	16.4	- .9	2.5	7.1	.1	2.0	13.9	0
	7.2	-3.0	4.8	9.9	18.3	-1.3	3.1	9.1	.2	2.5	12.6	0
	8.7	-3.1	4.8	9.5	19.1	-1.5	3.3	9.7	.1	2.7	12.0	.2
	9.6	-3.1	4.8	9.3	19.5	-1.5	3.4	10.0	.1	2.8	11.8	.3
	10.7	-3.2	4.8	9.1	20.5	-1.6	3.5	10.4	.1	2.9	11.5	.2
TANDEM AXLE WHEEL LOAD	2.65	-3.0	4.3	10.8	15.4	- .8	2.5	7.3	.2	1.8	20.3	.2
	4.5	-3.2	4.2	9.8	17.1	-1.3	3.9	8.7	.2	2.4	19.6	.2
	7.2	-3.5	4.1	8.8	18.6	-1.6	3.5	10.2	.2	2.9	19.1	.3
	8.7	-3.6	4.1	8.4	19.6	-1.8	3.7	10.8	.1	3.0	18.8	.3
	9.6	-3.7	4.1	8.2	20.0	-1.9	3.8	11.1	.2	3.1	18.7	.3
	10.7	-3.8	4.1	8.0	20.4	-2.0	3.9	11.6	.2	3.2	18.6	.3
	12.5	-3.8	4.1	7.7	21.0	-2.1	4.1	12.1	.2	3.4	18.4	.4

Table 4.1. Percent Change in Tangential Stress for Unit Variable Change to Low Values for Normal Pavement Condition

VARIABLE

		E_1	U_1	D_1	E_2	U_2	D_2	E_3	U_3	D_3	E_4	U_4
SINGLE AXLE WHEEL LOAD	2.65	2.3	-2.9	-10.1	-16.0	-0.4	2.2	-1.1	-0.2	-1.3	-3.4	-0.4
	4.5	2.4	-2.8	- 9.4	-15.9	-0.3	0.2	-1.3	0.0	-1.7	-3.7	-0.3
	7.2	2.7	-2.8	- 8.7	-17.8	-0.4	-1.7	-1.5	-0.1	-2.1	-4.1	-0.6
	8.7	2.7	-2.8	- 8.5	-18.2	-0.5	-2.4	-1.6	-0.1	-2.3	-4.3	-0.6
	9.6	2.8	-2.8	- 8.3	-18.4	-0.4	-2.7	-1.6	-0.1	-2.4	-4.3	-0.6
	10.7	2.8	-2.8	- 8.2	-18.6	-0.5	-2.1	-1.7	-0.1	-2.5	-4.4	-0.6
TANDEM AXLE WHEEL LOAD	2.65	2.8	-2.8	-10.0	-16.8	- .3	1.3	-1.2	0	-1.7	-5.0	- .5
	4.5	3.0	-2.3	-8.2	-16.7	- .3	- .4	-1.4	0	-2.0	-5.5	- .6
	7.2	3.2	-2.0	-7.6	-16.7	- .4	-2.1	-1.6	- .1	-2.5	-6.0	- .8
	8.7	3.3	-1.8	-7.1	-16.7	- .4	-2.8	-1.8	- .1	-2.7	-6.2	- .9
	9.6	3.3	-1.8	-6.8	-16.7	- .4	-3.1	-1.8	- .1	-2.8	-6.3	- .9
	10.7	3.3	-1.7	-6.5	-16.6	- .5	-3.5	-1.9	- .1	-2.9	-6.4	- .9
	12.5	3.4	-1.5	-6.1	-16.6	- .5	-4.0	-2.0	- .1	-3.0	-6.6	- .9

Table 4.2. Percent Change in Tangential Stress for Unit Variable Change to High Values for Normal Pavement Condition.

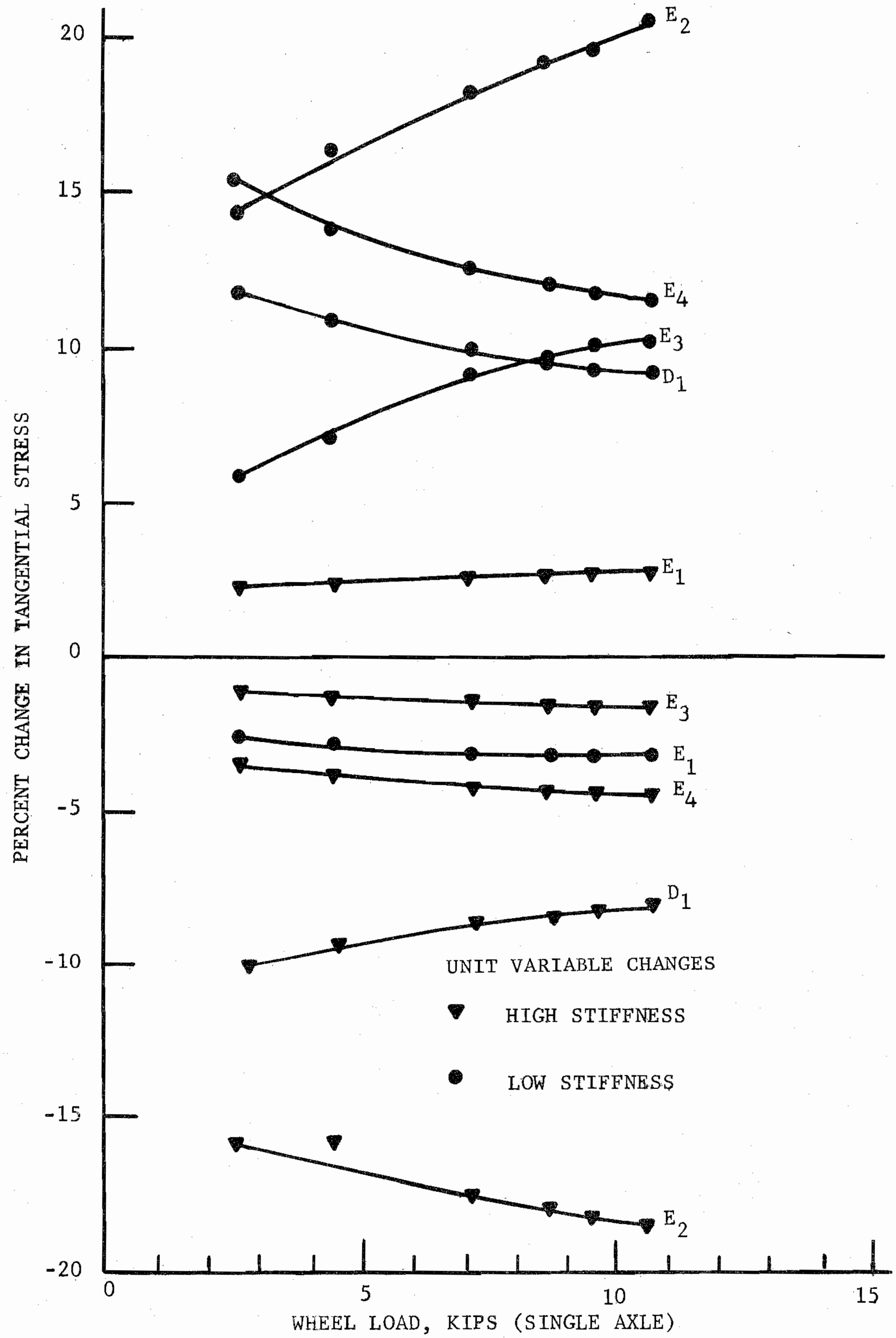

Fig 4.3. Percent Change in Tangential Stress versus Wheel Load for Unit Variable Changes

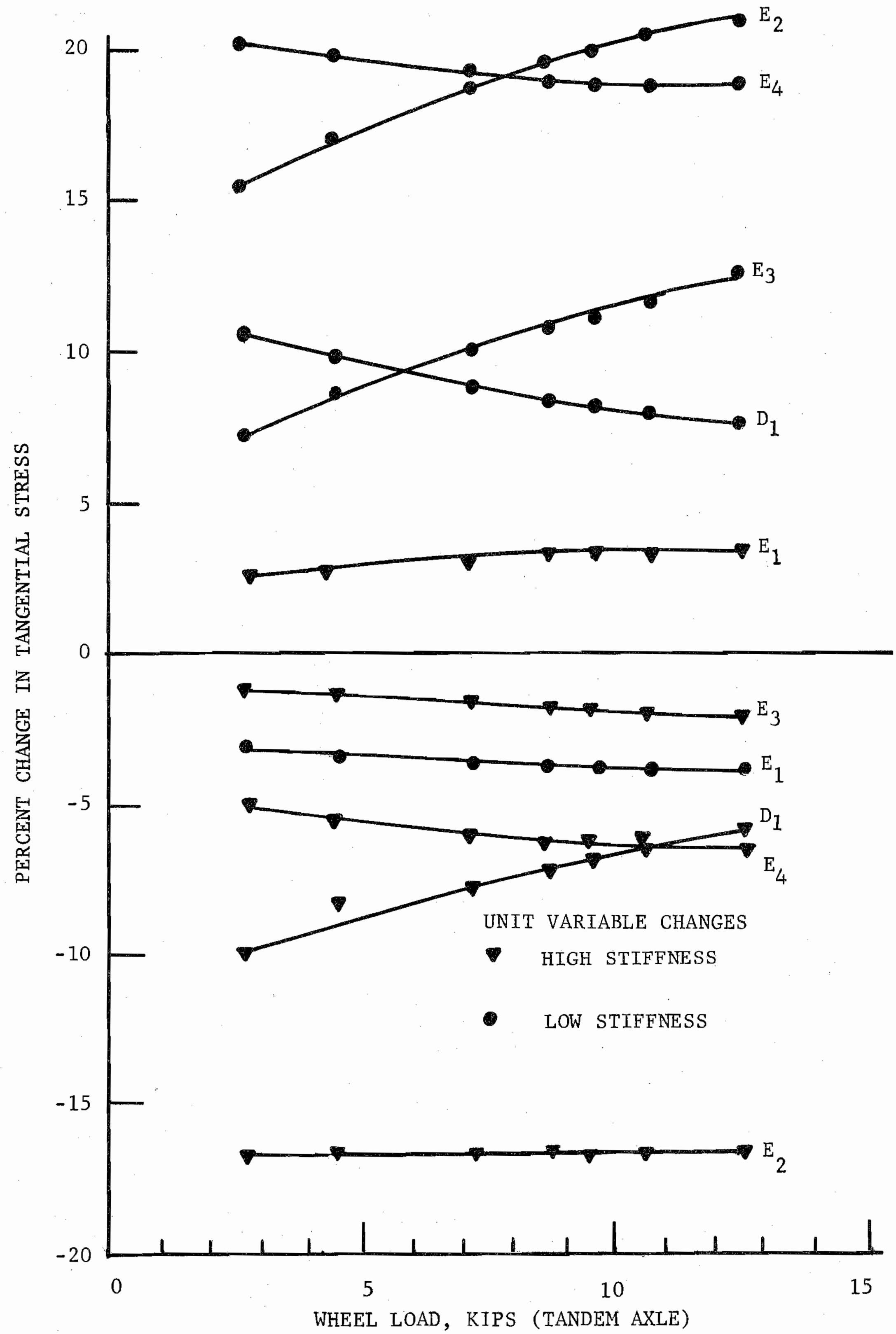

Fig 4.4 Percent Change in Tangential Stress versus Wheel Load for Unit Variable Changes

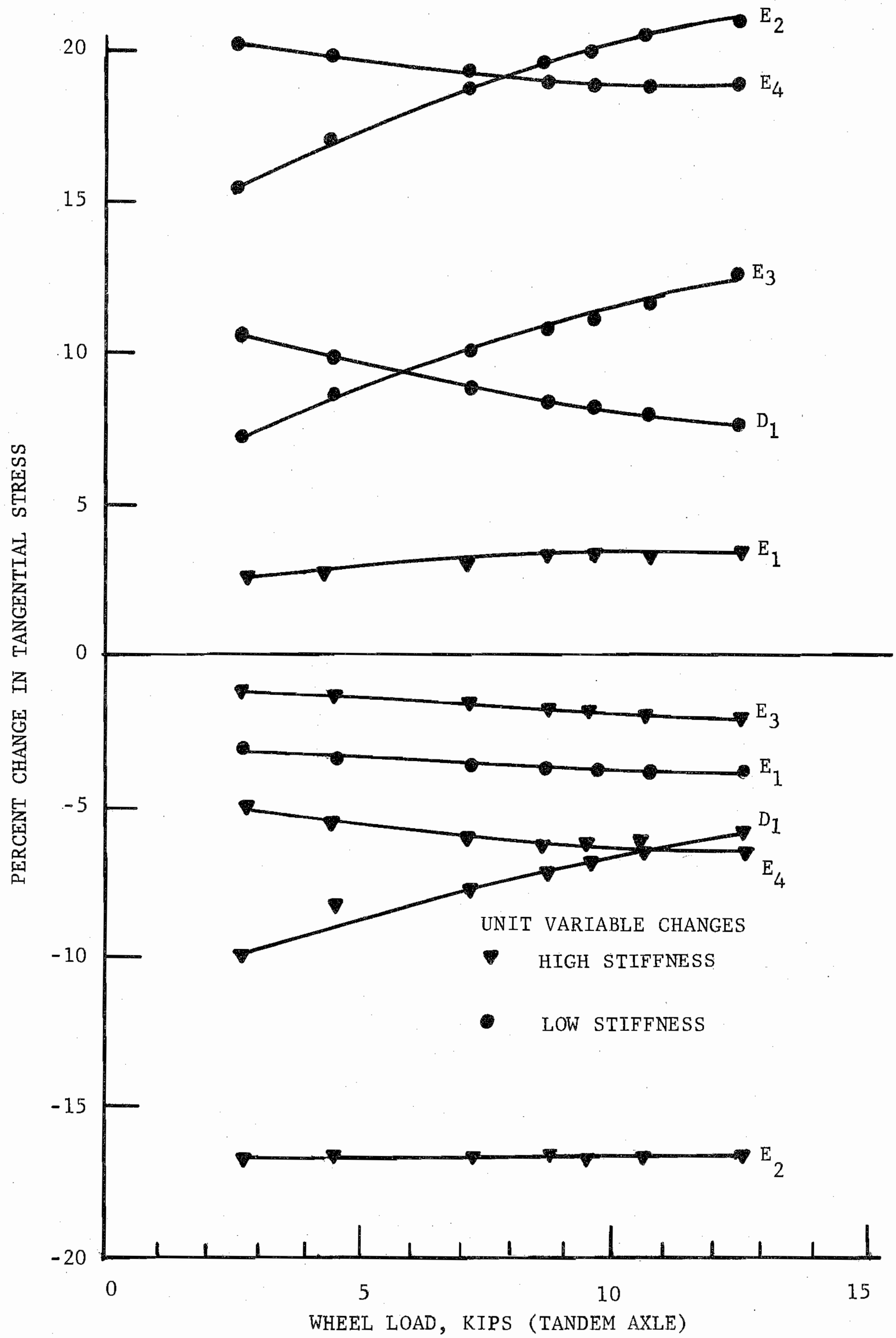

Fig 4.4 Percent Change in Tangential Stress versus Wheel Load for Unit Variable Changes

4.4 show these variations for the single and tandem axle wheel loads, respectively. It can be seen from these plots that the percent change varies more with variable changes than with wheel load magnitude.

Based on these observations, it was decided to show in graphical form the percent change caused by a unit variable change for only one wheel load. This would not give a complete report of the absolute sensitivity of tangential stress to the input material properties and thicknesses, but would give the relative importance of each input variable. Intutively, knowing that the larger wheel loads cause most of the damage to the pavement, the 10.7 Kip wheel load calculations were chosen to represent the entire system. In the next section, "Summary of Results", the percent change for each of the four pavement stiffness conditions will be shown for the 10.7 Kip wheel load. This will give a more meanful representation of the sensitivity of the system.

Summary of Results.- This section presents a selected summary concerning the sensitivity of tangential stress to the input material properties and layer thickness shown in Table 3.1. For the "Normal Stiffness" pavement, each of eleven material variables from Table 3.1 was varied one at a time from the low stiffness to high stiffness values. The results in terms of percent change are shown in Figures 4.5 and 4.6. Based on the observation that Poisson's Ratio has a small effect on tangential stress, Poisson's Ratio has been deleted from further study in this analysis. A summary of the percent changes in Tangential stress computed for "Walker County" pavement is shown in Figures 4.7 and 4.8. Figures 4.5 through 4.8 show that a variation in thickness of ± 2 inches for layers two and three change tangential stress less than 5%. In actual design problems, these depths are usually known or can be determined to an accuracy

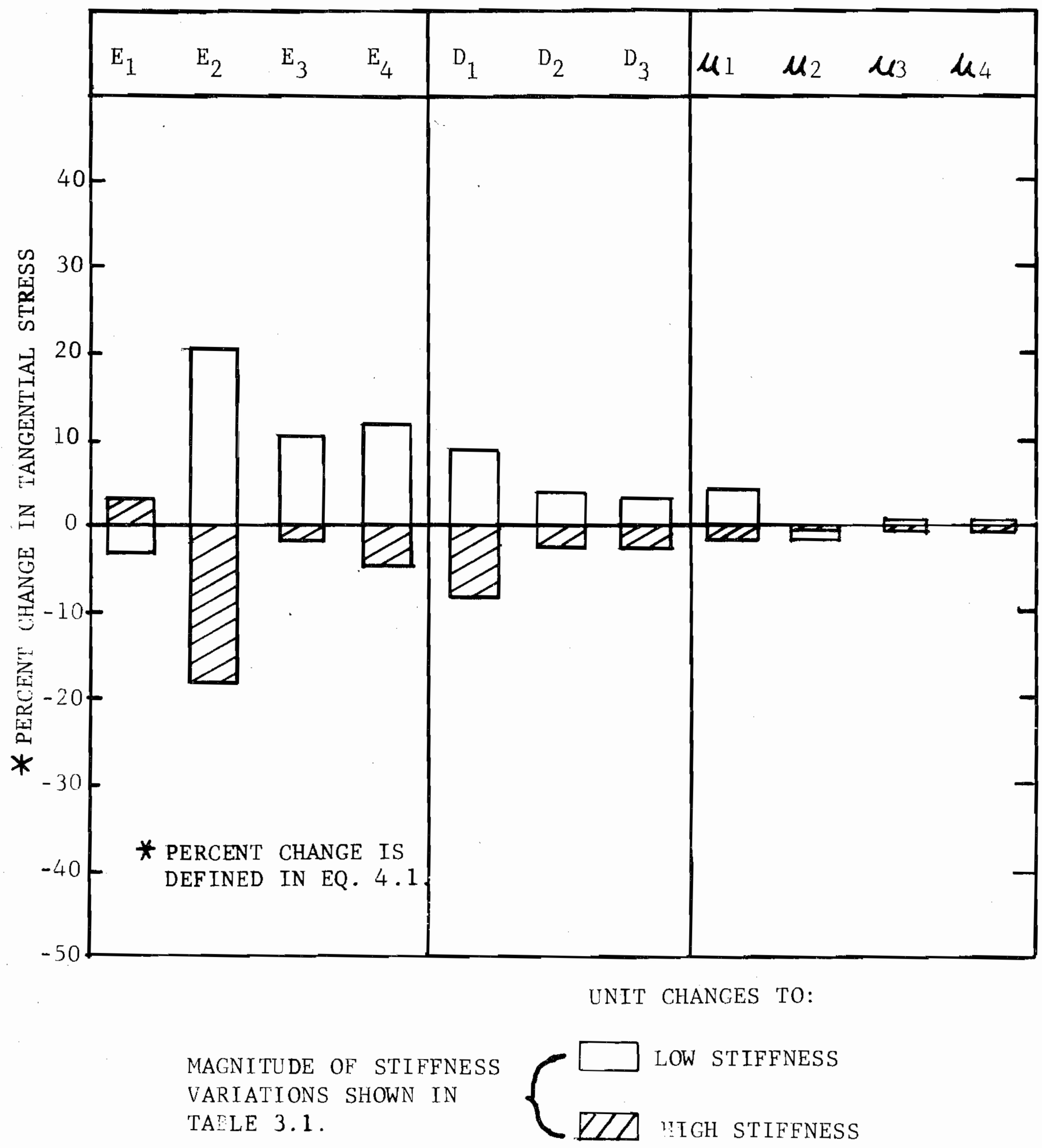

Fig 4.5. Summary of Percent Change in Tangential Stress for Normal Stiffness Pavement (Single Axle)

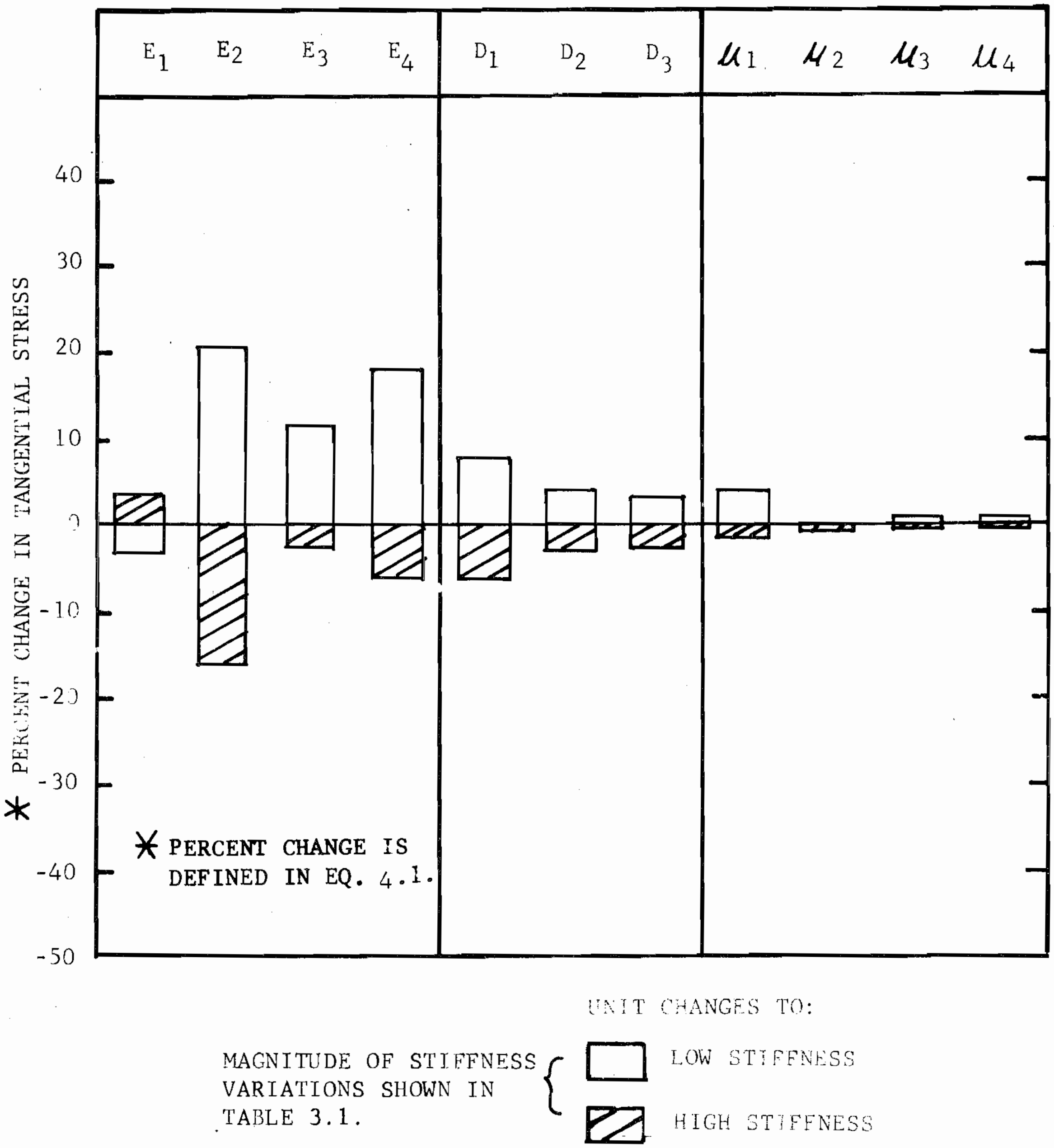

Fig 4.6. Summary of Percent Change in Tangential Stress for Normal Stiffness Pavement (Tandem Axle)

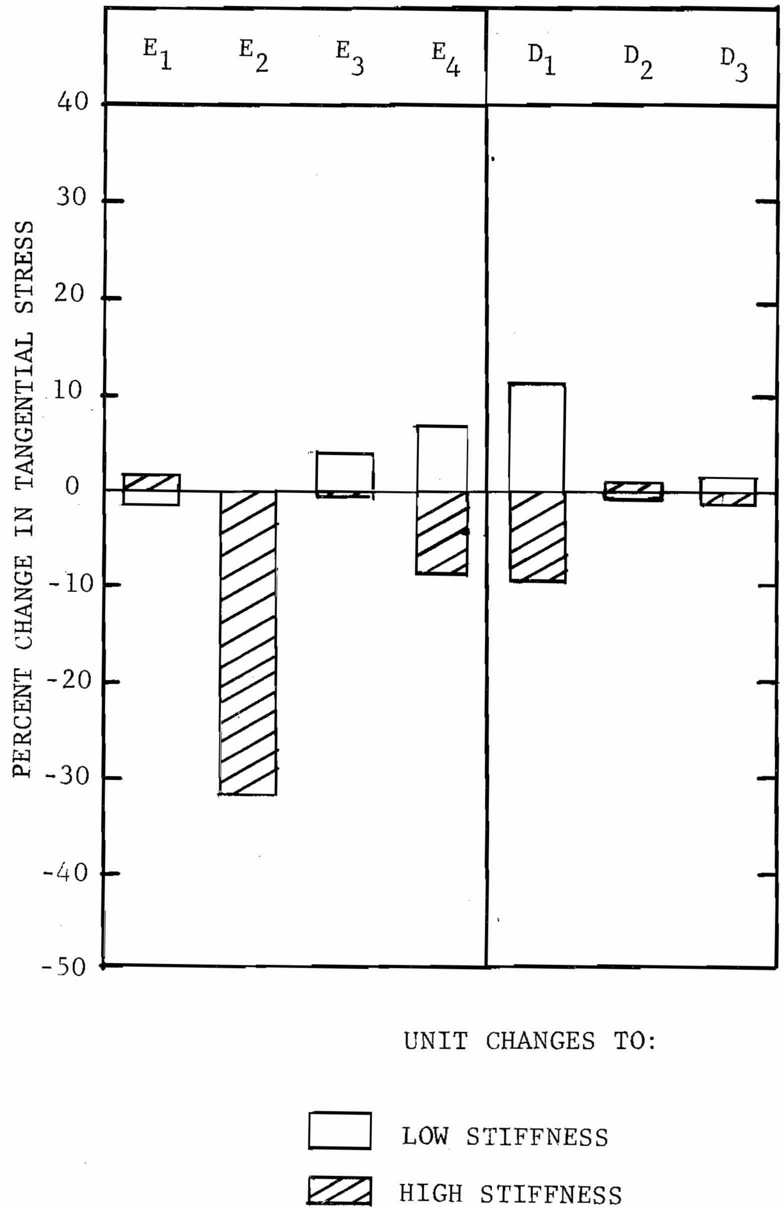

Fig 4.7. Summary of Percent Change in Tangential Stress for Walker County Pavement (Single Axle)

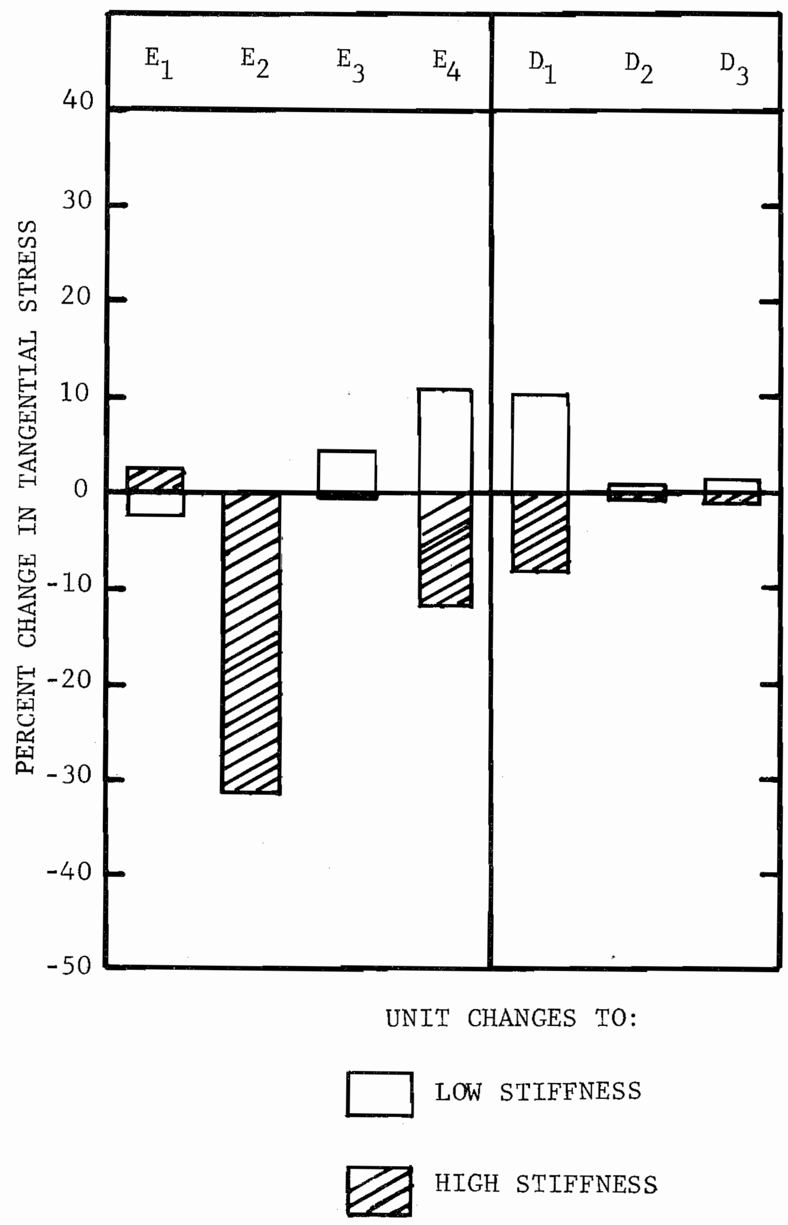

Fig 4.8. Summary of Percent Change in Tangential Stress for Walker County Pavement (Tandem Axle)

of ± 1 inch. From this, futher invertigation of possible variations in the thichness of layers two and three have been deleted.

Figure 4.9 shows the summary of computed percent changes for the "Low Stiffness" pavement; likewise, Figure 4.10 is a summary for "High Stiffness" pavement.

Summary.- Figures 4.5 through 4.10 show for the variables in Table 3.1 that elastic modulii (E_1, E_2, E_3, and E_4) and the thickness for layer one (D_1), create the largest change in tangential stress. The significance of each change will be discussed in the next chapter. The remaining unit changes for the variables shown in Table 3.1, Poisson's Ratios and thicknesses of layers 2 and 3 (μ_1, μ_2, μ_3, μ_4, D_2, and D_3) have been determined to be insignificant and will be eliminated from further discussion.

Modulus of Subgrade. The deflections of the pavement midway between the wheel loads were used to indicate changes in the modulus of elasticity for the subgrade layer (E_4). The LAYER program was used to compute deflections for each of the four pavement stiffness conditions. All variables were held constant except the elastic modulus of subgrade which was varied from 4100 to 20000 psi. The results of the computations are shown in Figure 4.11. As illustrated on the curve for the "High Stiffness" pavement, a unit change in deflection causes a much larger error in characterizing E_4 for the smaller deflection. However, this large error in characterizing E_4 is not critical in the represention of the entire system as discussed in Chapter 5.

Flexural Strength from Distress Survey. The first step in these calculations is to determine the fatigue equation for concrete

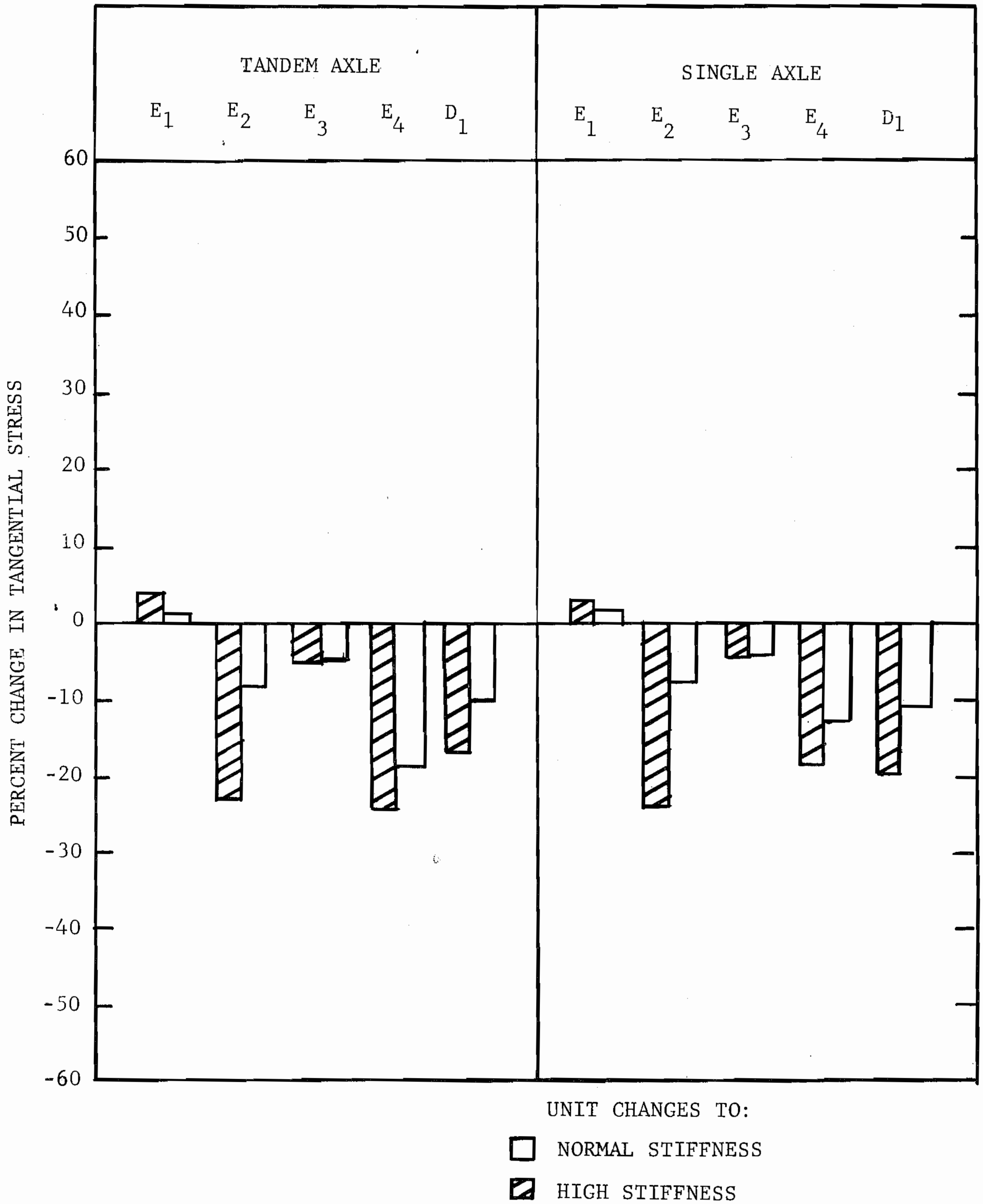

Fig 4.9. Summary of Percent Change in Tangential Stress for Low Stiffness Pavement (both Single and Tandem Axle)

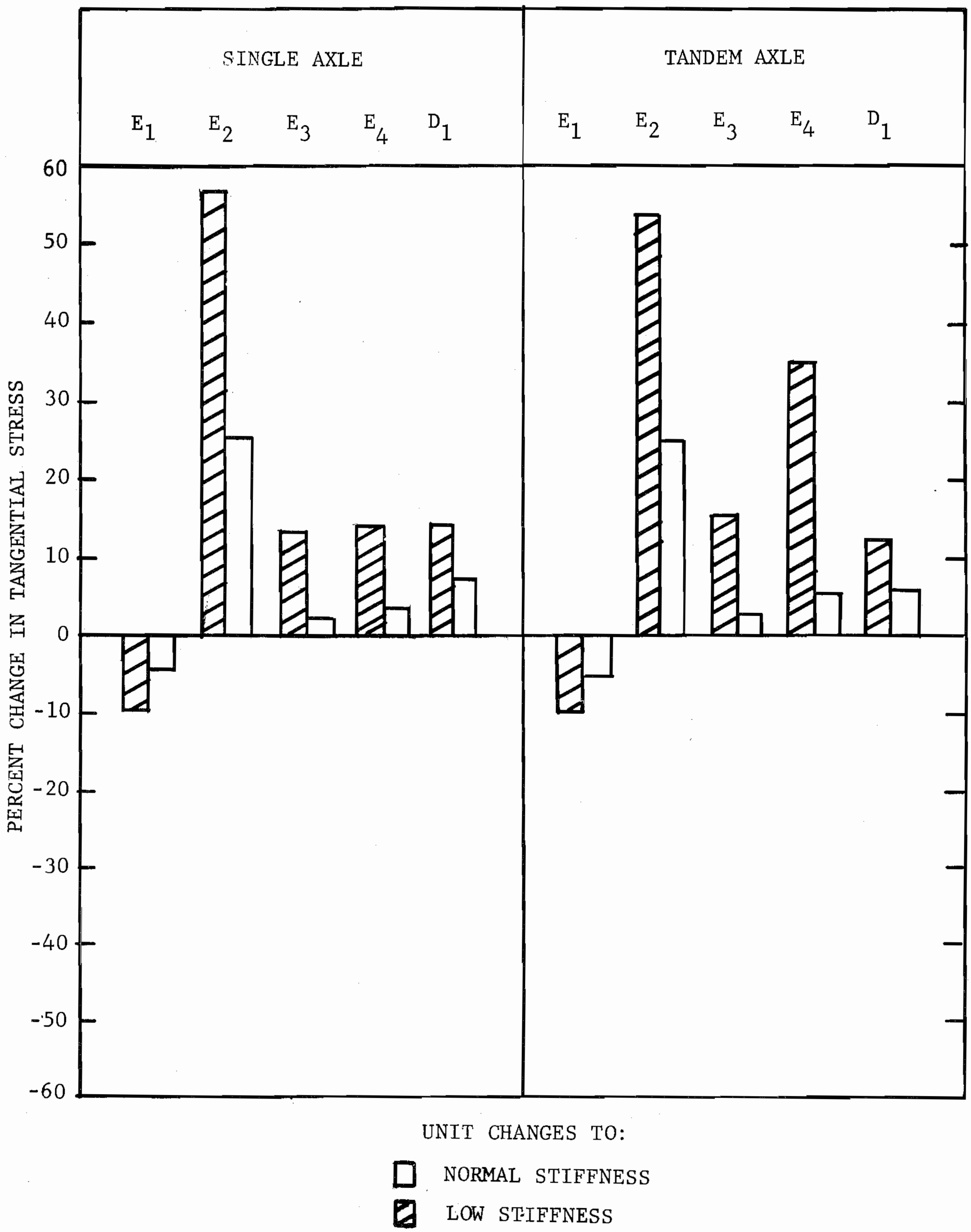

Fig 4.10. Summary of Percent Change in Tangential Stress for High Stiffness Pavement (both Single and Tandem Axle)

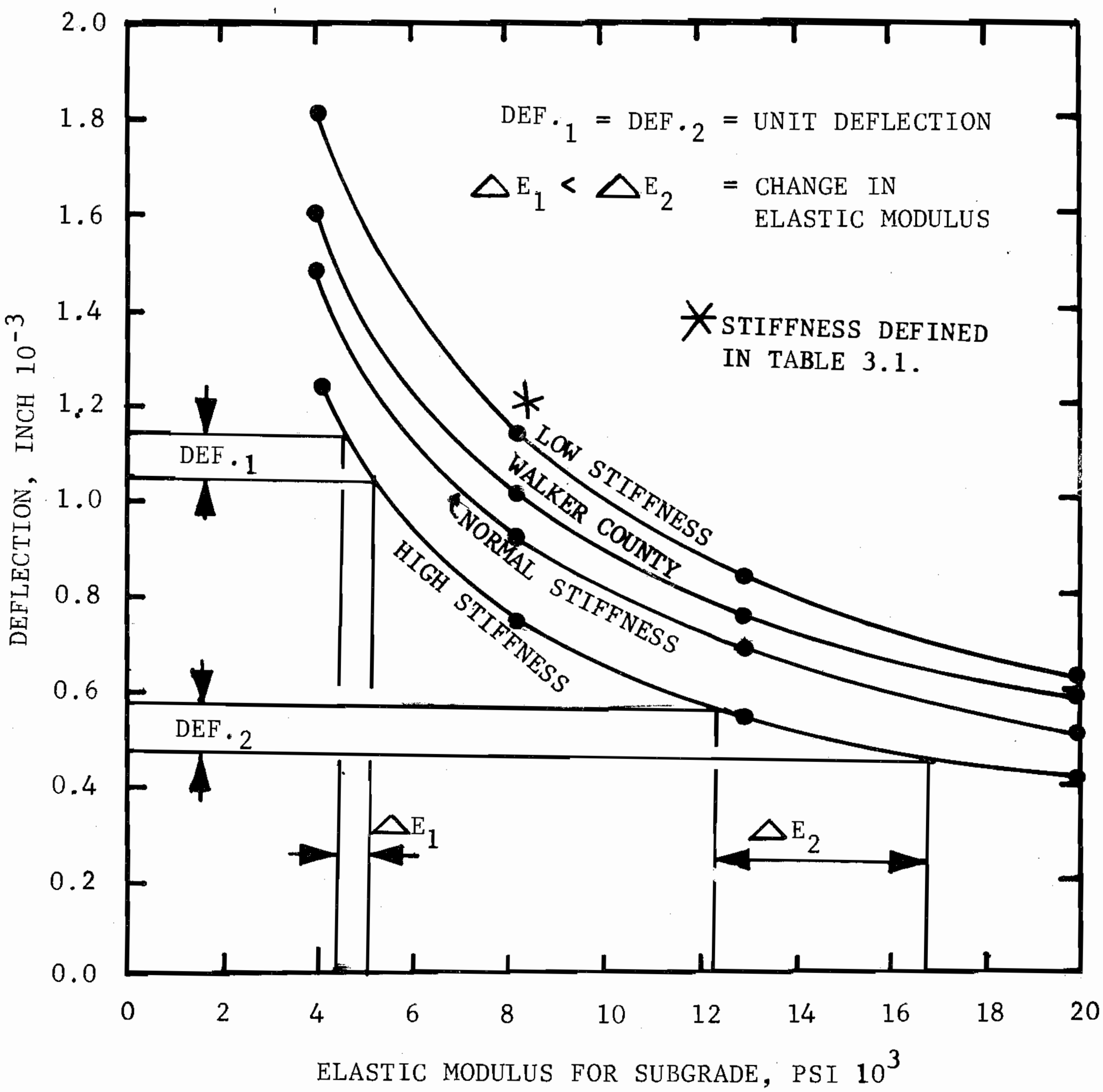

Fig 4.11. Deflection versus Subgrade Modulus (E_4)

that will cause the calculated cumulative damage to be 1.0. The fatigue equation in the POTS program is a combination of equations 2.1 and 2.5.

$$N_{c(j)} = \text{Antilog Log} \left[C \frac{f_c}{\overline{TS}_j}^{K} - t\,(\sigma_N) \right] \quad \text{. . . . . .4.1}$$

Where:

$N_{c(j)}$ = Cycles to failure for a given confidence

C,K = Constants for fatigue equation.

f_c = Flexural Strength; psi.

$\overline{TS}_j$ = Tangential Stress of Concrete; psi.

t = Normal table value for confidence level.

σ_N = Log of standard error of cycles to failure.

Figure 4.12 shows a plot of the fatigue equations for each of the four pavement conditions which calculates cumulative damage to be 1.0 for the traffic in Table 3.2. Remembering from Chapter 2 that:

$$\overline{RD} = \sum_{j=1}^{j=m} \frac{n\,(j)}{N\,(j)} \quad \text{. . . . .(2.3)}$$

Where:

$\overline{RD}$ = Cumulative damage.

n = Number of repetition for a specific wheel load group.

m = Number of wheel load groups.

The four plots were calculated by trial and error varing σ_N until the cumulative damage calculated was 1.0.

A cumulative damage of 1.0 is total damage to the pavement.

that will cause the calculated cumulative damage to be 1.0. The fatigue equation in the POTS program is a combination of equations 2.1 and 2.5.

$$N_{c(j)} = \text{Antilog Log} \left[C \frac{f_c}{\overline{TS}_j}^{K} - t\,(\sigma_N) \right] \quad \ldots\ldots\ldots 4.1$$

Where:

$N_{c(j)}$ = Cycles to failure for a given confidence

C,K = Constants for fatigue equation.

f_c = Flexural Strength; psi.

$\overline{TS}_j$ = Tangential Stress of Concrete; psi.

t = Normal table value for confidence level.

σ_N = Log of standard error of cycles to failure.

Figure 4.12 shows a plot of the fatigue equations for each of the four pavement conditions which calculates cumulative damage to be 1.0 for the traffic in Table 3.2. Remembering from Chapter 2 that:

$$\overline{RD} = \sum_{j=1}^{j=m} \frac{n\,(j)}{N\,(j)} \quad \ldots\ldots\ldots (2.3)$$

Where:

$\overline{RD}$ = Cumulative damage.

n = Number of repetition for a specific wheel load group.

m = Number of wheel load groups.

The four plots were calculated by trial and error varing σ_N until the cumulative damage calculated was 1.0.

A cumulative damage of 1.0 is total damage to the pavement.

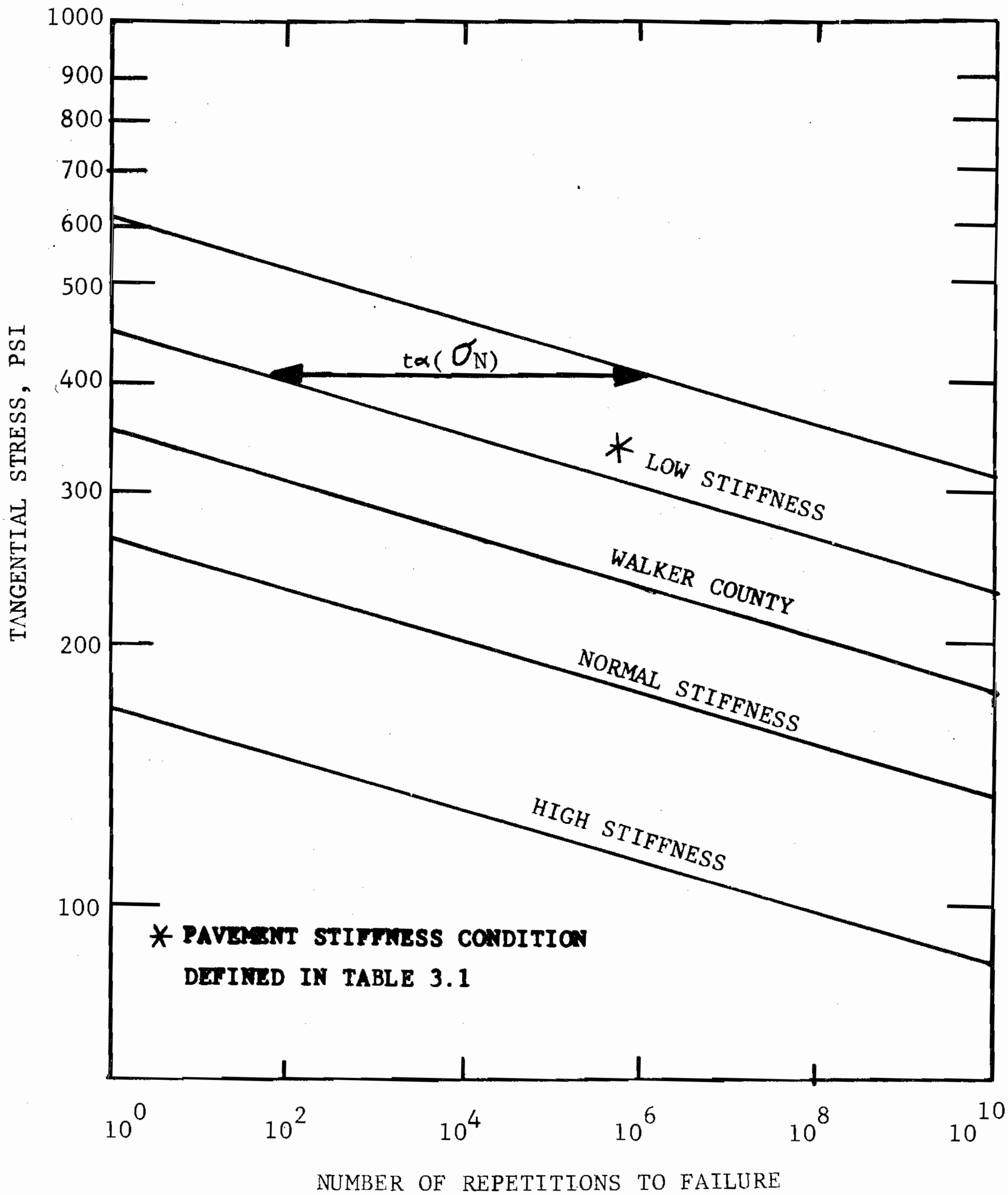

Fig 4.12. Fatigue Equation for Cumulative Damage Equal to 1.0

This definition should not be construed to mean the pavement is of no use or values; rather, it means total damage has occurred at a specific confidence level. If a pavement has 5% failures, then it can be said the pavement has total damage at the 95% confidence level. Using the predetermined plot in Figure 4.12 the horizontal distance form the average line to the plot of total failure can be measured. The horizontal distance, by definition, in the system is redefined as follows:

$$\overline{ND} = t_{\alpha} (\sigma_N) \quad (4.2)$$

Where:

$\overline{ND}$ = Horizontal distance or log of cycles.

t_{α} = Normal table value for a confidence level equal to the percent failures measured in the pavement.

σ_N = Log of standard error in estimating cycles to failure.

If we assume a log-normal distribution about the fatigue curve, the percent failures can be respresented as shown in Figure 4.13. Using this definition, standard error can be defined as follows:

$$\sigma_N = \frac{\overline{ND}}{t_{\alpha}} \quad (4.3)$$

Then:

Substituting into equation 2.4 of Chapter 2.

$$\sigma_{f_c} = f_c - \frac{f_c}{\text{antilog}\left(\frac{\log .5274}{34.25}\right)} \quad (4.4)$$

Figure 4.14 shows, for all four "Pavement Stiffness" conditions, the standard error of flexural strength of the concrete (σ_{f_c}) plotted as a function of precent failure (Ref 4) in the concrete.

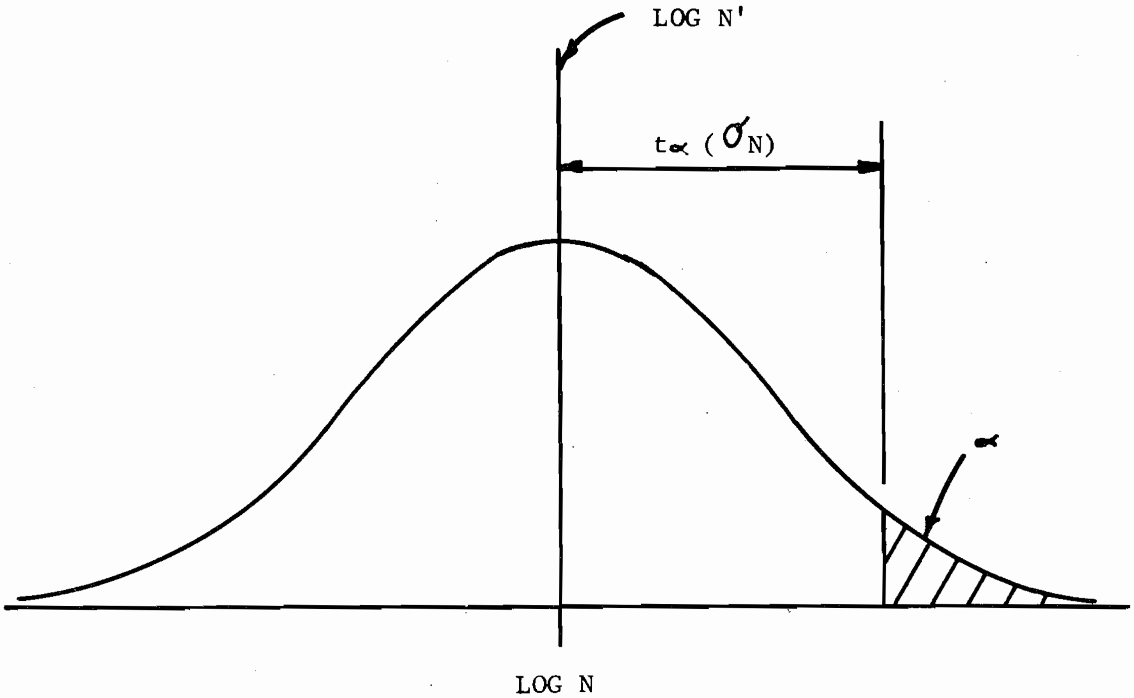

WHERE:

N = N' = $.527(fc/TS)^K$

α = FAILURES, %

tα = NORMAL TABLE VALUE AT α-CONFIDENCE

σ_N = STANDARD ERROR OF N

Fig 4.13. Conceptual Diagram Illustrating the Log-normal Distribution of Axle Applications for a given Flexural Strength

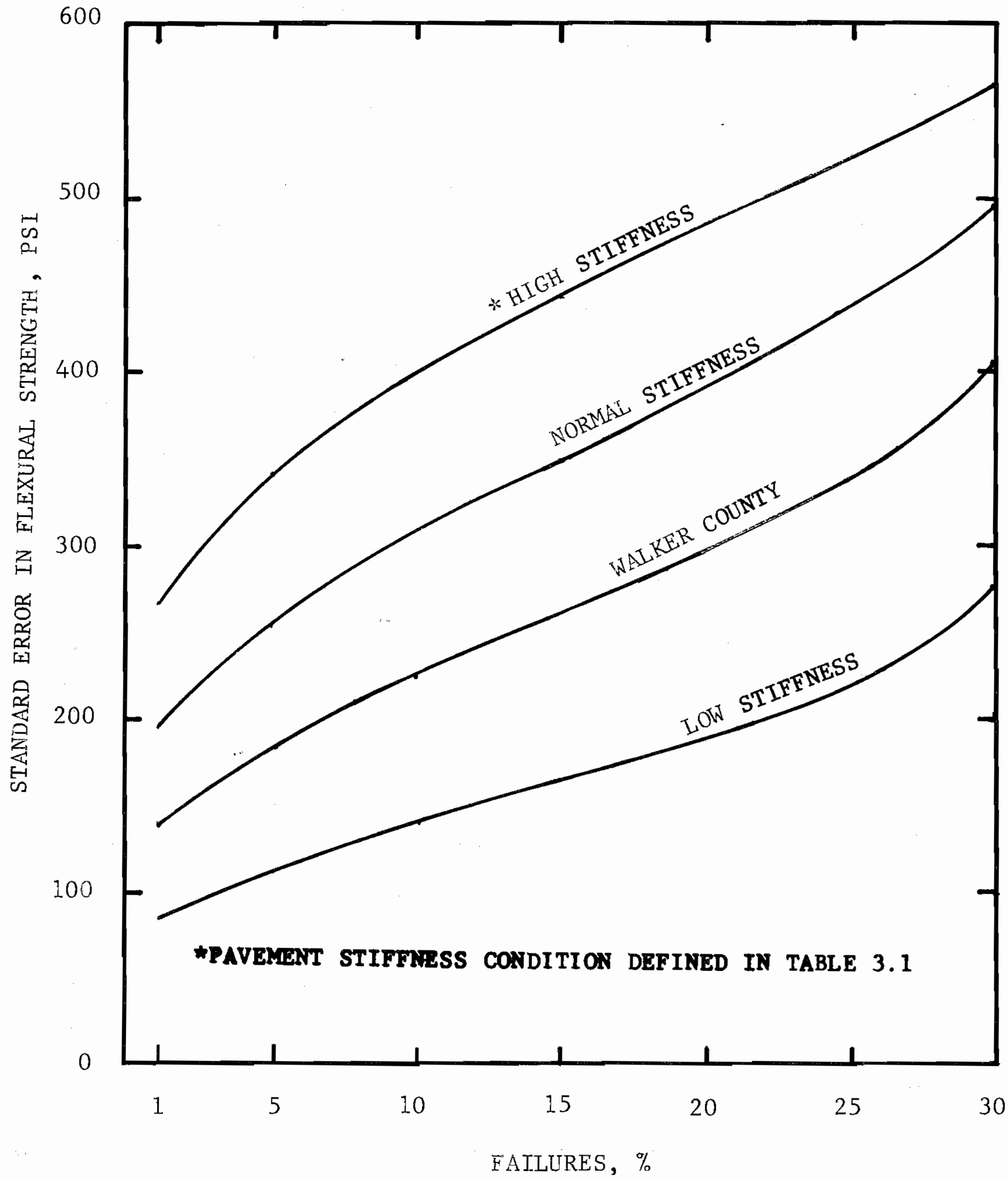

Fig 4.14. Standard Error in Flexural Strength versus Pavement Failures

Cumulative Damage. The basic inputs that affect this subsystem are tangential stress in the concrete, traffic, and flexural strength. The effect of each of these inputs on cumulative damage will be discussed in this section.

Tangential Stress in the Concrete. – Figures 4.15 and 4.16 show the effect of tangential stress on cumulative damage. The two figures show the results of damage calculations for traffic repetitions of 10,000 and 1,000,000, respectively. A new term has been added to these figures called "Design Static Flexural Strength" ($\hat{f}_c$). This term was added because of the limitations of the computer program to calculate damage directly for a number of flexural strengths. The program calculated cumulative damage at five confidence levels (99%, 95%, 90%, 80% and 50%) using a flexural strength of 620 psi and a standard error of 162 psi. The different confidence levels correspond respectively to the design flexural strengths of 320, 389, 431, 462 and 620. In the mathmatics of defining this term, equation 2.5 is altered as follows:

$$N_{c(j)} = C + \left(\frac{\hat{f}_c}{TS_j}\right)^K \quad \ldots\ldots\ldots\ldots\ldots\ldots \quad (4.5)$$

Where:

$\hat{f}_c$ = Design static flexural strength of concrete, psi

To obtain the design values shown in Figures 4.15 and 4.16 equation 2.5 and equation 4.5 were equated and $\hat{f}_c$ was solved as follows:

$$\hat{f}_c = \text{Antilog}\left(\log f_c - \frac{t(\sigma_N)}{K}\right) \quad \ldots\ldots\ldots\ldots \quad (4.6)$$

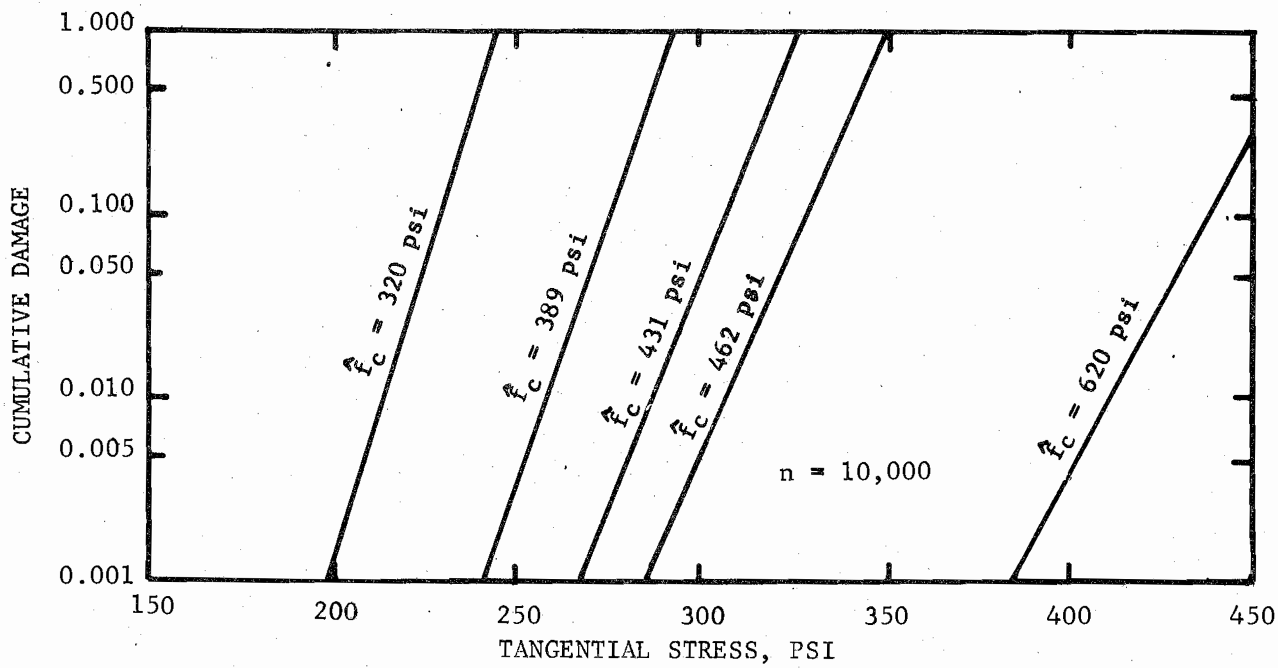

Fig 4.15. Cumulative Damage versus Tangential Stress for 10,000 Repetitions of Load

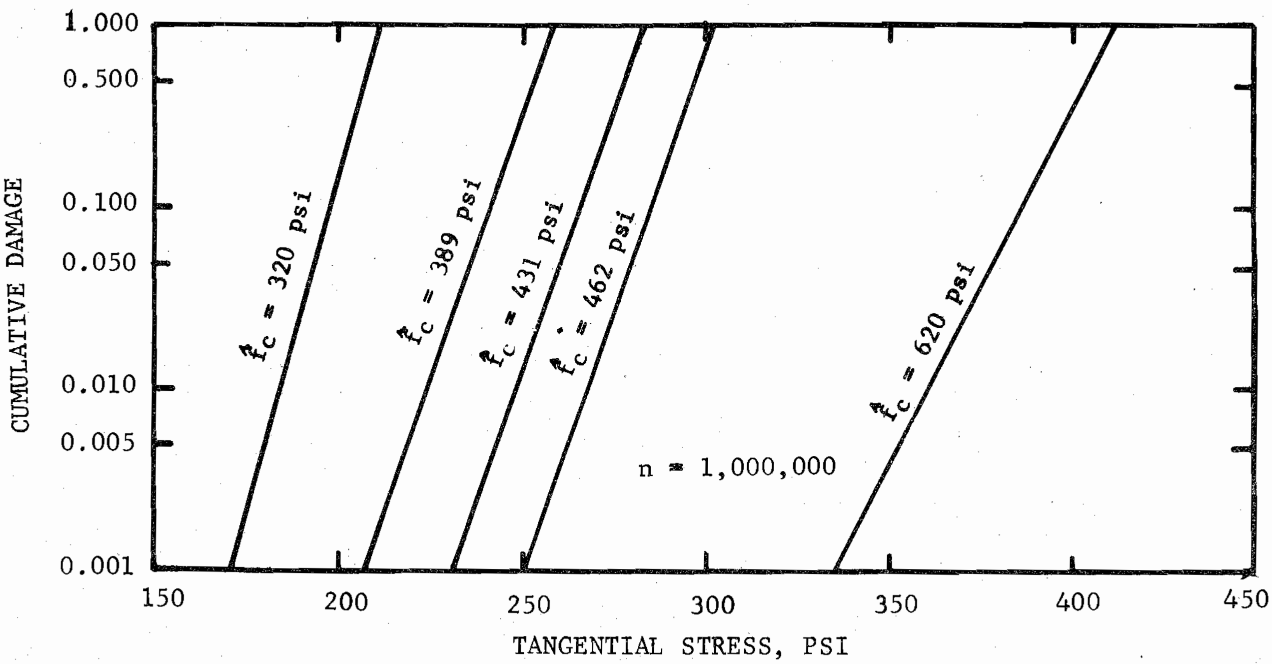

Fig 4.16. Cumulative Damage versus Tangential Stress for 1,000,000 Repetitions of Load

Where:

K = 34.25.

t = Constant from normal curve table for confidence level.

It should be remembered that the design static flexural strengths are not shown to represent average concrete strengths, but infrequent occurances of weak concrete which occur in the distribution.

Traffic Distributions.- Past traffic distributions obtained for the years 1965-1968 for the Walker County Project are shown in Table 4.3. Figure 4.17 shows for each of the yearly traffic distributions the percent change in cumulative damage from the damage values calculated for the average distribution of the four years.

Flexural Strength.- For each of the four pavement stress conditions, cumulative damage was computed for the range of flexural strengths. Figure 4.18 illustrates the pronounced effect of flexural strength on cumulative damage. This plot could also be thought of as a plot of the design flexural strength ($\hat{f}_c$) versus cumulative damage. For all four stress conditions a small change in flexural strenth of the concrete causes a large change in cumulative damages.

Constant - K.- The constant K as previously defined is used in the fatigue equation 2.2. Using 34.25, as used in all calculations, all of the significant damage is calculated for the four largest tandem axle wheel loads. In studying the fatigue equation, it was determined that the large value for the constant K was the reason for this

Axle Group* Kips	Average Wheel Load Kips	Total Past Applications (1961-1969) Based on Traffic Counts for Years			
		1965	1966	1967	1968
2-6 (SA)	2.6	1,178,884	885,783	840,359	827,298
7-11 (SA)	4.5	3,150,016	3,193,004	3,278,886	3,229,734
12-16 (SA)	7.2	491,004	587,001	698,373	821,066
17-18 (SA)	8.7	166,040	119,211	110,617	113,734
19-20 (SA)	9.6	78,276	36,216	39,624	51,414
21-22 (SA)	10.7	53,370	15,090	14,859	20,254
4-13(TA)	2.6	1,628,378	1,416,951	1,442,974	1,112,412
14-25(TA)	4.5	1,104,166	1,501,455	1,388,491	1,695,104
26-32(TA)	7.2	1,529,940	1,705,170	1,637,792	1,537,746
33-36(TA)	8.7	234,838	182,589	183,261	207,214
37-40(TA)	9.6	73,532	46,779	41,275	46,740
41-44(TA)	10.7	8,302	12,072	19,812	32,718
50(TA)	12.5	3,558	1,509	1,651	4,674

*SA - Single Axle
TA - Tandem Axle

Table 4.3. Estimated Traffic Volumes For Walker County Design

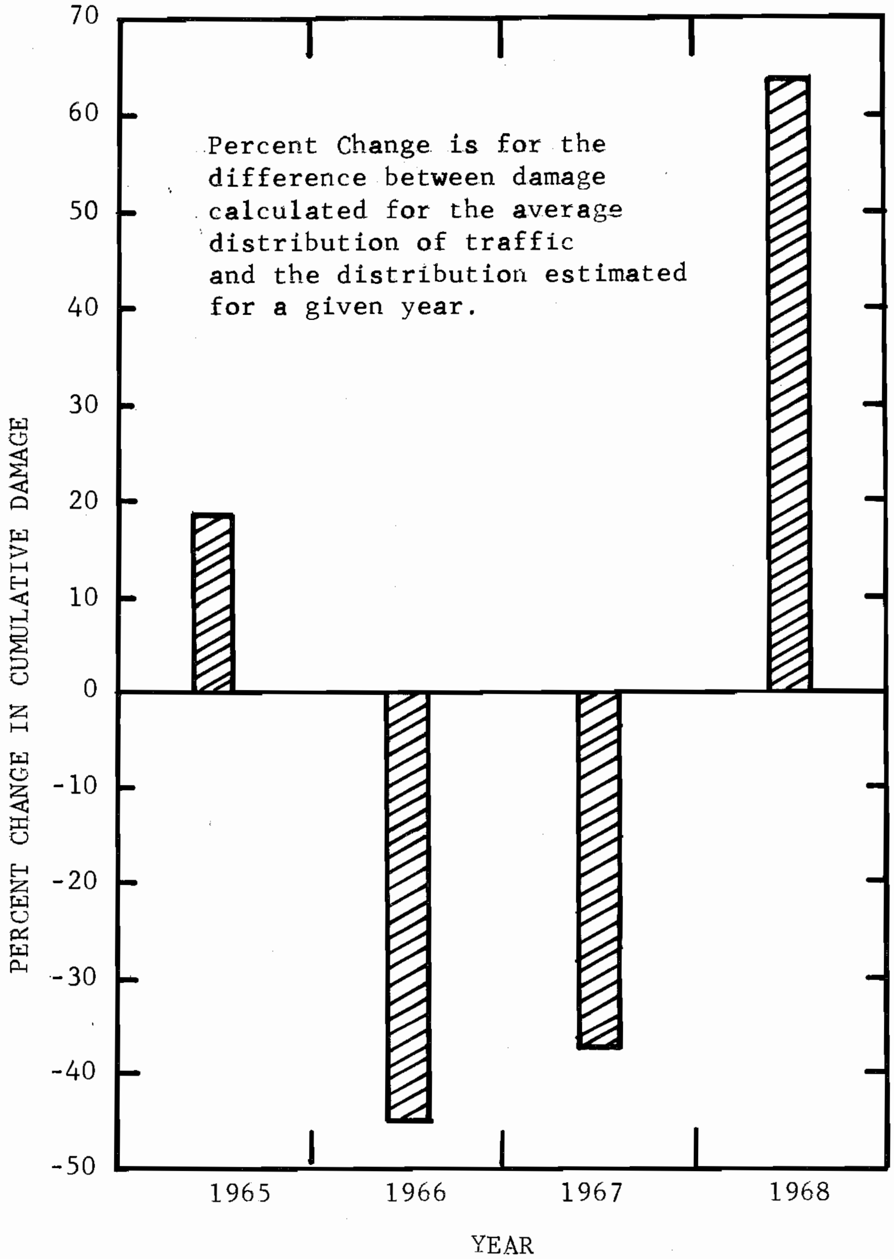

Fig 4.17. Percent Change in Cumulative Damage for the Four Estimates of Traffic Distributions given in Table 4.3.

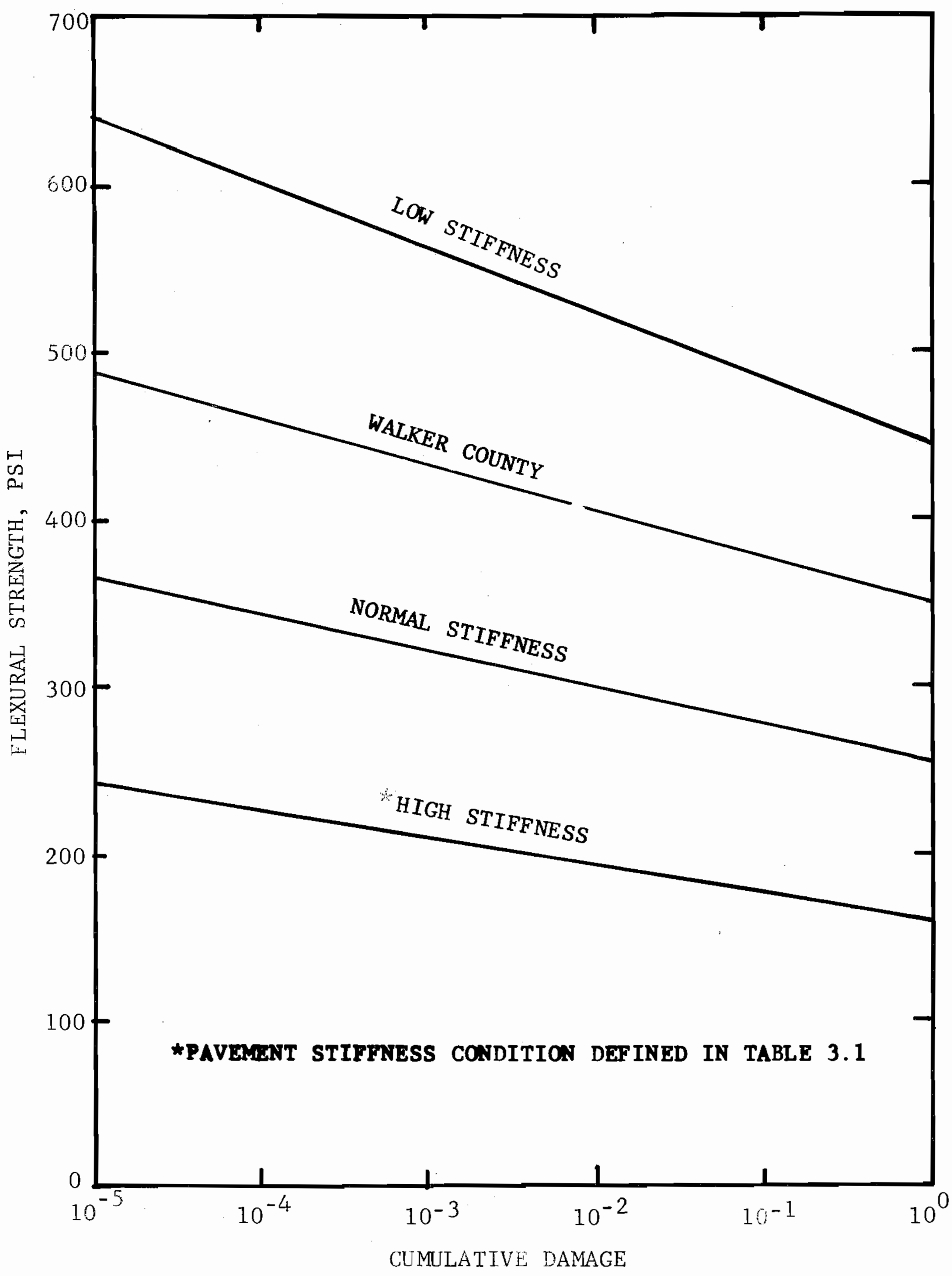

Fig 4.18. Flexural Strength versus Cumulative Damage

enon. To study the effect of changing the constant K, damage calculations were made varing K from 5 to 35. Figure 4.19 shows how the damage by each wheel load changes as the constant K is increased. Figure 4.19 gives the results of calculations made for the "Normal Stiffness" pavement only. Very similar results were obtained for each of the other three stiffness pavements defined in Table 3.1. For the past ten years, a number of states have been using the "18 Kip equivalent load" developed at the AASHO Road Test (Ref 1) for a measure of damage or fatigue to the pavement. Using the same distribution of traffic, the 18 Kip equivalent loads were calculated and percent of damage calculated for each wheel load was obtained. The cumulative effect of these wheel loads is superimposed on Figure 4.19 and labled "AASHO". The significance of these figures will be discussed in Chapter 5.

Subsystems For Overlaid Pavement.

This subsystem will be discussed in two parts, (1) the various variables affecting tangential stress in the concrete will be studied and (2) the variables affecting the final answer of the total system "Inches of Overlay", will be studied.

Tangential Stress in Concrete. First, the asphaltic concrete overlay thickness (D_o) and the elastic modulus of the overlay (E_o) were varied and tangential stress in the bottom of the concrete layer was calculated for the values shown in Table 3.3. Figures 4.20 and 4.21 show a graphical summary of the calculated tangential stress for the 10.7 Kip single and tandem axle-wheel loads, respectively. These graphs indicate that as the elastic modulus of the pavement overlay increases, thickness has less effect on tangential stress.

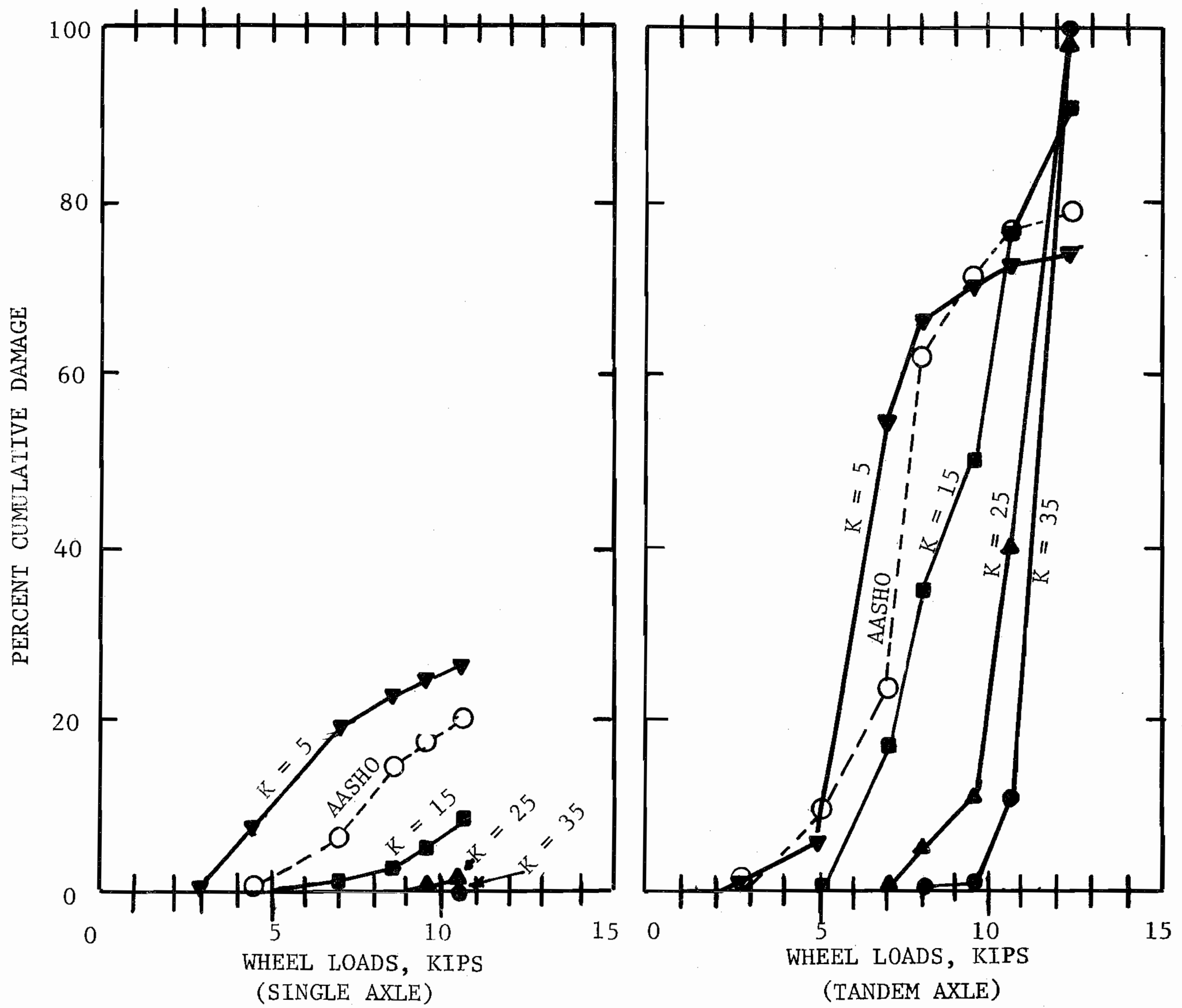

Fig 4.19. Cumulative Damage versus Wheel Load for Various Values of Slope in the Fatigue Equation

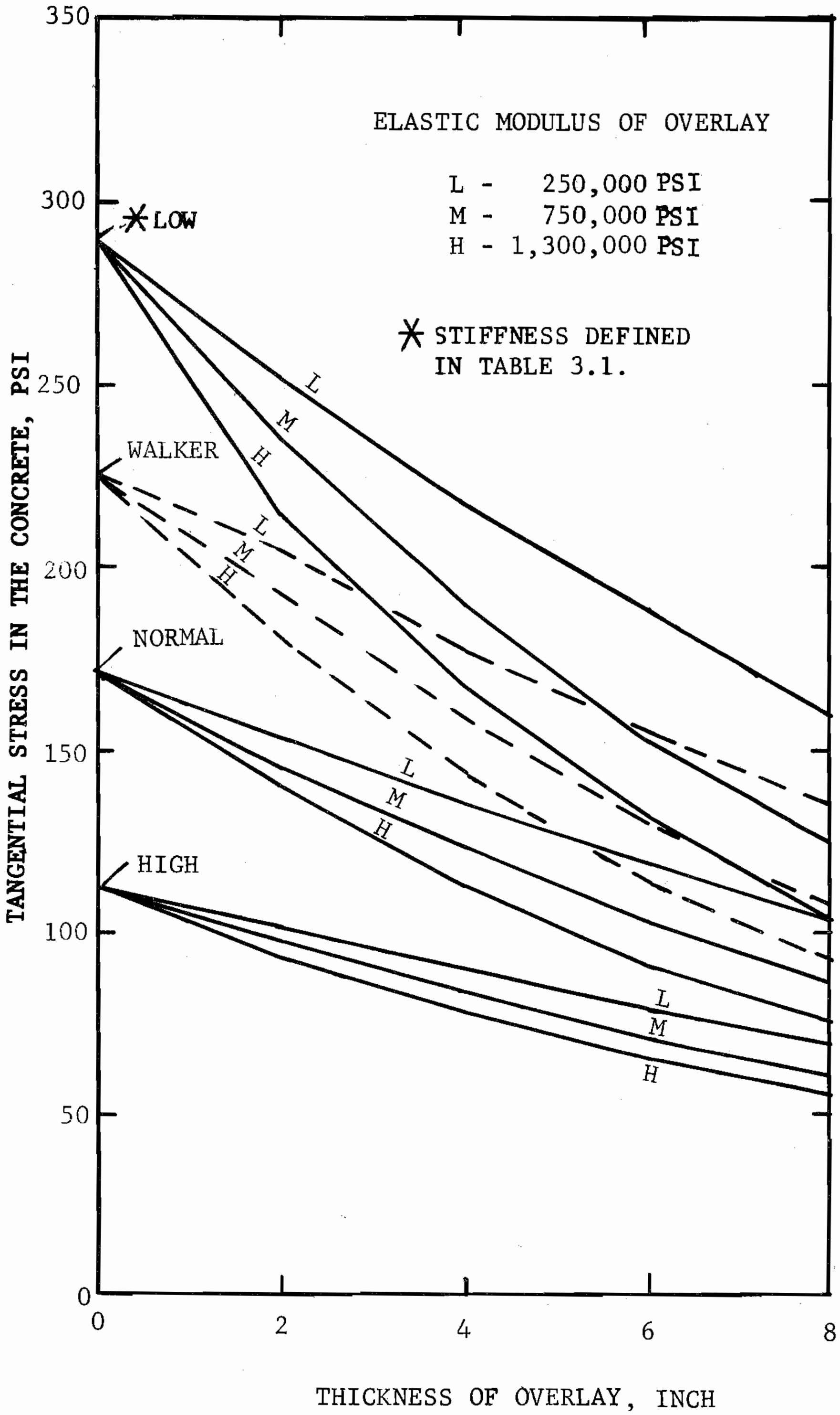

Fig 4.20. Tangential Stress versus Thickness of Overlay for Single Axle

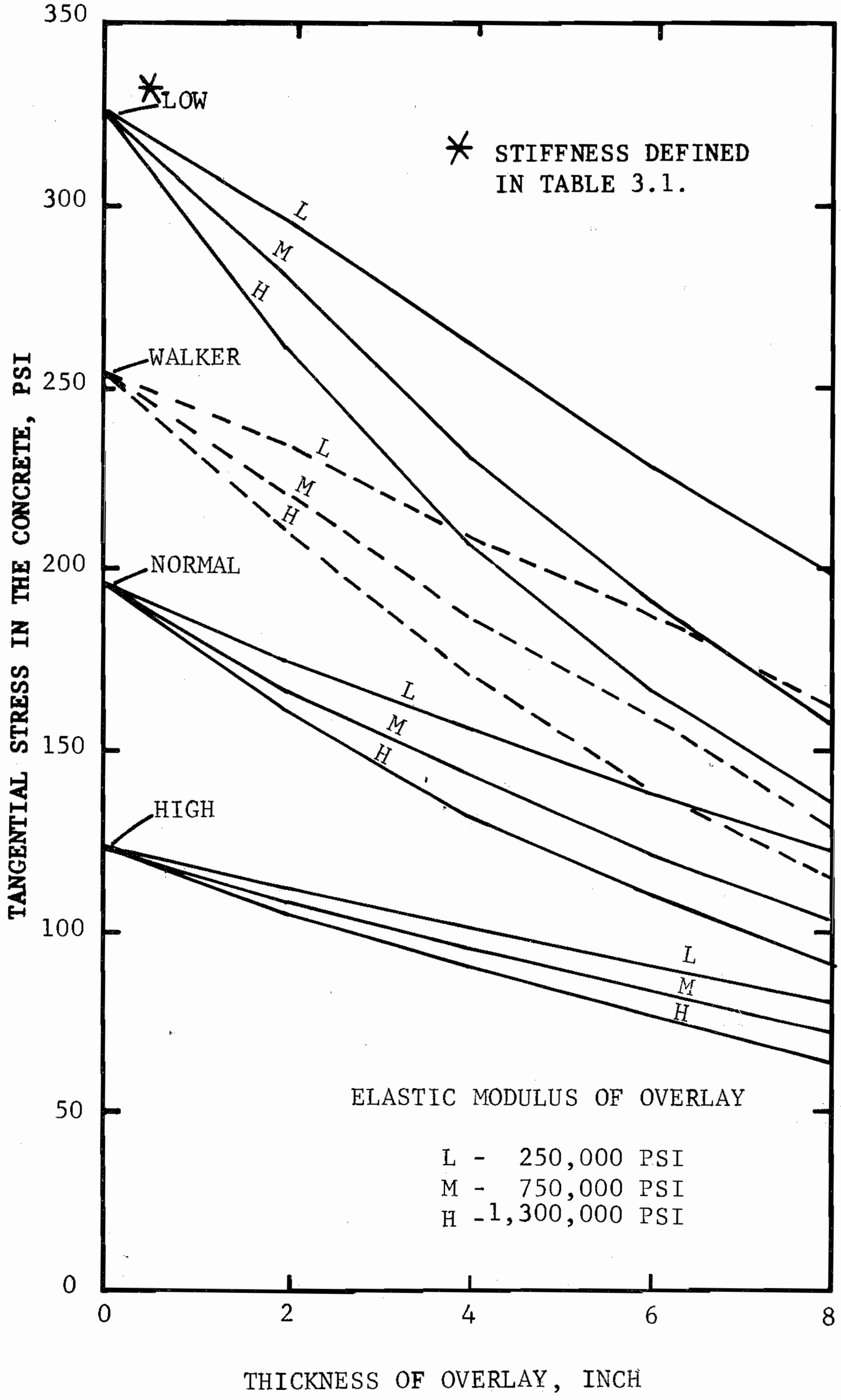

Fig 4.21. Tangential Stress versus Thickness of Overlay for Tandem Axle

Second, the variables for the existing pavement, previously shown in Table 3.1, were varied one at a time from the lowest to the highest stiffness condition. This was done only for the 4 inch overlay on the "Walker County" and "Normal Stiffness" pavement conditions at an elastic modulus of 750,000 psi. A summary of the percent change in stress caused by individual variable changes is shown in Figures 4.22 and 4.23. It should be noted that these plots are similar to Figures 4.5, 4.6, 4.7, and 4.8.

The percent changes in tangential stress for unit change in the "Low and High Stiffness" pavements variables are not shown. These variables were deleted for the reasons listed below:

1. For the "Low Stiffness" pavement, the tangential stresses calculated are so high that cumulative damage calculated is much larger than 1.0. This fact makes unit changes in stress insignificant.
2. For the "High Stiffness" pavement, the tangential stresses calculated are so low that the cumulative damage calculated is insignificantly small.
3. The percent change for the calculations made for the "Normal Stiffness" and "Walker County" pavements were very similar to the calculations made on the non-overlaid pavement. This further justifies the claim that any more calculations would be repetitious of the calculations made previously.

<u>Thickness of Overlay</u>. Calculations were made to determine how pavement stiffness, past cumulative damage, future traffic, and the

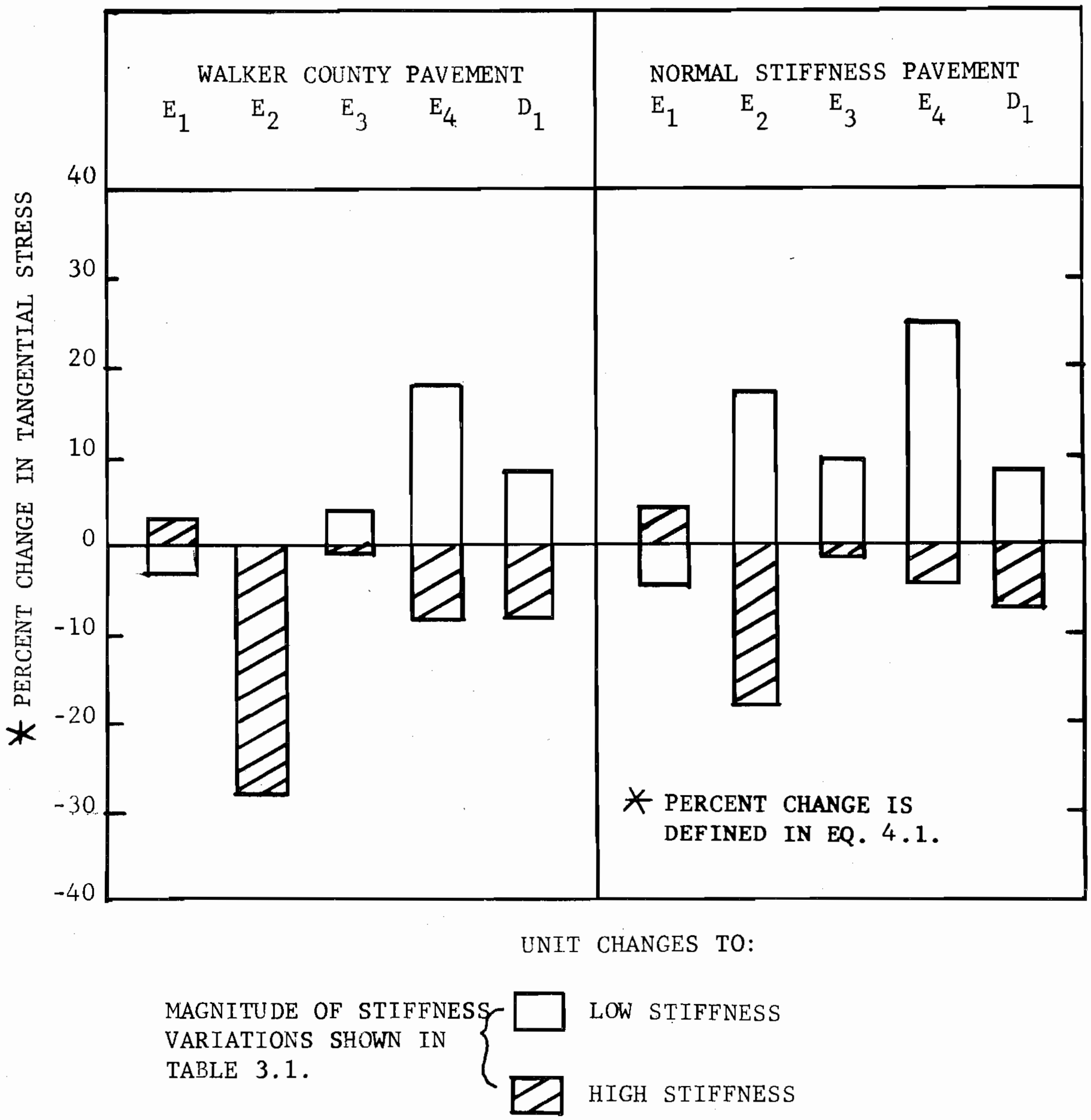

Fig 4.22. Summary of Percent Change in Tangential Stress for Overlaid Pavement (Single Axle)

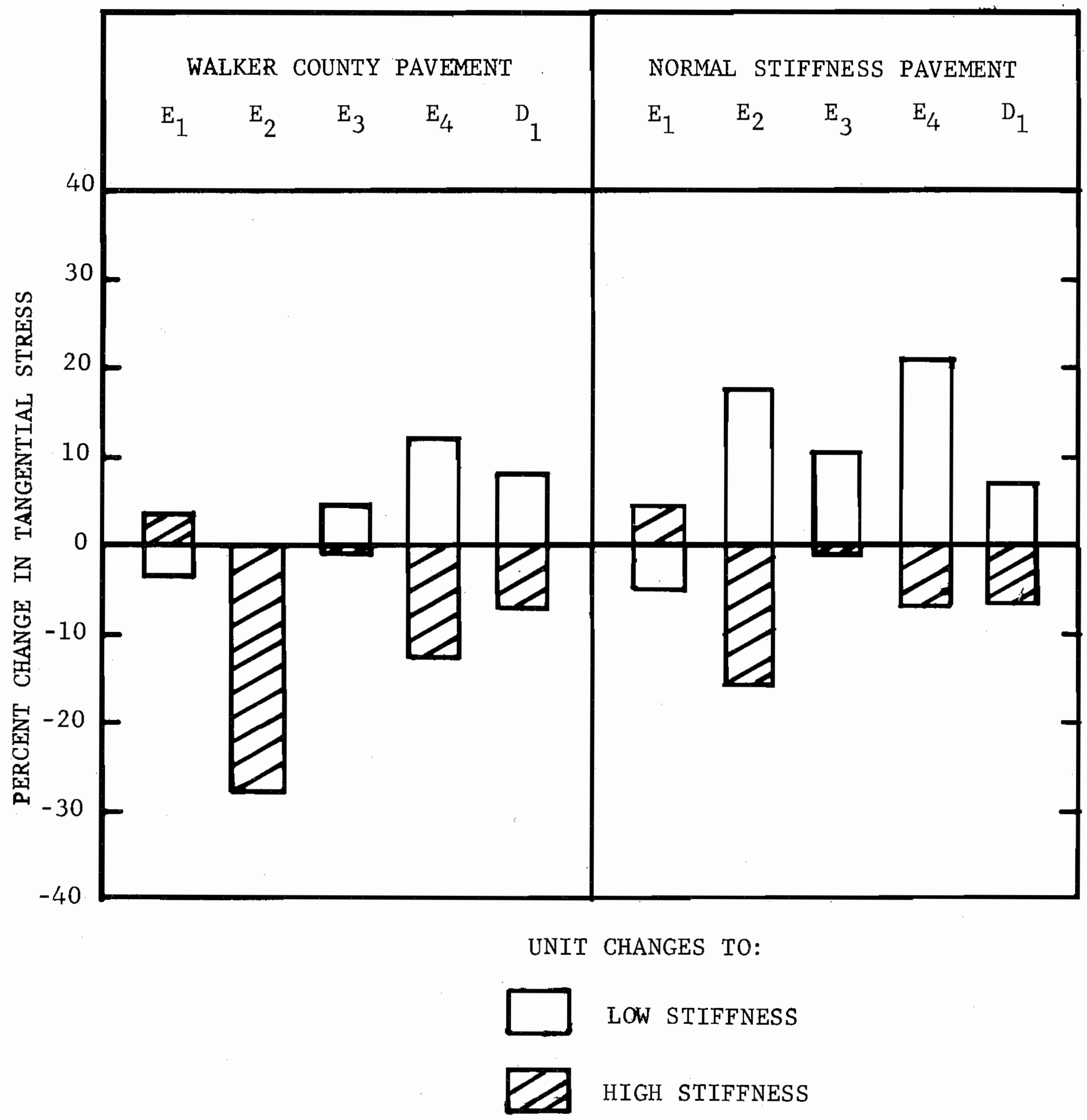

Fig 4.23. Summary of Percent Change in Tangential Stress for Overlaid Pavement (Tandem Axle)

elastic modulus of overlay thickness affected the calculated future damage to the pavement. Then, the future damage and each of the above variables were studied to see how they affected thickness of overlay. No study of the effect of traffic volumes and traffic distributions is made directly in this section. It was shown in Figure 4.19 that only the larger wheel loads effected the cumulative damage calculated. In fact, over 80% of the cumulative damage due to traffic is caused by the repetitions of the largest tandem axle wheel load. Taking this into consideration, the distribution of traffic can be said to be negligible, provided that the number of wheel load applications for the largest tandem axle group is known. Also, the damage calculated is proportional to traffic volume. For instance, if the traffic in consideration is three times the volume used in this study, the cumulative damage calculated would also be increased three times.

For each of the four pavement conditions, cumulative damage after overlay was calculated for various overlay thickness with the results of these calculations shown in Figures 4.24, 4.25, 4.26 and 4.27. Past cumulative damage, when added to future cumulative damage, must by definition be approximately 1.0. Using this knowledge, Figures 4.24 through 27 may be used to study the effect of cumulative damage for both before and after overlaying. For the above, computations were divided into four parts one for each of the asphalt concrete stiffness estimated for the different temperatures of the year. Traffic was assumed to be equal uniformly distributed year round for each stiffness.

Figure 4.28 shows cumulative damage calculations for the "Normal Stiffness" pavement with a design flexural strength of 320 psi.

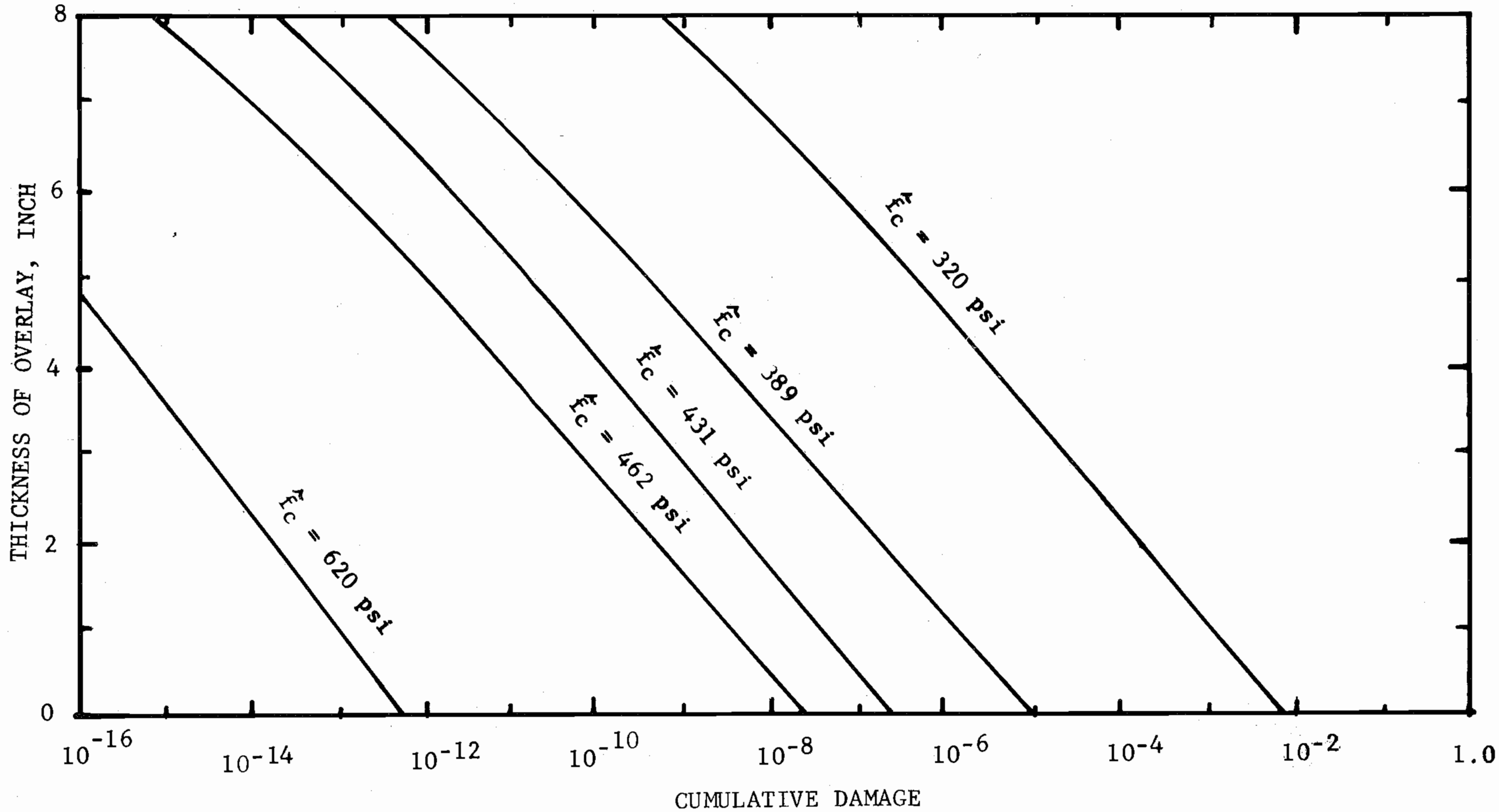

Fig 4.24. Overlay versus Damage for Normal Stiffness Pavement

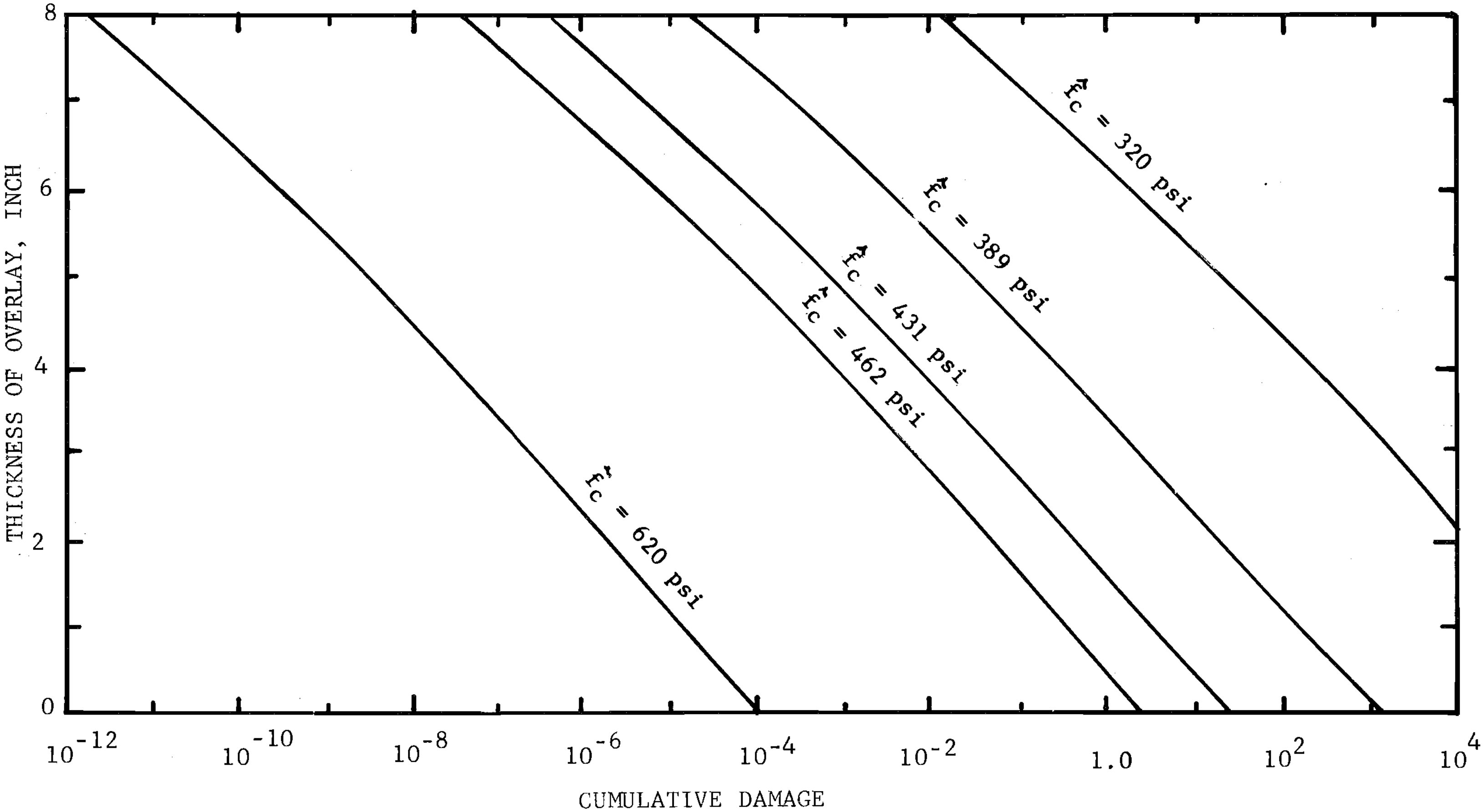

Fig 4.25. Overlay versus Damage for Low Stiffness Pavement

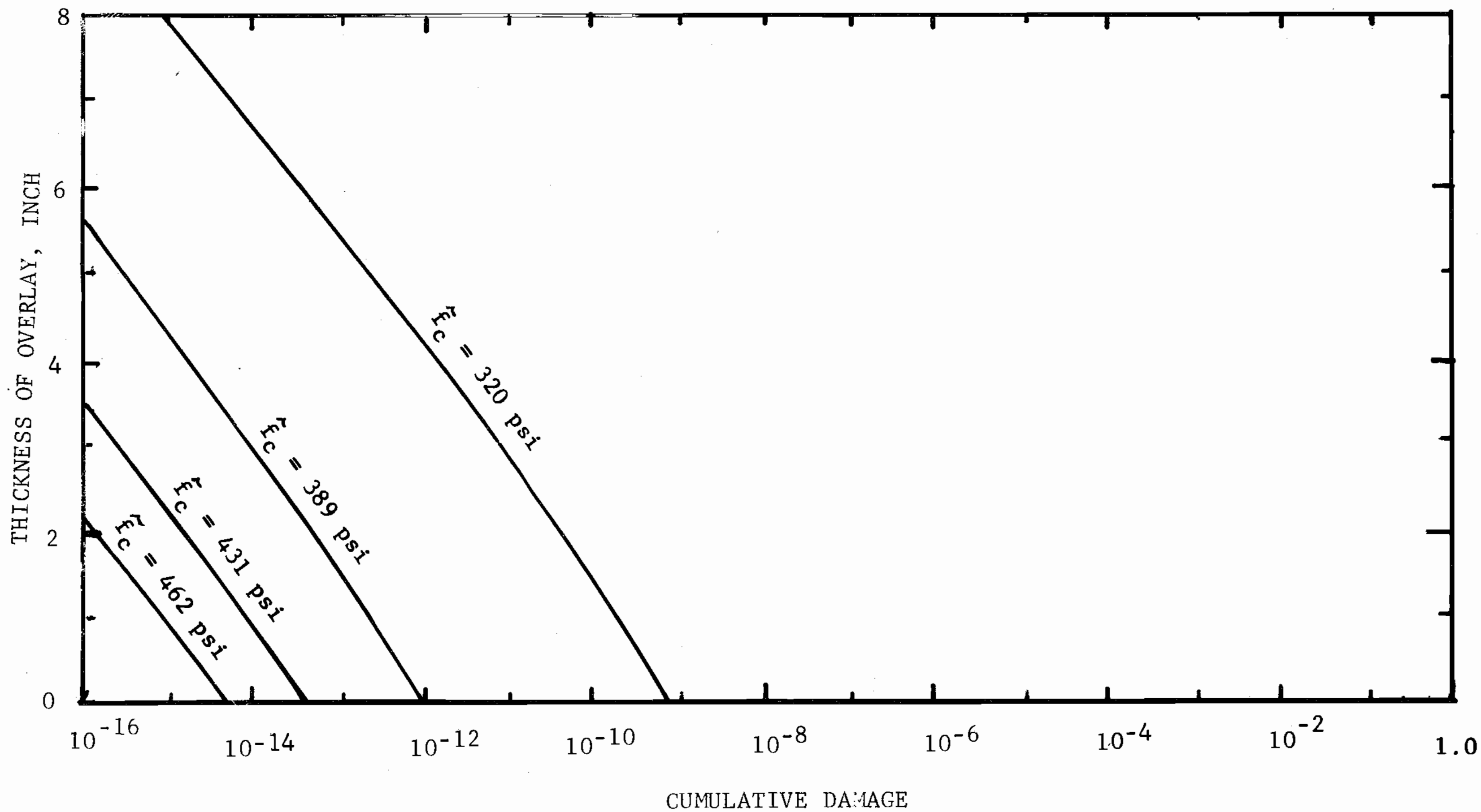

Fig 4.26. Overlay versus Damage for High Stiffness Pavement

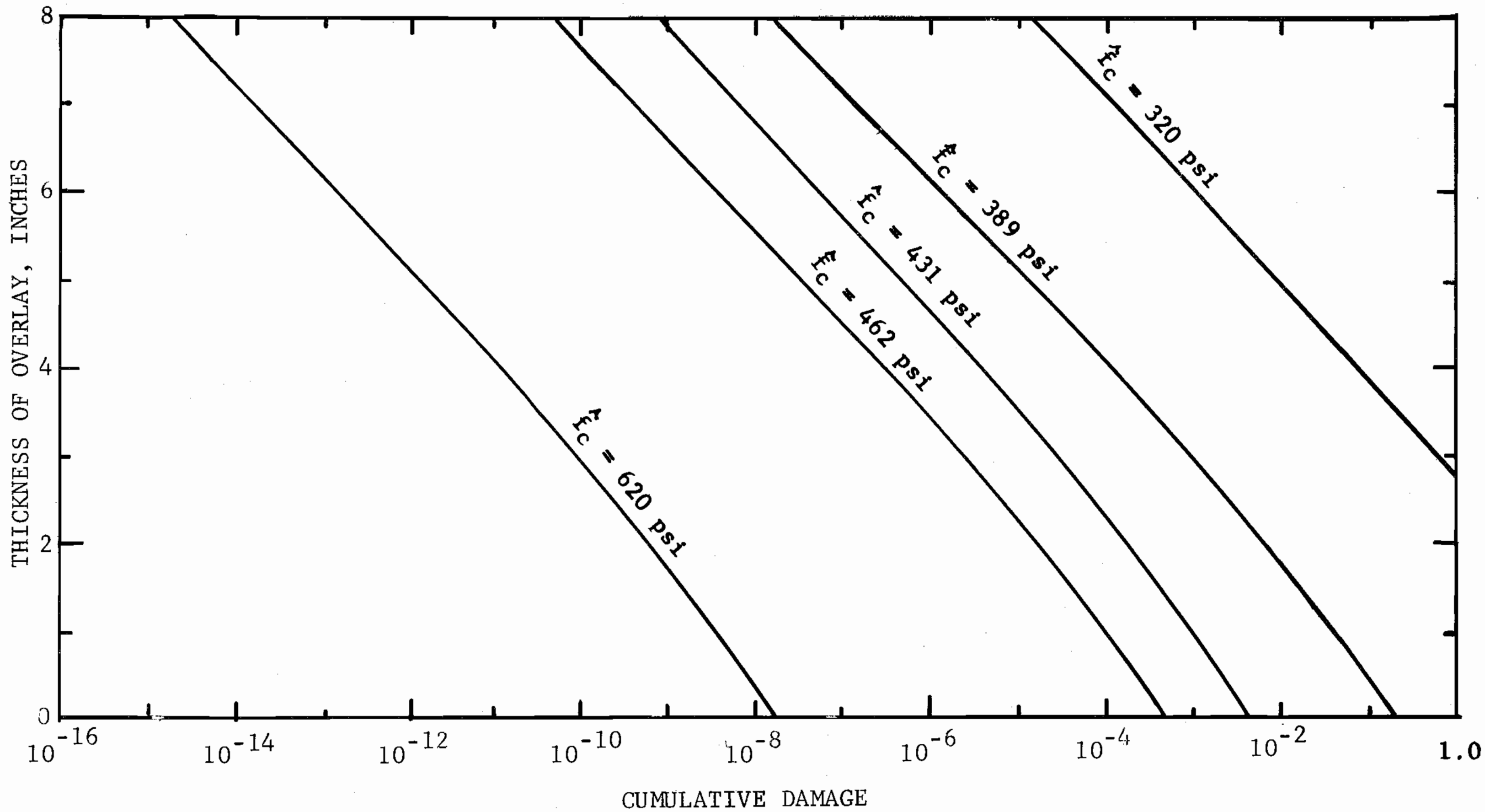

Fig 4.27. Overlay versus Damage for Walker County Pavement

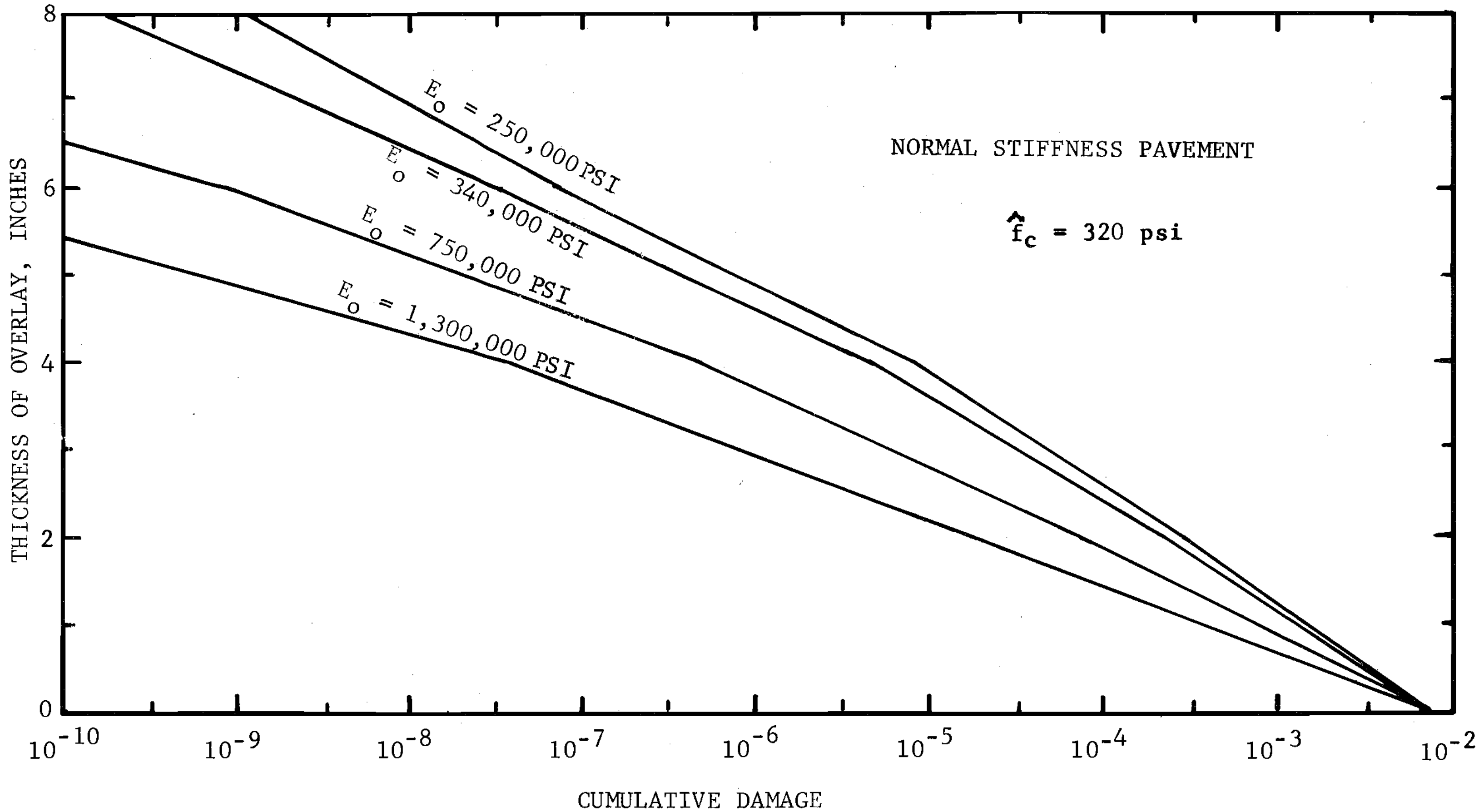

Fig 4.28. Overlay versus Damage for Normal Stiffness Pavement

Each line represent calculations made for cumulative damage assuming the elastic modulus is a constant year round. These plots are made to show the possible error involved if seasonal or temperature effects are not taken into consideration.

Summary.

In summary, this chapter presents the results of the sensitivity study in the form of a number of figures. For a few of these figures, certain approximations and judgements were made before presenting the figures in their final form. The approximations and judgements made will be listed as follows:

1. Tangential stress versus wheel load is approximated by a circular curve.

2. "Percentage Change" in tangential stress, as defined in Equation 4.1, remains relatively constant for all wheel loads. That is, relatively constant when compared to the "percent change" caused by the different input variations shown in Table 3.1. This allows a study of the variations caused by a unit variable change for one wheel load only.

3. The percent change created by a unit change in Poisson's Ratio for all layers, and the thicknesses of layers 2 and 3 are insignificant and are eliminated from further discussion.

CHAPTER 5. ANALYSIS OF RESULTS

The discussion in this chapter covers each subsystem in the order of occurrence as shown in Chapter 4. Due to the complexity of the system, the results of the computations are not analyzed statistically. Each variable and its effect on the subsystem in which it is used is discussed. The interaction between subsystems is indicated by showing how the output of a specific subsystem affects the output of another subsystem.

Subsystem for Existing Pavement.

Computations for the existing pavement structure are made in four subsystems as presented in Chapter 4. The effect of inputs on the first three systems will be discussed individually; then, as shown in Figure 3.1, the outputs from these three subsystems are studied in order to determine the effect on the fourth subsystem.

Tangential Stress in Concrete. In general, it was found that the modulus of elasticity had more effect on tangential stress than the other material properties. The one exception is the modulus of elasticity of the concrete (E_1), as illustrated in Figures 4.5 through 4.10. In viewing these figures, it must be remembered that a unit change in the elastic modulus of layer 1 (E_1) is relatively small compared to a unit change in the modulii of elasticity for the other layers. The unit change is made small because concrete is more homogeneous than the other pavement materials, thus making its modulus more constant. If a low modulus for concrete (light weight concrete) is used in a design, additional analysis to determine the effect of variation for the low modulus concrete would be necessary.

The modulus of the second layer (E_2) was found to have the most significant effect on tangential stress. The range of elastic modulus for layer 2 is 10,000 psi to 300,000 psi, which is the largest range used. Modulus values for layer 2 greater than 300,000 psi would be expected when stabilized materials are used. When this larger value is used, however, stresses calculated by the linear elastic design would be very small and would have little effect on this fatigue design system. It appears that if lab procedures can determine the modulus of layer 2 within an accuracy of one order of magnitude, the resulting error will be satisfactorly small.

The modulus of the third layer (E_3) was found to have less significant effect on tangential stress than the modulii of either layers 2 and 4. This is caused, in part, by the fact that the lower type base materials, or stabilized subgrades, usually used in this layer is further removed from the concrete than layer 2, which in turn causes the linear elastic theory to reduce its effect on the stress in the concrete.

The subgrade modulus (E_4) has a pronounced effect on tangential stress. The range of modulii values chosen covers the majority of subgrade materials which are encountered in highways today. Since the subgrade layer is the thickest layer and, in fact, in the LAYER program it is assumed to be semi-infinite, it has a strong effect on the tangential stress calculated anywhere in the pavement.

A unit change in the thickness of the layers had little or no effect on the tangential stress in the concrete. The thickness of the concrete (D_1) is varied from 7.0 to 8.0 inches which gives the largest change in stress for any of the changes in thickness. Although the unit change of ± ½ inch for an estimate of concrete thickness appears to be large, this change was not considered an unreasonable value. This is based on the fact that the data obtained in the Walker County project (Ref 15) had a variation of ± ½ inch for the effective thickness at the 90% confidence level. This unit change gave an error in tangential stress of approximately ± 10%.

The thickness of layers 2 and 3 had little effect on the tangential stress in the concrete even though varied, ± 2 inches. Considering that the thickness of these layers can usually be estimated or measured to the closest inch, it can be said that unit changes in estimating layer thicknesses are not significant. Although not computed in this analysis, the thickness of subgrade can affect stress calculations. This effect on stress is small as indicated by McCullough's work(Ref 15).

Poisson's ratio (μ) proved to have no significant effect on the computed tangential stress except in layer 1. The range from .12 to .20, however, covers the entire range in values for portland cement concrete pavements (Ref 26). For specific highway pavements having a high concrete modulus, it is believed that this input can be estimated closer than the unit changes selected for analysis. The maximum change in stress is only 4% for the unit changes in Poisson's Ratio of layer 1 as used in this study.

Modulus of Subgrade (E_4). The sensitivity of this input variable with respect to deflection was shown previously in graphical form in Figure 4.11. It can be seen in that E_4 is more sensitive to the smaller deflections. The most sensitive range of deflections is when the values of E_4 are determined to be between 10,000 and 20,000 psi. By referring to Figures 4.5 and 4.6 it can be seen that errors in E_4 between the values of 10,000 and 20,000 psi are not critical. For example, in Figure 4.5 the varying of E_4 from the "Normal Stiffness" value of 10,000 psi to the "High Stiffness" value of 20,000 psi created a percent change in tangential stress of only 4.4.

Flexural Strength from the Distress Survey. For the normal and high stiffness pavements, where the stresses calculated are low, this system assumes the cause of failure to be attributed to a weak flexural strength in the concrete. This phenomenon is illustrated by the standard error in flexural strength versus percent damage plots in Figure 4.14. When a pavement has a high percent damage and the computed stress condition is low, the standard error for flexural strength is found to be unreasonably high; i.e., the "Normal Stiffness" pavement is found to have 10% failures which indicates a standard error of 308 psi. If lab testing of the concrete proved this to be far from true, then an adjustment would have to be made in the system. One adjustment could be made by modifying the tangential stresses in the concrete for edge or corner load effects.

Cumulative Damage. This section is divided into four parts with each part discussing how cumulative damage is affected by (1) tangential stress in concrete, (2) traffic, (3) flexural strength and (4) constant - K.

Tangential stress in Concrete ($\overline{TS}$).- The cumulative damage, as can be seen in Figure 4.15 and 4.16, indicates that a change in the tangential stress of 50 psi will change the damage calculated from 0.001 to 1.0 for any of the design curves shown. If a design problem has tangential stress in the range of 200 to 300 psi, and error of 13% to 25% in stress would cause errors in cumulative damage in the neighberhood of 100 times the damage calculated using the true value for tangential stress.

Traffic.- If the distribution of traffic remains constant, the cumulative damage is directly proportional to traffic volumes. Figure 4.17 illustrated that cumulative damage can vary up to 60% by holding traffic volumes constant and varying traffic distribution estimates for the four traffic counts (Table 4.3) taken one year apart on the same highway. Studies by Heathington and Tutt (Ref 10) show that the estimated percentages of trucks for the larger axle weights have coefficients of variation ranging from 250% to 1000%. This error in estimating would cause cumulative damage to be in error 2.5 to 10.0 times the damage that would be calculated using the actual or true traffic.

Flexural Strength (f_c).- For each of the stress conditions shown in Figure 4.18, a change in flexural strength of 50 psi will cause a change in cumulative damage values from 0.001 to 1.0. When the design flexural strength is greater than 325 psi, no significant damage will be calculated if the pavement's stress condition is as low as calculated for "Normal Stiffness" pavement. Usually, we would expect the design flexural strength to be much larger than 325 psi. The flexural strength is specified to be approximately 600 psi and the standard error of flexural strength is usually in the range of 45 psi to 82 psi (Ref 14). The Walker County value of 162 psi was uncommonly high.

Constant-K.-The value for the constant K used in ghe general analysis was 34.25. It can be seen in Figure 4.19 that only the larger tandem axle wheel loads had any effect on damage. Even for a constant K of the 25, it was found that 99% of the damage was created by the four large tandem axle wheel loads. The above is in contrast to the AASHO Road Test equation which for the same traffic would have predicted only 75% of the damage to have been created by all the tandem axles. From Figure 4.19 it can be seen that an equivalent constant K for the AASHO Road Test equation would be between 5 and 15. The large difference between this value and the K value of 34.25 used in this analysis should be studied in the lab and the field to determine the true K value. Because of the great sensitivity of the system to K, its magnitude must be accurately determined before the system's answers can be used with confidence.

Subsystems for Overlaid Pavement.

This subsystem is discussed in three sections, with the first section covering the variables effecting tangential stress, the second section discussing the variables directly affecting the depth of the overlay, and the third section covering the effect of future traffic.

Tangential Stress on Concrete (TS). As previously shown in Figure 4.20 and 4.21, the thickness and elastic modulus are both effective in reducing tangential stress. For existing concrete pavements, where the initial stress condition is low, these two variables have the least significant effect on tangential stress. This is particularly evident in the calculations for stress made on the "Normal and High

Stiffness" pavements. In practice, it would be a rare condition when a highway pavement with tangential stress as low as 200 psi for 42.8 Kip axle weight would need overlaying for the reason of reducing stress.

The percent changes in tangential stress caused by unit changes in the variables describing the existing (see Table 3.1) pavement are similar for both before and after overlaying. This is demonstrated by comparing Figures 4.22 and 4.23 with Figures 4.5 through 4.8. The actual size of the change in tangential stress for the overlaid pavement is approximately 20 percent smaller. This is true because all stresses have been reduced because of the 4 inch ACP overlay.

Thickness of Overlay. Figures 4.24 through 4.27 can be used directly or indirectly to study the effect of existing pavement conditions, past cumulative damage, and future traffic on the depth of ACP overlay.

Pavement Condition. Each of the four pavement conditions defined in Table 3.1, are represented in Figures 4.24 throuth 4.27. If we consider a damage of 0.1% as the smallest meaningful cumulative damage after overlay, then the "Low Stiffness" pavement is the only pavement which calculates meaningful damage values for what is usually considered to be a typical flexural pavement design strength. A typical design strength for a 99% confidence level would be in the range of 400 to 500 psi.

Past Cumulative Damage. For a design, the total cumulative damage for before and after overlaying should be 1.0. This means the 1.0 minus cumulative damage after overlay (RDo) should be equal to the past cumulative damage (RD). Using this principal, these plots can be used to study the effect of past damage on thickness of overlay.

Future Traffic. Figures 4.24 through 4.27 were calculated for the same traffic distribution and volume. In the previous analysis of the constant K, the first part of this chapter indicated that approximately 80% damage due to traffic is caused by the repetitions of the largest tandem axle wheel load. Taking this into consideration, the distribution of traffic can be considered negligible, provided that the number of wheel loads for the largest axle group is known. The damage calculated is proportional to the traffic volume. For instance, if the traffic in consideration for a pavement condition is three times the volume used in the study, then the damage would be three times the amount read from Figures 4.24 through 4.27. For example, using the normal pavement condition, a design flexural strength of 320 psi and an overlay thickness of 2 inches indicates that the damage read from Figure 4.24 is approximately 0.00013. For a traffic three times the size used, the damage would be 0.00039.

Summary.

The following comments summarize the findings in the calculations made on the subsystems for existing pavement:

1. Table 5.1 gives the relative effect of the input elastic properties and layer thicknesses on tangential stress calculated for the concrete layer. This relative rating is based on the summaries of "percent change in tangential stress of the concrete" presented in Chapter 4 and discussed in this chapter. In general, the first two variables (E_2 and E_4) are the most sensitive and the designer should exsert most of the effort of data collection for this subsystem on these

Order of Effect	Input Variable	Range of Variables Input	Comments
1.	E_2	10,000 to 3000,000 psi	Large change in stress for a large range of input variables.
2.	E_4	4,100 to 20,000 psi	Large change in stress caused by a large input variation and assumption of infinite thickness of the layer.
3.	E_3	10,000 to 100,000 psi	Smaller change in stress because of smaller variation and it has less effect than E_2 because it is further removed from concrete.
4.	D_1	7 to 8 inches	Large range for ability to measure this input.
5.	E_1	4,500,000 to 5,500,000 psi	Small changes in tangential stress for variation of input.
6 & 7	D_2 & D_3	4 to 8 inches	Small change in stress for large input variation.
8.	μ_1	.12 to .20	Small change in stress for large input variation input.
9, 10, & 11	μ_2, μ_3, & μ_4	.35 to .50	No significant change in stress for large input variation

Table 5.1. Relative Effect of Input Variable on Tangential Stress in Concrete.

two variables. The next three variables (E_3, D_1, and E_1) have less effect than the first two and, in general, less time is needed to develop inputs for these variables. The last five variables (D_2, D_3, μ_1, μ_2, μ_3, and μ_4) had little effect on tangential stress which means the accuracy of approximating them is even less critical. If measurements of the last five variables are not available an Engineering guess is sufficient, provided the values are known to be within the range of the variables used in this sensitivity study.

2. For any stiffness pavement, where the tangential stresses are calculated to be low, this design system will attribute failure to be caused by a weak flexural strength in the concrete.

3. A small error in tangential stress in the concrete will cause a large error in the calculated cumulative damage.

4. Using present techniques for estimating the number of larger tandem axle wheel loads can cause errors in calculating cumulative damage by a multiple of 2.5 to 10.0.

5. A small error in the flexural strength of the concrete will cause large errors in the calculation of cumulative damage.

6. Because of the large value for the constant K used in the fatigue equation, 34.25, only the larger tandem axle wheel loads have any effect on the cumulative damage calculations.

The following comments summarize the findings in the calculations made on the subsystems for overlaid pavements:

1. Tangential stress in the concrete can be lowered by reducing the thickness or the elastic modulus of the overlay.

2. The effect of the input elastic properties and layer thick-

nesses of the exesting pavement or tangential stress is approximately the same for both before and after overlay. Table 5.1 is still applicable for these variables in the after overlay conditions.

3. The pavement stiffness condition has a pronounced affect on the design overlay thickness. This is attributed to the affect of stiffness on the calculated tangential stress.

4. An error in past cumulative damage in the order of ten will cause a 1 inch error in the thickness of overlay.

5. The same error in the volume of traffic also causes a 1 inch error in the thickness of overlay.

CHAPTER 6. REVISED SYSTEM

This chapter describes changes made in the design system in developing this sensitivity study and suggests changes in the system that could be made to reduce the man hours of work required and to help eliminate computation errors. Additionally, a method is suggested for using the deflection basin measured by the Dynaflect to characterize the material properties.

Use of Dynaflect.

One advantage of the system, as now used, is that a majority of the non-destructive deflection measuring instruments can be used. These instruments include the Benkelman Beam and the California Reflectometer which are described in reference 15. If the Dynaflect is used, the system can be revised to obtain more information from the measured deflection basin. These basins are relatively easy to measure with the Dynaflect, whereas most of the other instruments would require considerably more work. The deflection basin measured provided an additional tool to the user of the system for determining the elastic constant of the existing pavement. Appendix B illustrates one attempt to match calculated deflection basins with actual measured basins. The basins were computed using the LAYER program previously discussed in Chapter 3.

From the linear elastic theory, it can be shown that tangential stress is a function of the bending or curvature of a rigid slab and the elastic properties and depth of the slab. It can be said that if the correct value of the elastic properties, the thickness of layer 1 and the correct curvature of the slab is used, then the correct tangential stress can be predicted by the linear elastic theory. Thus, in effect, tangential stress is not only a function of the different elastic and physical components of the subbase and subgrade but also may be a function of the combined effect of these components on curvature. This leads to the possibility of the modeling of the existing pavement structure as only two layers and solving for elastic properites by trial and error using the LAYER program.

Modeling the problem as a two-layer pavement is not considered within this study. It is believed to have possibilities for future use in this system to reduce computer time and to cut down on lab work in determining elastic constants.

Revised Computer Programs.

In general, the revision of programs to improve the working of the system is considered beyond the limits of this study. In the process of conducting the study, however, it was found that certain changes to programs within the system were necessary in order to conduct an efficient sensitivity study. These changes consist of (1) approximating tangential stress, (2) printing out cumulative damage for each wheel load and (3) the ability to input standard error of fatigue in terms of standard error of flexural strength. Most of these changes have been discussed before or referred to in discussions in the Appendices. These changes were written to minimize the change in the calculated values from the original system and to save on computer time and computer coding. The following sections will summarize the changes made.

LAYER Program. Even though this program was not changed, a number of computer runs were eliminated. Instead of using this program to calculate tangential stresses in the concrete for 13 different axle weights, tangential stresses were calculated for two wheel loads for both the single and tandem axles. Another program was then written to approximate the remaining wheel loads assuming a circular distribution. This program and its approximating technique and credibility is discussed in detail in Appendix A.

POTS Program. This program was revised to include the approximations discussed above concerning tangential stress. POTS was additionally revised to print out cumulative damage for each individual wheel load. The ability to input standard error in terms of flexural strength was added. The old program previously had standard error input in terms of the error in predicting the number of repetitions to failure. This old process necessitated a tedious hand calculation when standard error of flexural strength is input. The original program had the advantage of handling data taken directly from fatigue tests.

Desired Revisions to System.

In the study of this system, it became apparent that a number of features of the system could be revised to save time in using the system and to reduce the possibility of error in calculations. Most of these changes can be justified on a time saving basis, only if the system will be used frequently. This section will direct its discussion to these types of revisions.

PROFILE ANALYSIS Program. The choosing of design sections for both subgrade and pavement failures is now a decision made by the designer based on judgement. This program is used to verify or reject the designer's choice based on a statistical technique, "Analysis of

Variance". It would be desirable to have a computer program to choose design sections based on sound statistical basis rather than on the designer's judgement alone. This could be accomplished by modifying the PROFILE ANALYSIS program to choose the design section, possibly using analysis of variance, similar to that now used. In addition, a graphic output that would contain input data as well as the design sections chosen would be desirable.

Adjust Damage to Agree with Distress. For each design section, a tedious procedure is necessary to compute the adjusted standard error of flexural strength. The procedure now used is to compute cumulative damage by varying the standard error of flexural strength. A graphic plot is used to interpret for a damage of 1.0.

Once the standard error has been determined, it becomes necessary to calculate the remaining life for the pavement; i.e., the percentage of the pavement which has not failed. This is accomplished for a desired confidence level specified by the Engineer. For the present system, numerous computer runs are necessary to establish design charts to solve for this remaining life value. It would be advantageous to the system to develop a single program to accomplish this task.

Computations for Overlaid Pavement. The system now used is shown in Figure 2.2 and discussed in Chapter 2. If this procedure is to be used a number of times, it would be worth developing a composite computer program to compute the desired answer, "Thickness of Overlay", in one program run.

Computations for Tangential Stress after Overlaying. Figure 6.1 verifies that the plot of tangential stress before overlay versus

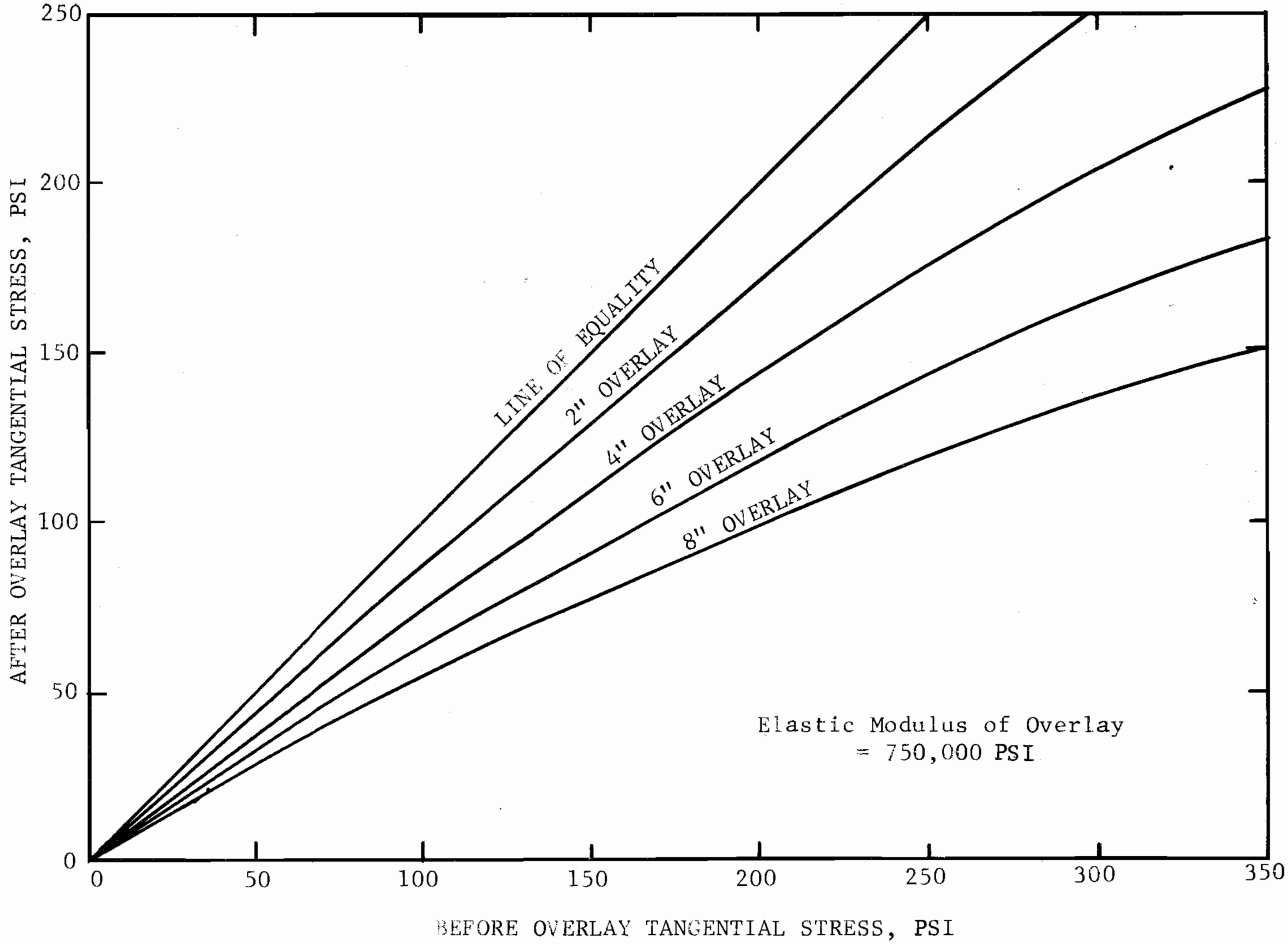

Fig 6.1. Tangential Stress Before and After Overlay

tangential stress after overlay will be a smooth curve for each thickness of overlay with an elastic modulus of 750,000 psi. The family of curves for different elastic modulii are similar to those shown. Based on these curves it is suggested that statistical regression analysis could be used to develop a regression equation that would estimate tangential stress after overlaying when given the following:

1. Tangential stress for desired wheel loads before overlaying.
2. Thickness of overlay.
3. Elastic modulus of overlay.

If the equation suggested above were developed and incorporated into a computer program, a number of costly computer runs on the LAYER program could be eliminated.

Summary.

This chapter describes changes made in the design system in developing this sensitivity study and suggests changes in the system that could be made to reduce the man hours of work required and to help eliminate computation errors. Additionally, a method is suggested for using the deflection basin measured by the Dynaflect to characterize the material properties of the pavement. The following comments are made to enumerate these changes and suggestions.

1. The deflection basin measured by the Dynaflect can be used to determine if the elastic properties of the concrete, subbase, and subgrade are correct. The properties are varied by trial and error until the deflections predicted by the LAYER program coincide with the measured deflections.

2. Tangential stress versus wheel load was approximated by the equation of a circle.

3. In this study, the POTS program was modified to print damage values for each wheel load.

4. For use in this study, the POTS program was modified to read-in standard error in terms of flexural strength. This may be useful in the working of the system when fatigue studies are not available.

5. A program to choose statistically different design sections based on a profile of measurement would be desirable.

6. A program to adjust the standard error of flexural strength to agree with measured pavement distress or failure could reduce man hours.

7. It would be advantagious to the system to have a program that would make all the necessary trial and error calculations to determine the thickness of overlay in the Subsystem "Computations on Overlaid Pavement" (see Fig 2.2).

8. A program could also be developed to replace the function of the LAYER program in the subsystem "Computation on Overlaid Pavement". This program could include a regression equation to predict tangential stress after overlaying.

CHAPTER 7. CONCLUSIONS AND RECOMMENDATIONS

This study was conducted to determine the sensitivity of the system with respect to its input variables, to give information to the designer as to which variables are important and where more time should be spent in developing inputs for the system. An additional goal was to recommend revisions to the system, where desireable, and to enumerate the advantages and disadvantages of using the system. It must be remembered that the conclusions reached in this study are limited to the range of variables considered in this analysis.

Conclusions.

1. The constant-K in the concrete fatigue equation is the most important input of the system. This constant is costly to determine, but is necessary before a confidence can be placed on the design system.

2. The design flexural strength of the concrete is the second most important variable. In order to account for its stochastic nature, it is input into the system in three parts. The flexural strength and its standard error are used along with the designer's choice of confidence levels to determine the design flexural strength. The confidence level chosen has a very strong effect on this variable. This makes the choice of the confidence level the most important decision the designer makes in using the system.

3. Tangential stress in the concrete is the third most important variable used in the system. Although it is not an independent variable input directly into the system, it is established by defining the pavement structure and the wheel loads. Each of the variables

defining the structure, such as elastic properties, layer thickness, and the estimated wheel loads, has varying effects as previously discussed in Chapter 5.

4. The distributions and volumes of traffic are the fourth most important class of variables used in the system. It is important to the system to accurately estimate the number of large tandem axle wheel load repetitions. The system, as now used for all four pavement stiffnesses described in Table 3.1, calculated that more than 95% of the cumulative damage was caused by the three largest wheel load groups.

Recommendations

1. For this system, further investigation is necessary to determine the characteristics of the fatigue curve and flexural strength of the concrete. For determining standard error of flexural strength, more consideration should be given to developing a pavement distress survey because of the sensitivity of the standard error of flexural strength to the distress measurement.

2. Methods of predicting the number and weight of the larger axle loads should be studied. Consideration of additional traffic counts should be made if presents techniques are not adequate. One method for surveying traffic that could be studied is the "Portable Scale for Weighing Vehicles in Motion", developed at the University of Texas at Austin (Ref 23).

3. If the Dynaflect is available for making deflection measurements, the designer should make use of the deflection basins measured. One example could be a trial and error fit of the basins as discussed in Appendix B.

4. In the modeling of the pavement structure and the load conditions, no account is given to edge loadings, possible voids in the subbase, or cracks in the concrete. It is recommended that the modeling of these features be studied, and the system's model be revised according to the present best state-of-the-art. An application to this problem may be the SLAB program (Ref 11) developed at The University of Texas at Austin.

5. Considering the vast variations in deflections that actually occur within ever design project, it is believed that the present deflection measuring instruments are adequate to meet the needs of the design system. A study should be undertaken to determine how to best account for variations that occur in deflection. For the present, a good rule of thumb is to take deflection measurements at linear intervals down the roadway as often as the designer would be willing to change the design of the overlay.

6. If this system is used frequently, consideration should be given as suggested in Chapter 6 to revising the computer programs to make the "System" more efficient to use.

7. Each designer, when first using this system, will probably have input variables which do not fit within the range of variables used in this study. When this is the case, the designer should run a small sensitivity study of the variables in question. Once this type investigation is done for a design problem, a much better confidence in the system's answer will be obtained.

Weak versus Strong Points of The Overlay Design System.

The overlay design system studied is based on sound fundamentals. The system uses the best state-of-the-art measuring techniques to determine the load carrying capacity of the existing pavement; and then, these measurements are used directly in the design procedure.

A weak point of the system is that a flat slope in the fatigue curve (Equation 2.2) causes the design overlay thickness to be very sensitive to the following variables: flexural strength, tangential stress in concrete, distribution of wheel loads, and the confidence level chosen. Considering the possible variation of each of these variables, a strong confidence cannot be placed on the thickness chosen for any individual design section.

A strong point of the system is that design projects can be divided into pavement sections of significantly different load carrying capacities. The relative difference in the thickness of the overlay is established with sound procedures. Because of the economical fact that most overlay design projects are financed with limited funds, this design procedure is useful in determining where the most money or thickest overlay should be placed within the design project in question.

APPENDIX A

USING A CURVE TO APPROXIMATE TANGENTIAL STRESS LEADING TO THE CALCULATION OF CUMULATIVE DAMAGE

Note: If a sufficient number of readers should so request, a manual will be made available for adaptation to the solution of specific problems.

APPENDIX A. USING A CURVE TO APPROXIMATE TANGENTIAL STRESS LEADING TO THE CALCULATION OF CUMULATIVE DAMAGE

Introduction.

In this appendix, an analysis of how and why a circle was chosen to approximate tangential stress and how this applies to the calculation of resultant damage will be shown. In the design system, the "LAYER" Program was used to compute tangential stress at the bottom of the concrete pavement. These stresses were then used in the "POTS" Program to calculate resultant damage for all wheel loads applied to the pavement. Neither the theory nor the derivation of the calculations within these programs are explained in this presentation.

Problem.

The coding and computer time necessary to calculate tangential stress and cumulative damage at thirteen different wheel load groups as previously used in this design system, using the POTS Program and the LAYER Program, is very time consuming and expensive. For use in this sensitivity study, a computer program was sought to estimate tangential stress for each of the individual wheel load groups, provided that the stress for two of these groups was known. Also, for use in the study it was desirable to calculate, at the same time, cumulative damage for each wheel load group at different confidence levels. The program developed to solve this problem was written to calculate tangential stress for thirteen individual wheel loads (i.e., six single axle wheel loads and seven tandem axle wheel loads) and the calculation of cumulative damage due to these individual wheel load applications at five confidence levels (i.e., 50%, 85%, 90%, 95%, 99%). One must realize, however, that this program can be modified to calculate tangential stress for any wheel load and resultant damage due to these wheel loads at any confidence level. The development of the program is explained later in this presentation.

Assumptions.

It is known that the heavier wheel loads cause the most stress, resulting in the largest damage. Based on previous work done by McCullough (Ref 15) and data from the AASHO Road Test (Ref 22), a constant contact pressure of 70 psi was used in calculating resultant damage for all wheel loads. While this is a conservative estimate for the smaller wheel loads, it is approximately equal to the measured contact pressure for the heavier wheel loads. The program is not limited to using only 70 psi but the contact pressure used must be constant for all wheel loads, or the curve approximated will be in error. It may be noted that in this study, wheel loads are assumed to have an upper limit of 10.7 Kip for single axle groups and 12.5 Kip for tandem axle groups. The program written for this special use does not have the ability to analyze seasonal effects of temperature on the stiffness of asphaltic concrete pavement. With minimum programming, the seasonal effect could be incorporated into this program or the POTS program could be modified to include a tangential stress approximating curve. Another limitation in using the approximate calculation for tangential stress is that all tandem axles are assumed to be the same distance apart. This assumption is necessary to apply the principle of superposition for calculating stress due to the combined effect of both axles.

Development Of The Program.

Two attempts were made to fit the equation of a function to the graph of the tangential stresses in question before an accurate approximation was found that would generate the desired stresses.

Figure A.1 indicates that tangential stress is directly proportional to wheel load magnitude. The curve for tangential stress shown here is for the pavement condition described in Chapter 2.

Straight Line Interpolation Method.

The equation for a straight line can be defined as

$$y_i = mx_i + b_i \quad \ldots\ldots\ldots\ldots \text{A.1}$$

Where:

m = the slope of the line.

b_i = the y intercept of the line.

To solve for the y-intercept, the straight line was forced through the known points P_1, P_2. P_1 and P_2 correspond to the known tangential stresses for the 4.5 Kip wheel load and the 10.7 Kip wheel load, respectively. Referring to the y-intercept, equation A.1 becomes

$$y_i = X_i M + (y_i - mx_1) \ldots\ldots\ldots\ldots \text{A.2}$$

The slope m, can be defined as

$$m = \frac{X_2 - X_1}{Y_2 - Y_1} \quad \ldots\ldots\ldots\ldots \text{A.3}$$

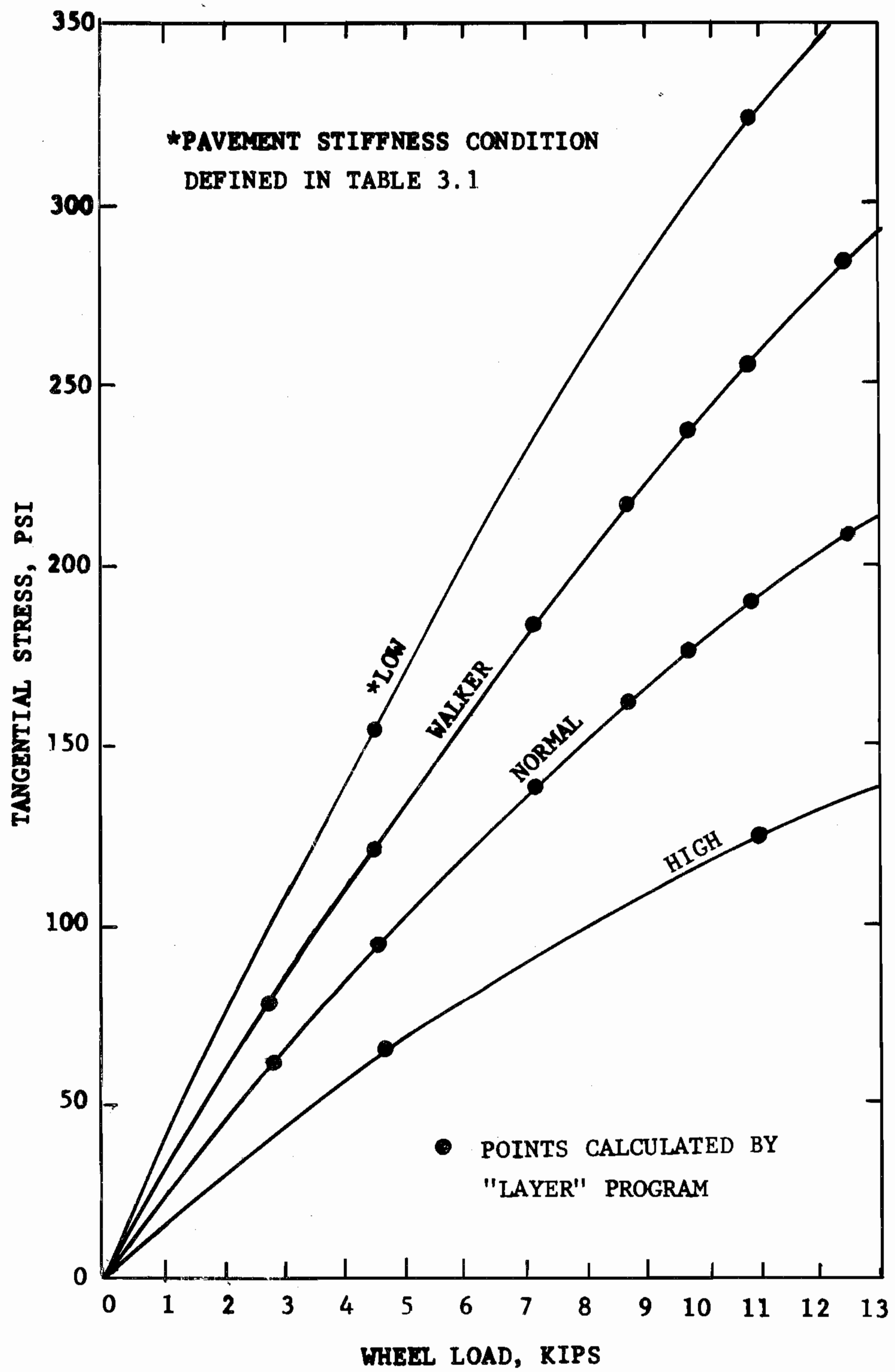

Fig A.1. Tangential Stress versus Wheel Load For Tandem Axle

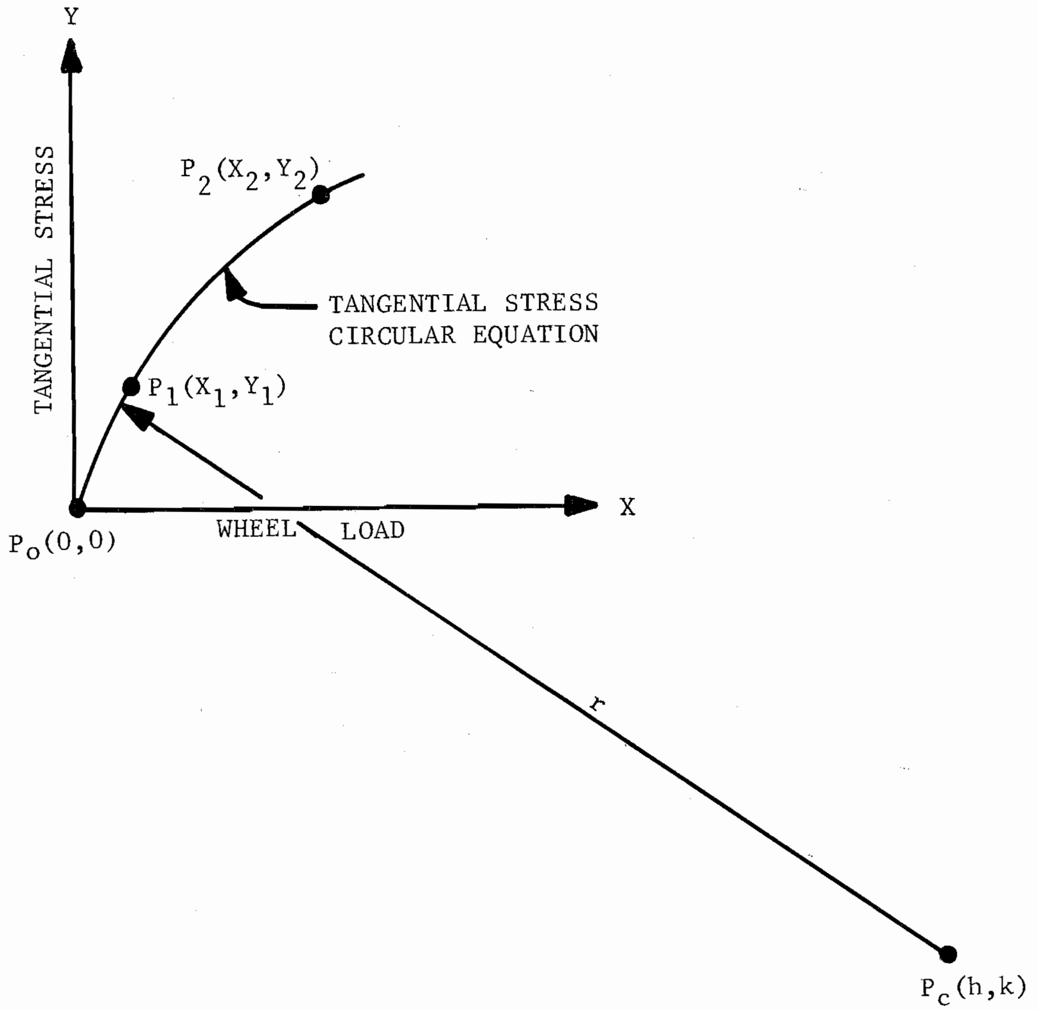

Figure A.2. Coordinates for Circular Curve Approximation of Tangential Stress

From this, equation A.2 can be expanded to

$$y_i = (\frac{X_2 - X_1}{y_2 - y_1})xi + y = (\frac{y_2 - y_1}{X_2 - X_1})X \; . \; . \; . \; . \; . \; . \; . \; . \; . \; . \; . \; . \; . A.4$$

By applying this criteria to figure A.5, equation A.4 can be written as

$$y_1 = (\frac{TS_2 - TS_1}{WL_2 - WL_1})\ Xi + \left[y_1 - (\frac{TS_2 - TS_1}{X_2 - X_1})\ X_1 \right] . \; . \; . \; . \; . A.5$$

The point TS_1 corresponds to the known tangential stress for the 4.5 Kip wheel load and the point TS_2 to the stress for the 10.7 Kip wheel load. A computer program was then written to generate a straight line through these two points and calculate tangential stress and cumulative damage for the desired wheel load groups.

Circular Curve Fix Method.

The next locus used to approximate the curve of tangential stress was a circle. A circle can be defined as an infinite set of points in a two-dimensional plane, all points being equidistant from a fixed point (Figure A.2). From analytic geometry, the general equation of a circle with its center at a distance, (h, k), from the origin can be defined as

$$(x_i - h)^2 + (yi - k)^2 = r^2 \; . \; . \; . \; . \; . \; . \; . \; . \; . \; . \; . \; . \; . \; . \; . \; . \; . A.6$$

If the point (h, k) is the origin of the circle, i.e., P (h, k) = P (o,o), equation A.6 can be written.

$$x_i^2 + yi^2 = r^2 \; . \; A.7$$

It was assumed that a circlar curve has a point in common, i.e., $P_1(x_1, y_1)$, with the curve of tangential stress. It was also assumed that the center of this curve lies some x-distance (h) and some y-distance (k) from the point P_1. Applying this to the above criteria, the equation of the circle can be written a

$$(x_1 - h) + (y_1 - k)^2 = r^2 \text{. . . . . A.8}$$

Another point, P_2 (x_2, y_2), can also be placed so as to satisfy both the equations of tangential stress and that of the circle defined. This point, $P_2(x_2,y_2)$, assuming the same center as point Pc, can be put in the general form for the equation of a circle.

$$(x_2 - h)^2 + (y_2 - k)^2 = r^2 \text{ . . . . A.9}$$

Since the circle which contains points P_1 and P_2 can also be assumed to contain the point Po (o,o), a third equation can be written defining the circle described.

$$(o - h)^2 + (o - k)^2 = r^2 \text{ . . . . A.10}$$

$$h^2 + k^2 = r^2 \text{. . . . . A.11}$$

Equations A.8, A.9, and A.11 can be reduced to

$$x_1^2 + y_1^2 - 2\,hx_1 - 2ky_1 + h^2 + K^2 = r^2 \text{. . . . . A.12}$$

$$x_2^2 + y_2^2 - 2\,hx_2 - 2ky_2 + h^2 + K^2 = r^2 \text{. . . . . A.13}$$

$$h^2 + K^2 = r^2 \text{ . . . . A.14}$$

By applying equations A.12, A.13, and A.14 to Figure A.16, they can be written as

$$WL_1^2 + TS.^2 - 2h\ WL, - 2K\ TS_1 = h^2 + K^2 = r^2 \quad \text{A.15}$$

$$WL_2^2 + TS_2^2 - sh\ WL_2 - 2K\ TS_2 + h^2 + K^2 = r^2 \quad \text{A.16}$$

$$h^2 + K^2 = r^2 \quad \text{A.17}$$

By mathematical manipulation of equations A.15, A.16, and A.17 and determinants, the values for the variables h, k, and r can be determined by any three specific points, P_o, P_1 and P_2, all lying on both the tangential stress curve and the circular curve. From the above criteria, a computer program was written to predict tangential stress and resultant damage for the desired wheel load groups.

Results.

For two different pavement stiffness conditions, the Walker County Pavement and the Normal Stiffness Pavement, described in Chapter 3, Table 3.1, tangential stress was calculated in the LAYER Program for all wheel loads under consideration. The results of the two programs developed for accurately approximating tangential stress are shown in Tables A.1, A.3, A.5, and A.7. These tables show the errors in estimating tangential stress for both pavement stiffness conditions. Tables A.2, A.4, A.6, and A.8 show the error in calculating cumulative damage using the approximate stresses.

It is noted that the errors in estimating tangential stress are small, in all cases, with the largest errors being under 8%. The largest error for the circular approximation is 1.7%. For The larger and more critical wheel loads, errors in tangential stress are well under 1% by both approximations.

Although the stress approximations appear accurate, it is noted that small errors in stress, for the larger wheel loads, cause a much larger error in estimating cumulative damage. From the tables noted above, it can be determined that the circular approximation is much more accurate than the straight line. The error in calculating total cumulative damage for the Walker County Pavement is approximately 6%. In reviewing the damage calculation of the main report it should be remembered that errors of this size could occur from calculations caused by the approximation made above.

The stresses for the 4.5 and 10.7 Kip wheel load were used as "force points" for the curve of approximation, because they appeared to give the best fit for tangential stress for the wheel loads considered. It was later established, after the sensitivity study was completed, that by changing the two "force points" to 10.7 and 12.5 kip wheel load, respectively, that total cumulative damage could be more accurately approximated. For the Walker County Pavement, Table A.3 show a comparison of approximate and actual tangential stresses. Tabel A.4 shows the cumulative damage caused by these stresses. Table A.7 and A.8 compare the stresses and damage, respectively, for the Normal Pavement Condition.

Summary of Findings and Limitations

A circular curve can be used to approximate tangential stress versus wheel load in this design system, provide it is used within the limitation and assumptions by which it was derived. The assumption and limitation are as follows:

1. Constant contact pressure for all wheel loads.
2. Tandem axles for all wheel load groups have approximately the same spacing.
3. Wheel load distributions can be divided into the wheel load groups choosen.
4. Tangential stress should not be extrapolated for wheel load much larger than the input wheel load or force points.
5. Tangential stress calculated is based on calculations in the "LAYER " program or similar theory.

A sample listing and output for the curve fit method is given in Appendix D.

Walker County Pavement Condition

Single Axle Wheel Loads (Kips)	Actual Stress* (psi)	Straight Line Interpolation* (psi)	Percent Difference	Curve Approximation*	Percent Difference
2.65	71.0	76.5	7.7	69.3	2.4
4.5	110.5	110.5	0	110.5	0
7.2	163.3	160.2	2.0	163.3	0
8.7	190.4	187.8	1.4	190.9	.3
9.6	206.1	204.4	.8	206.3	.1
10.7	224.6	224.6	0	224.6	0
Tandem Axle Wheel Loads					
2.65	78.5	84.0	7.0	76.8	2.2
4.5	123.3	123.3	0	123.3	0
7.2	183.7	180.6	1.7	184.5	.4
8.7	215.0	212.5	1.2	215.7	.3
9.6	233.3	231.6	.7	233.6	.1
10.7	254.9	254.9	0	254.9	0
12.5	288.9	293.1	1.5	288.2	0

* "force points" for approximation are tangential stresses for 4.5 and 10.7 Kip wheel loads.

Table A.1. Comparison of Tangential Stress

Walker County Pavement Condition

Single Axle Wheel Loads (Kips)	Actual Stress* (psi)	Straight Line Interpolation* (psi)	Percent Difference	Curve Approximation*	Percent Difference
2.65	$.25 \times 10^{-16}$	$.32 \times 10^{-15}$	88	$.11 \times 10^{-16}$	56
4.5	$.37 \times 10^{-9}$	$.37 \times 10^{-9}$	0	$.37 \times 10^{-9}$	12
7.2	$.51 \times 10^{-4}$	$.26 \times 10^{-4}$	49	$.57 \times 10^{-4}$	12
8.7	$.15 \times 10^{-2}$	$.97 \times 10^{-3}$	640	$.17 \times 10^{-2}$	12
9.6	$.84 \times 10^{-2}$	$.63 \times 10^{-2}$	25	$.87 \times 10^{-2}$	4
10.7	$.58 \times 10^{-1}$	$.58 \times 10^{-1}$	0	$.59 \times 10^{-1}$	2
Tandem Axle Wheel Loads					
2.65	$.13 \times 10^{-14}$	$.14 \times 10^{-13}$	92	$.62 \times 10^{-15}$	469
4.5	$.67 \times 10^{-8}$	$.67 \times 10^{-8}$	0	$.67 \times 10^{-8}$	0
7.2	$.67 \times 10^{-2}$	$.38 \times 10^{-2}$	43	$.78 \times 10^{-2}$	16
8.7	$.16 \times 10^{-0}$	$.18 \times 10^{0}$	125	$.18 \times 10^{0}$	13
9.6	$.60 \times 10^{-0}$	$.47 \times 10^{0}$	22	$.63 \times 10^{0}$	5
10.7	$.62 \times 10^{-1}$	$.62 \times 10^{1}$	0	$.62 \times 10^{1}$	0
12.5	$.43 \times 10^{-2}$	$.71 \times 10^{2}$	65	$.40 \times 10^{2}$	5
Totals	$.50 \times 10^{-2}$	$.78 \times 10^{2}$	55	$.47 \times 10^{2}$	6

* At the 99% confidence level.

Table A.2 Comparison of Cumulative Damage

Walker County Pavement Condition

Single Axle Wheel Loads (Kips)	Actual Stress* (psi)	Curve Approximation* (psi)	Percent Difference
2.65	71.0	68.4	3.6
4.5	110.5	109.5	.9
7.2	163.3	163.2	.1
8.7	190.4	190.4	0
9.6	206.1	206.1	0
10.7	224.6	224.7	0
Tandem Axle Wheel Loads			
2.65	78.5	75.4	3.9
4.5	123.3	121.9	1.1
7.2	183.7	183.5	.1
8.7	215.0	215.1	0
9.6	233.3	233.3	0
10.7	254.9	255.0	0
12.5	288.9	288.9	0

*"force points" for approximation are tangential stresses for 10.7 and 12.5 Kip wheel loads.

Table A.3. Comparison of Tangential Stress

Walker County Pavement Condition

Single Axle Wheel Loads (Kips)	Actual Stress* (psi)	Curve Approximation*	Percent Difference
2.65	$.25 \times 10^{-16}$	$.70 \times 10^{-17}$	272
4.5	$.37 \times 10^{-9}$	$.27 \times 10^{-9}$	27
7.2	$.51 \times 10^{-4}$	$.50 \times 10^{-4}$	2
8.7	$.15 \times 10^{-2}$	$.15 \times 10^{-2}$	0
9.6	$.84 \times 10^{-2}$	$.84 \times 10^{-2}$	0
10.7	$.58 \times 10^{-1}$	$.59 \times 10^{-1}$	2
Tandem Axle Wheel Loads			
2.65	$.13 \times 10^{-14}$	$.33 \times 10^{-15}$	246
4.5	$.67 \times 10^{-8}$	$.45 \times 10^{-8}$	33
7.2	$.67 \times 10^{-2}$	$.65 \times 10^{-2}$	3
8.7	$.16 \times 10^{0}$	$.17 \times 10^{0}$	6
9.6	$.60 \times 10^{0}$	$.60 \times 10^{0}$	0
10.7	$.62 \times 10^{1}$	$.63 \times 10^{1}$	2
12.5	$.43 \times 10^{2}$	$.43 \times 10^{2}$	0
Totals	$.50 \times 10^{2}$	$.50 \times 10^{2}$	0

* At the 99% confidence level.

Table A.4. Comparison of Cumulative Damage

Normal Pavement Condition

Single Axle Wheel Loads (Kips)	Actual Stress* (psi)	Straight Line Interpolation* (psi)	Percent Difference	Curve Approximation*	Percent Difference
2.65	56.2	61.8	9.1	55.6	1.1
4.5	87.1	87.1	0	87.1	0
7.2	127.0	123.9	2.4	127.0	0
8.7	146.9	144.4	1.7	147.0	.1
9.6	158.3	156.7	1.0	158.3	0
10.7	171.7	171.7	0	171.7	0
Tandem Axle Wheel Loads					
2.65	61.0	66.7	9.3	60.2	1.3
4.5	95.3	95.3	0	95.2	.1
7.2	140.0	137.0	2.1	140.2	.1
8.7	162.7	160.2	1.5	162.9	.1
9.6	175.7	174.1	.9	175.8	.1
10.7	191.1	191.0	.1	191.1	0
12.5	214.9	218.9	1.9	214.8	0

* "force points" for approximation are tangential stress for 4.5 and 10.7 Kip wheel loads.

Table A.5. Comparison of Tangential Stress

Normal Pavement Condition

Single Axle Wheel Loads (Kips)	Actual Stress* (psi)	Straight Line Interpolation* (psi)	Percent Difference	Curve Approximation*	Percent Difference
2.65	$.83 \times 10^{-20}$	$.22 \times 10^{-18}$	100	$.56 \times 10^{-20}$	20
4.5	$.11 \times 10^{-12}$	$.11 \times 10^{-12}$	0	$.11 \times 10^{-12}$	0
7.2	$.92 \times 10^{-8}$	$.40 \times 10^{-8}$	46	$.96 \times 10^{-8}$	4
8.7	$.21 \times 10^{-6}$	$.12 \times 10^{-6}$	43	$.22 \times 10^{-6}$	5
9.6	$.10 \times 10^{-5}$	$.70 \times 10^{-6}$	600	$.10 \times 10^{-5}$	0
10.7	$.59 \times 10^{-5}$	$.59 \times 10^{-5}$	0	$.59 \times 10^{-5}$	0
Tandem Axle Wheel Loads					
2.65	$.24 \times 10^{-18}$	$.50 \times 10^{-17}$	79	$.15 \times 10^{-18}$	37
4.5	$.98 \times 10^{-12}$	$.98 \times 10^{-12}$	0	$.96 \times 10^{-12}$	2
7.2	$.61 \times 10^{-6}$	$.29 \times 10^{-6}$	52	$.65 \times 10^{-6}$	7
8.7	$.12 \times 10^{-4}$	$.69 \times 10^{-5}$	567	$.12 \times 10^{-4}$	0
9.6	$.36 \times 10^{-4}$	$.27 \times 10^{-4}$	25	$.37 \times 10^{-4}$	3
10.7	$.32 \times 10^{-3}$	$.32 \times 10^{-3}$	0	$.32 \times 10^{-3}$	0
12.5	$.17 \times 10^{-2}$	$.32 \times 10^{-2}$	88	$.17 \times 10^{-2}$	0
Totals	$.21 \times 10^{-2}$	$.36 \times 10^{-2}$	114	$.21 \times 10^{-2}$	0

*At the 99% confidence level.

Table A.6. Comparison of Cumulative Damage

Normal Pavement Condition

Single Axle Wheel Loads (Kips)	Actual Stress* (psi)	Curve Approximation* (psi)	Percent Difference
2.65	56.2	56.0	.4
4.5	87.1	87.6	.6
7.2	127.0	127.3	.2
9.6	158.3	158.4	.1
10.7	171.7	171.7	0
Tandem Axle Wheel Loads			
2.65	61.0	60.2	1.3
4.5	95.3	95.2	.1
7.2	140.0	140.3	.2
8.7	162.7	162.9	.1
9.6	175.7	175.8	.1
10.7	191.1	191.1	0
12.5	214.9	214.9	0

*force points" for approximation are tangential stresses for 10.7 and 12.5 Kip wheel loads.

Table A.7. Comparison of Tangential Stress

Normal Pavement Condition

Single Axle Wheel Loads (Kips)	Actual Stress* (psi)	Curve Approximation*	Percent Difference
2.65	$.83 \times 10^{-20}$	$.74 \times 10^{-20}$	11
4.5	$.11 \times 10^{-12}$	$.13 \times 10^{-12}$	18
7.2	$.92 \times 10^{-8}$	$.10 \times 10^{-7}$	10
8.7	$.21 \times 10^{-6}$	$.23 \times 10^{-6}$	10
9.6	$.10 \times 10^{-5}$	$.10 \times 10^{-5}$	0
10.7	$.59 \times 10^{-5}$	$.59 \times 10^{-5}$	0
Tandem Axle Wheel Loads			
2.65	$.24 \times 10^{-18}$	$.15 \times 10^{-18}$	38
4.5	$.98 \times 10^{-12}$	$.95 \times 10^{-12}$	3
7.2	$.61 \times 10^{-6}$	$.66 \times 10^{-6}$	8
8.7	$.12 \times 10^{-4}$	$.12 \times 10^{-4}$	0
9.6	$.36 \times 10^{-4}$	$.37 \times 10^{-4}$	2
10.7	$.32 \times 10^{-3}$	$.32 \times 10^{-3}$	0
12.5	$.17 \times 10^{-2}$	$.17 \times 10^{-2}$	0
Totals	$.21 \times 10^{-2}$	$.21 \times 10^{-2}$	0

*At the 99% confidence level.

Table A.8. Comparison of Cumulative Damage

APPENDIX B

DYNAFLECT DEFLECTION BASINS

APPENDIX B. DYNAFLECT DEFLECTION BASINS

This study compares the deflection basins measured by the Dynaflect with deflection basins predicted by the Chevron Linear Elastic Layer Program (Ref 25). Field measurements with the Dynaflect were taken in January, 1969, in conncection with an asphaltic concrete overlay design project conducted by Dr. B. F. McCullough. The project site was on Interstate Highway 45 in Walker County, Texas. Figure B.1 shows the location of the project site.

A typical section for the Walker County project is shown in Figure B.2. The Dynaflect load wheels were placed approximately 3 to 4 feet from the outside 10 foot shoulder, with the first sensor for deflection placed between the two load wheels, and the remaining four sensors placed parallel to the shoulder edge at one foot intervals. The position of the Dynaflect sensors during testing is shown in Figure B.11.

For predicting deflections in the LAYER program, the elastic and physical properties of the materials were obtained from values determined in the previous mentioned design project and are shown in Table B.1.

<u>Deflection Basins</u>.

Figure B.3 and B.4 show actual deflection measurements taken from two different subgrade design sections. Superimposed on these two plots are predicted deflections using material properties from Table B.1.

These plots indicate that measured deflection basins, when compared with calculated basins, have similar shapes as long as the geophone 1 deflections are small (deflection between load wheels). In an attempt to explain the difference between the measured and calculated deflection basins, the hypothesis was made that the error in the deflection prediction can come from anyone of the three places. The first place for error was that a reduction in the effective modulus of the concrete pavement had occurred because of loss of load transfer at wider than usual transverse cracks. The second place for error was that a reduction in the effective modulus of the subbase had occurred because of a local increase in moisture or because of pumping action of the slab. The third place for error was that a reduction in the effective depth of the concrete had occurred because of normal variation of the concrete depth and/or poor consolidation of the concrete caused by lack of vibrating.

Modulus of Concrete (E_1).

Figure B.5 shows four calculated deflection basins for four subgrades at two levels of stiffness of the concrete pavement. As E_1 is reduced from 5,000,000 psi to 3,000,000 psi the deflection basins become steeper.

In Figures B.6 and B.7 the measured deflections for two different design sections are shown superimposed over the deflections calculated using an E_1 of 3,000,000 psi.

It appears that the calculated deflection for an E_1 of 3,000,000 psi tends to fit measured condition closer than deflection basins for the higher E_1 of 5,000,000 psi shown previously in Figures B.3 and B.4.

Modulus of Subbase (E_2).

For an E_4 of 8200 psi, E_1 of 5,000,000 psi, and E_2 for 5,000 psi and 30,000 psi, deflection basins were calculated and are shown in Figure B.8. Then, E_1 was changed to 3,000,000 psi and the results of this computations are shown in Figure B.9. However, neither of these two plots shows a significant change in the deflection basin for a change in E_2 from 5,000 psi to 30,000 psi.

Depth of Concrete (D_1).

Deflection basins calculated for concrete depths of 7.5 inches and 8.0 inches for each of four subgrades are shown in Figure B.10. The changes in deflection basins are small for the stronger subgrades.

Conclusions.

1. The majority of measured deflections could be predicted by calculations made by the Chevron Layer Program, using conventional procedures for determining the modulus of elasticity as used in the design project.
2. For concrete pavements having relatively steep and large deflection basins, special consideration should be given to the continuity of the slab (pavement cracks), local moisture conditions, slab pumping and depth of concrete. If any of these conditions have an adverse effect on the deflections, then the values effected should be modified before using them in the LAYER program.
3. A decrease in the effective modulus of the concrete and subbase will increase the slope of deflection basins.

4. A decrease in the depth of the concrete will cause an increase in the slope of the deflection basins.
5. A change in the modulus of the subgrade has by far the greatest effect on the magnitude of the deflection, but causes little change in the slope of the deflection basin.
6. The increase in slope of the deflection basin was small for a reduction in depth of the concrete pavement from 8 inches to 7.5 inches, and for a subgrade modulus greater than 8000 psi. For subgrades with modulii of less than 8000 psi, the increase in the deflection basin slope does become significant.

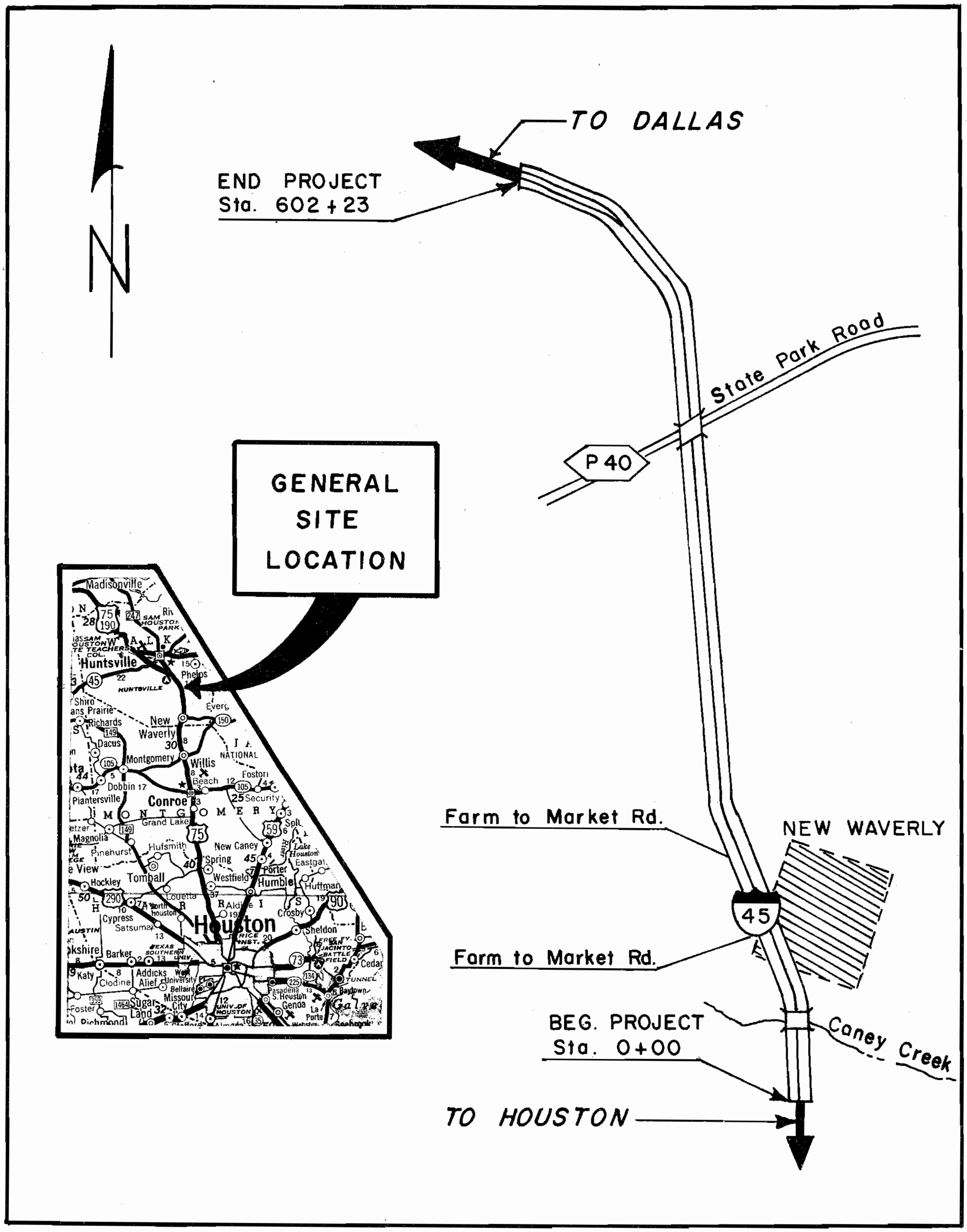

Fig B.1. Location of the Walker County Project

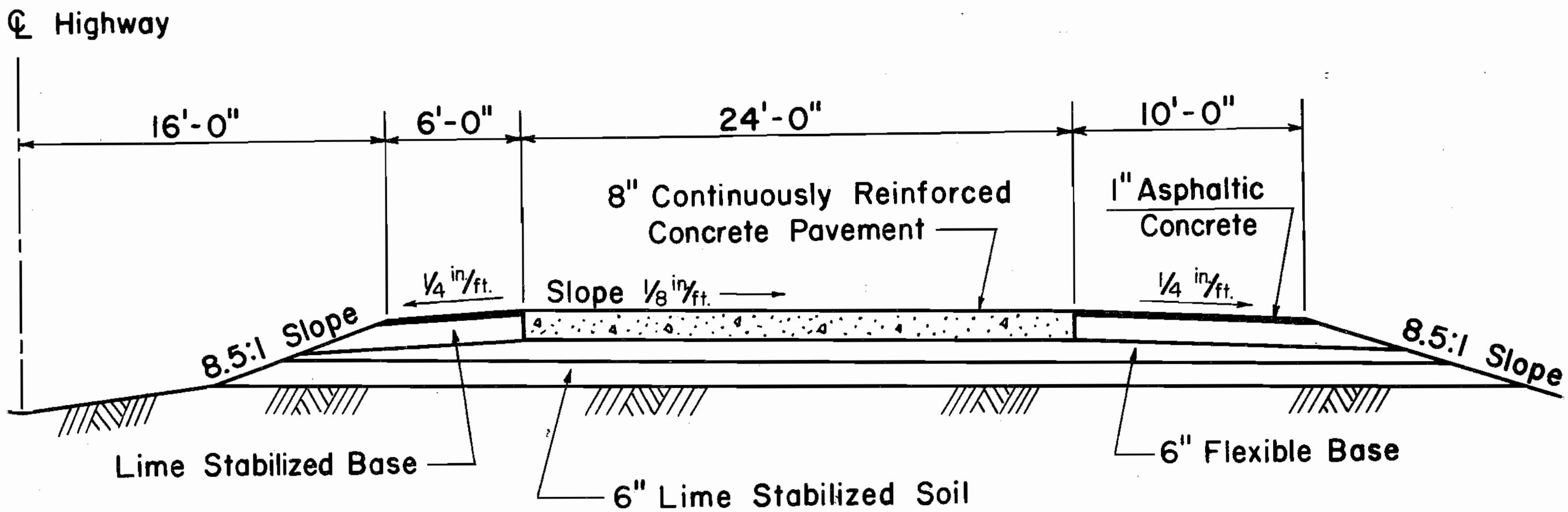

Fig B.2. Typical Half Section for Walker Project

Concrete Pavement	$^{*}E_1$	5,000,000 psi
	U_1	0.20
	D_1	8.0"
Subbase	E_2	10,000 psi
	U_2	0.40
	D_2	6.0"
Treated Subgrade	E_3	80,000 psi
	U_3	0.35
	D_3	6.0"
Subgrade	E_4	4,100 to 20,000 psi
	U_4	0.45

$^{*}E_i$ = Elastic Modulus of i^{th} Layer

U_i = Poisson's Ratio of i^{th} Layer

D_i = Thickness of i^{th} Layer

Table B.1. Layer Thickness and Elastic Properties

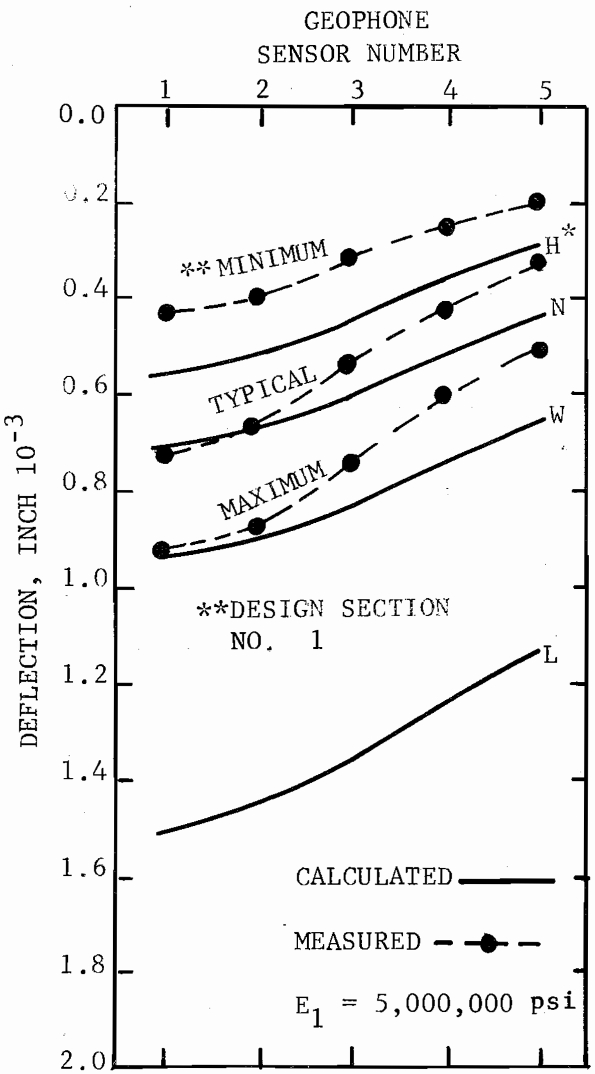

Fig B.3. Measured and Calculated Deflection Basins for Design Section No. 1 (E_1 = 5,000,000 psi)

*SUBGRADE MODULUS
H = 20,000
N = 13,000
W = 8,200
L = 4,100

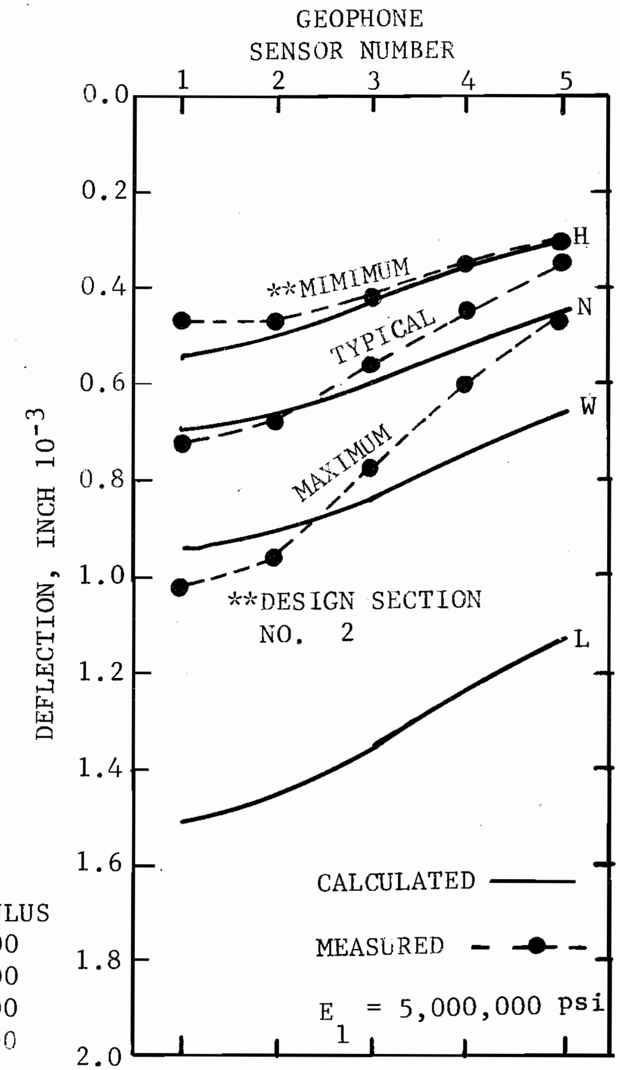

Fig B.4. Measured and Calculated Deflection Basins for Design Section No. 2 (E_1 = 5,000,000 psi)

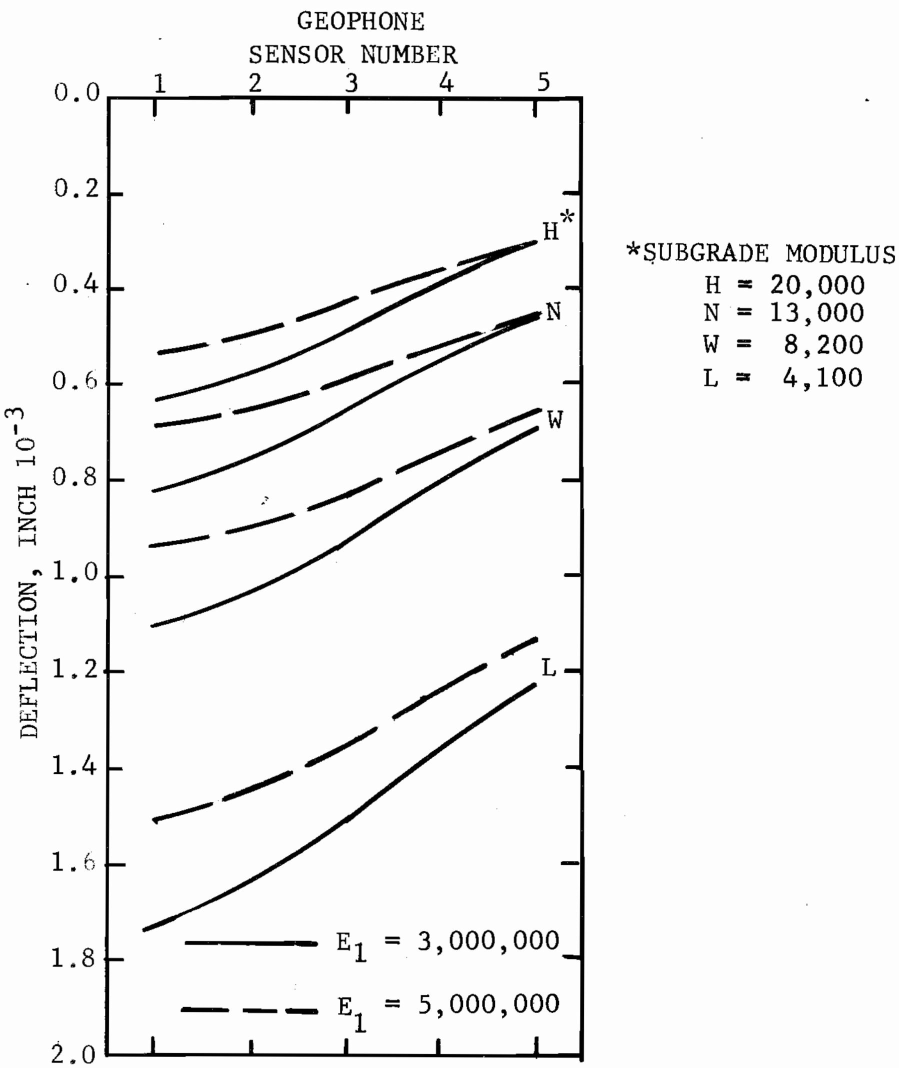

Fig B.5. Calculated Deflection Basin Showing the Effect of Varying the Elastic Modulus of Layer 1

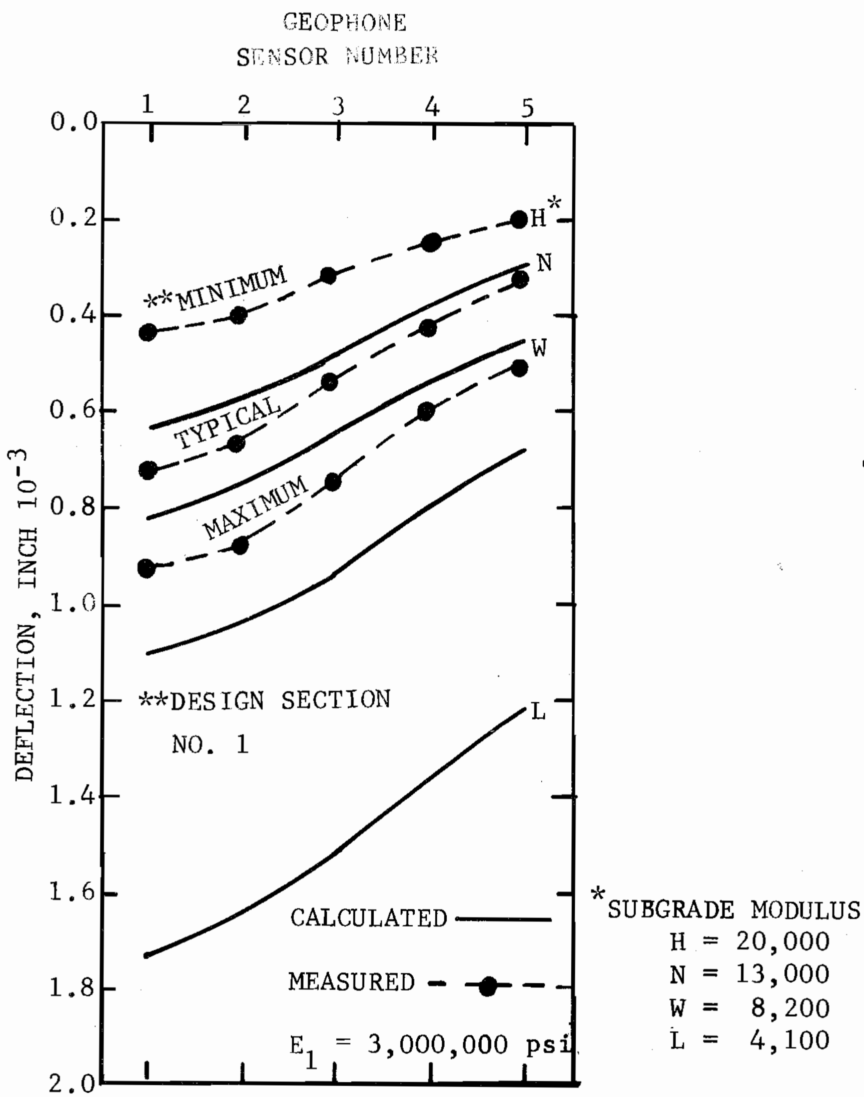

Fig B.6. Measured and Calculated Deflection Basins for Design Section No. 1 (E_1 = 3,000,000 psi)

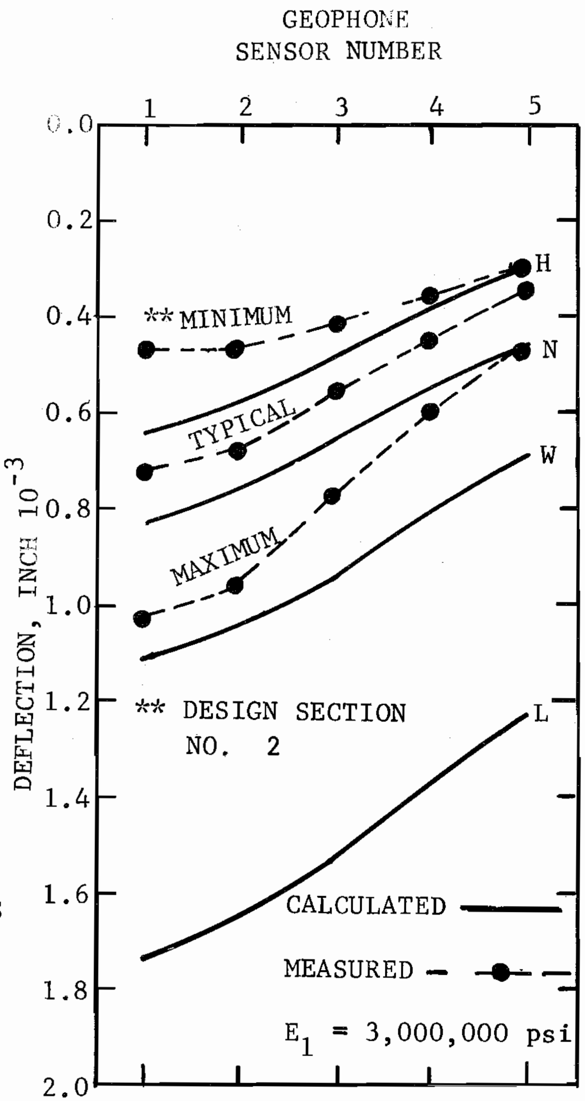

Fig B.7. Measured and Calculated Deflection Basins for Design Section No. 2 (E_1= 3,000,000 psi)

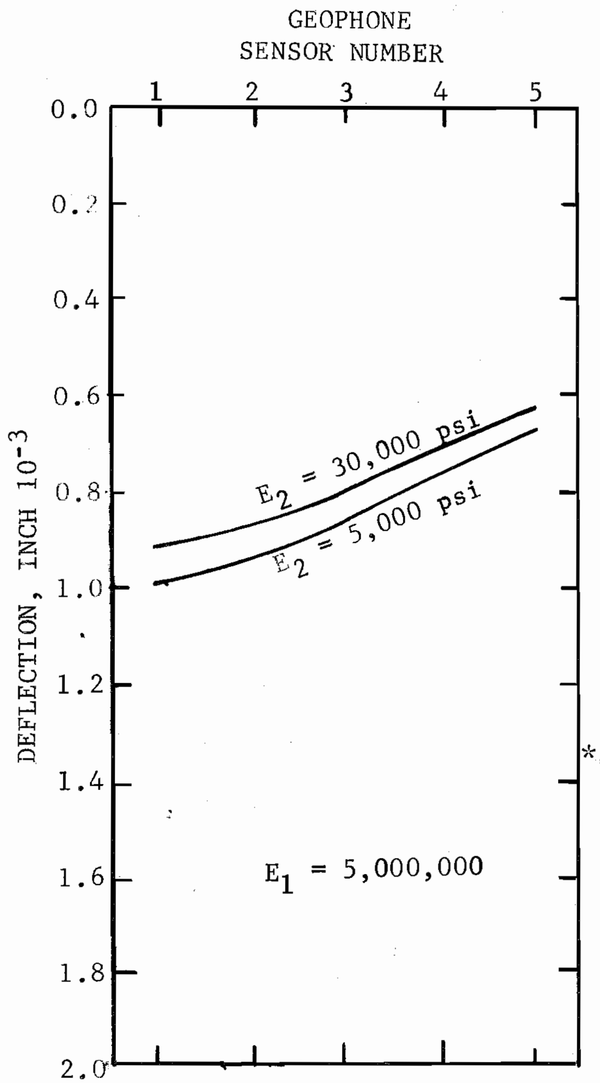

*SUBGRADE MODULUS
H = 20,000
N = 13,000
W = 8,2000
L = 4,100

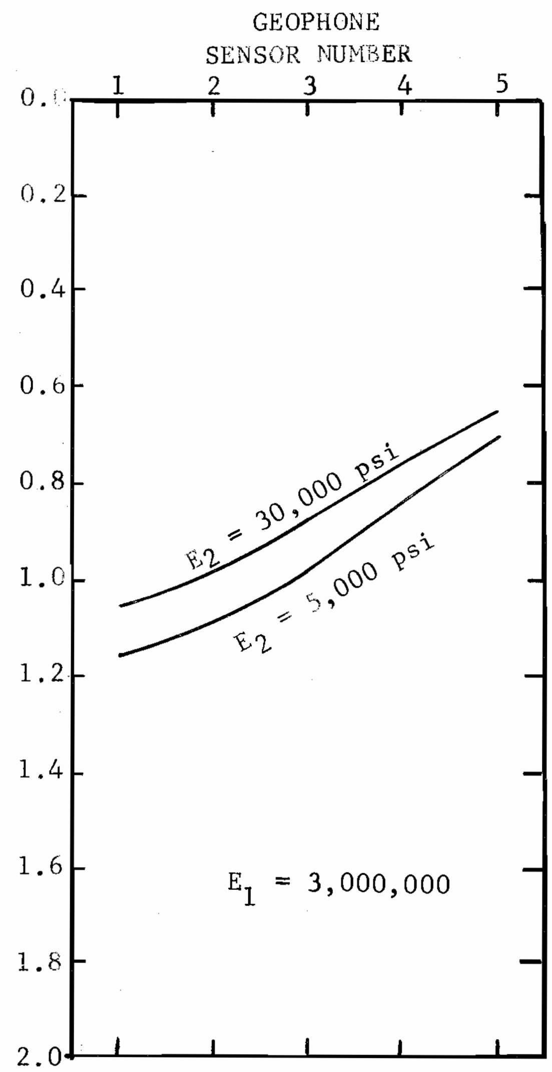

Fig. B.9. Calculated Deflection Basins Showing the Effect of Varying the Elastic Modulus of Layer 2 (E_1 = 5,000,000)

Fig B.9. Calculated Deflection Basins Showing the Effect of Varying the Elastic Modulus of Layer 2 (F_1 = 3,000,000)

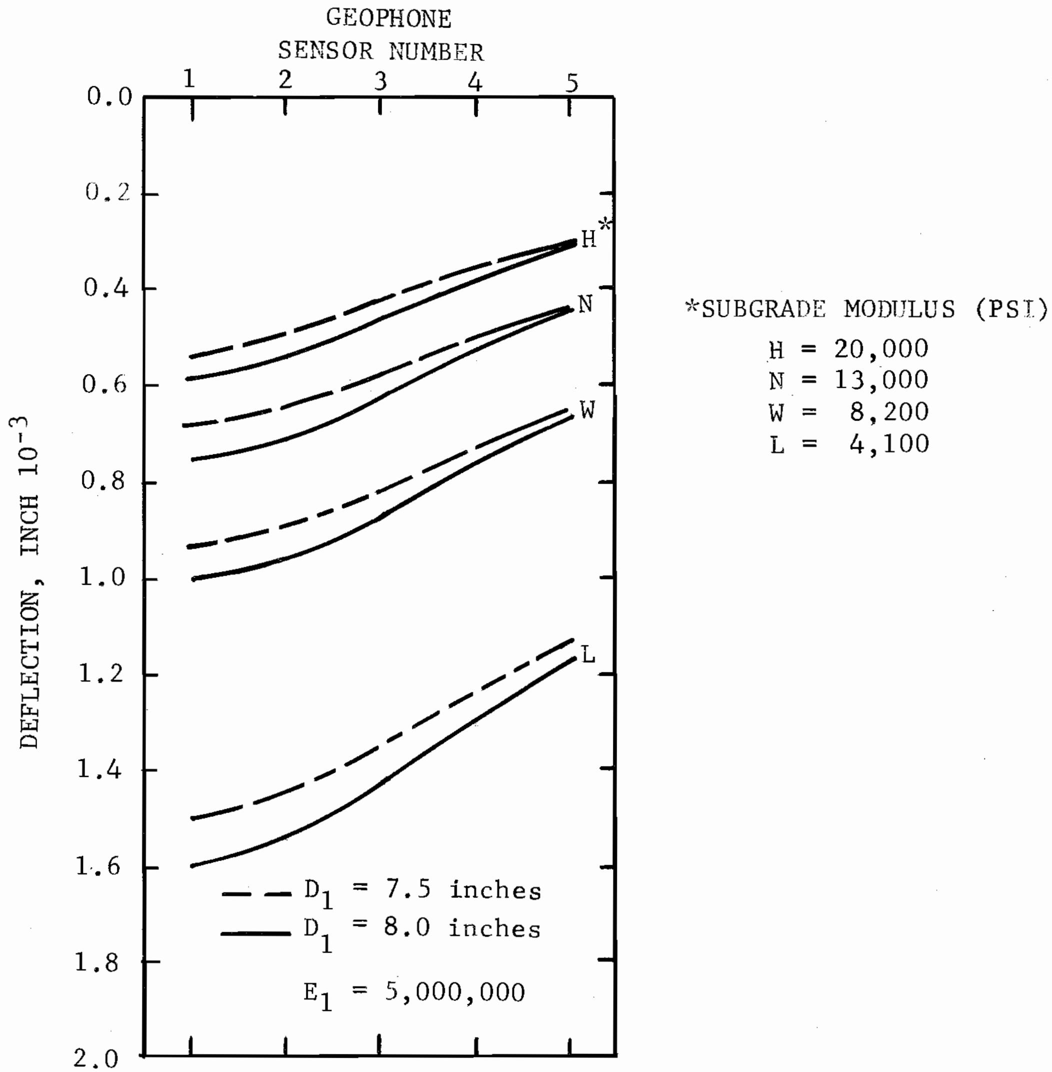

Fig B.10. Calculated Deflection Basins Showing the Effect of Varying the Thickness of Layer 1 (E_1 = 5,000,000)

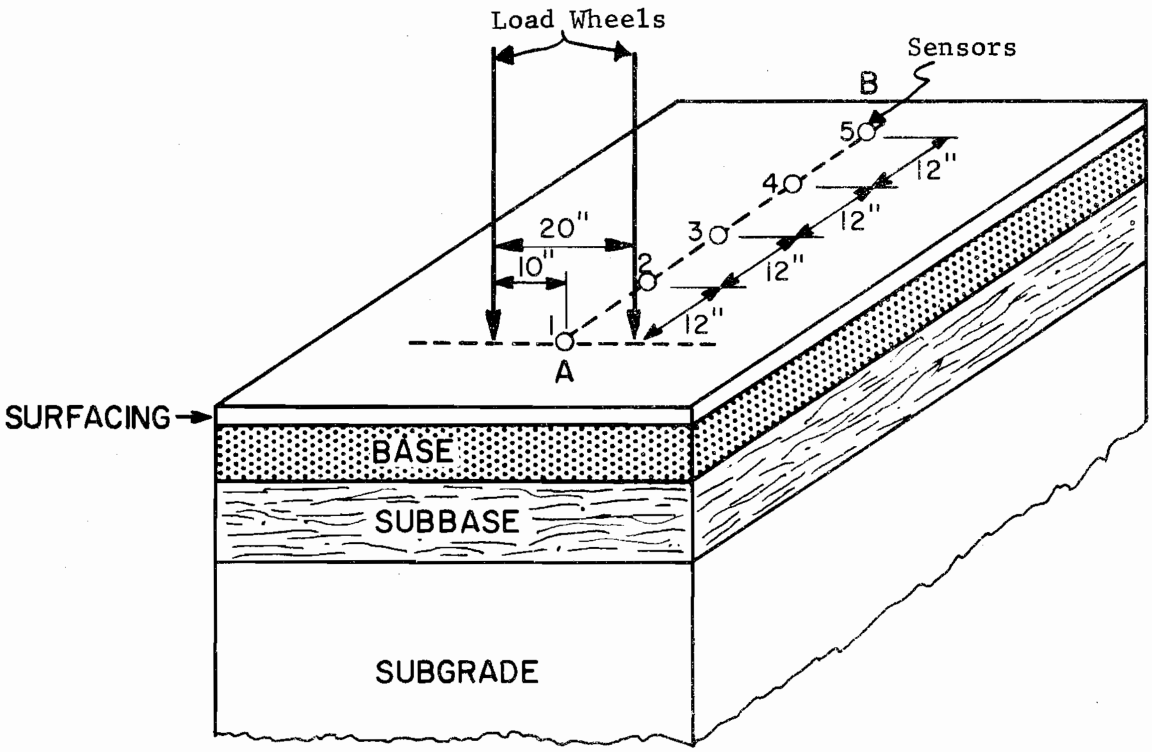

Figure B.11. Position of Dynaflect Sensors During testing

APPENDIX C

COMPUTER PROGRAM TO DETERMINE THE SIGNIFICANT DIFFERENCE BETWEEN DESIGN SECTIONS AND A SAMPLE OUTPUT OF THE PROGRAM-PROFILE ANALYSIS

MAIN

```
      REAL*8 STA
      DIMENSION STA(500),X1(500),NN(21),KOUNT(21),IXDATE(2)
      COMMON X(250,2),NUM(2)
  800 READ(5,1,END=829) IDIST,C01,C02,C03,C04,ICONT,ISECT,IJOB,HWY1,HWY2
     *,DATE1,DATE2,NOSE
    1 FORMAT(3X,I2,3A4,A2,I4,2I2,A4,A3,2A4,I2)
      PRINT 100
  100 FORMAT (1H1,///)
      PRINT 22
   22 FORMAT(33X,'TEXAS HIGHWAY DEPARTMENT',/)
      PRINT 33, IDIST
   33 FORMAT(31X,'DISTRICT ',I2,' - DESIGN SECTION',/)
      CALL DATE(IXDATE)
      PRINT 34, IXDATE
   34 FORMAT(30X,'THIS PROGRAM WAS RUN - ',2A4,/)
      PRINT 36,HWY1,HWY2
   36 FORMAT(30X,' PROFILE ANALYSIS FOR   ',A4,A3,/)
      PRINT 29
   29 FORMAT(7X,'DIST.        COUNTY       CONT.  SECT.  JOB  HIGHWAY    D
     1ATE   NO. OF SECT.')
      PRINT 57,IDIST,C01,C02,C03,C04,ICONT,ISECT,IJOB,HWY1,HWY2,DATE1,DA
     *TE2,NOSE
   57 FORMAT( 8X,I2,5X,3A4,A2,2X,I4,4X,I2,4X,I2,2X,A4,A3,3X,2A4,6X,I2,/)
C
C
C     NT     - NUMBER OF DATA POINTS IN PROJECT
C     X1(I) - LIST OF DATA POINTS AS RECORDED ON PROJECT
C
C
      N5 = 0
      KN = 1
      KOUNT(1) = 1
      NN(1) = 1
      K = NOSE + 1
      READ 99, (NN(I), I = 2,K)
   99 FORMAT(20I3)
      N = NN(K)
      DO 10 I = 1,N
   10 READ 3, STA(I),X1(I)
    3 FORMAT(A7,F5.3)
      NT=NN(K)
      PRINT 102
  102 FORMAT(31X,'REFERENCE       STA.       INPUT',/,
    1         31X,' POINTS                    DATA',/)
      NLINE = 0
      DO 190 I = 1,NT
      PRINT 101,I,STA(I),X1(I)
  101 FORMAT(33X,I3,7X,A7,2X,F10.3)
```

MAIN

```
      NLINE = NLINE + 1
      IF (NLINE.LT. 40) GO TO 190
      PRINT 100
      PRINT 33,IDIST
      PRINT 36, HWY1,HWY2
      PRINT 102
      NLINE = 0
  190 CONTINUE
      PRINT 107,(NN(I),I=1,K)
  107 FORMAT(/,8X,'INPUT BREAK PTS. AT ',13(1X,I3),/,28X,8(1X,I3))
      IF ( N5.EQ.0) GO TO 193
  191 CONTINUE
      PRINT 100
      PRINT 22
      PRINT 33,IDIST
      PRINT 36, HWY1,HWY2
      CALL DATE(IXDATE)
      PRINT 34, IXDATE
      PRINT 29
      PRINT 57,IDIST,CO1,CO2,CO3,CO4,ICONT,ISECT,IJOB,HWY1,HWY2,DATE1,DA
     *TE2,NOSE
      PRINT 103
  103 FORMAT(//,21X,'AVERAGE AND STANDARD DEVIATION FOR DATA DIVIDED',/,
     1          21X,' INTO GROUPS OF SIGNIFICANT DIFFERENCE ', //  )
      PRINT 104, (NN(I), I = 1,K)
  104 FORMAT(  8X,'BREAK POINTS AT ',13(1X,I3),/,24X,8(1X,I3),/)
      PRINT 105
  105 FORMAT(14X,'REF. POINTS        AVERAGE        STANDARD          F
     1           F',/,16X,'LIMITS             OF            DEVIATION
     2  CALC.         TABLE',/,14X,'OF SECTIONS        SECTIONS        OF S
     3ECTIONS                     VALUE',/)
C
  193 CONTINUE
      I = 0
      I = I + 1
      N1 = 1
      N2 = NN(2)
      GO TO 76
   75 N1 = NN(I) + 1
   73 N2=NN(I+1)
   76 CONTINUE
C
C     CALCULATE AVERAGE AND STANDARD DEVIATION
C     SUM - SUM OF GROUP IN ARRAY X1(I)
C     AK - NUMBER OF VARIABLES IN GROUPP (X1(N1 TO N2)
C     SD - STANDARD DEVIATION OF GROUP X1(N1 TO N2)
C
      SUM = 0.
```

MAIN

```
      IF (N1 .EQ. N2) GO TO 86
      DO 80  J = N1,N2
   80 SUM =  SUM + X1(J)
      AK = N2 - N1 + 1
      AVR = SUM / AK
      SD = 0.
      DO 85  J= N1,N2
      IF ( AVR - X1(J) .EQ. 0.) GO TO 85
      SD = SD + (AVR -X1(J))**2
   85 CONTINUE
      IF ( SD .EQ. 0.) GO TO 90
      SD =  SQRT(SD /(AK -1))
      IF(N2.EQ.NT) GO TO 93
      GO TO 90
   86 AVR = X1(N2)
       SD = 0
   90 CONTINUE
C
C
C     OBTAIN F(CALCULATED ) AND F1(TABLE VALUE) FOR ANALYSIS
C       OF VARIANCE FOR X1(N1-N2) COMPARED WITH X1(N3-N4)
C
C
      L = 0
      DO 91 J = N1, N2
       L = L+1
   91 X(L,1) = X1(J)
      N3 = N2 + 1
      IF (N3 .GT. NN(K) ) GO TO 93
      N4 = NN(I +2)
      LL = 0
      DO 92 J = N3, N4
      LL = LL + 1
   92 X(LL,2) = X1(J)
      NUM(1) = L
      NUM(2) = LL
      CALL FTAB (F1)
      CALL ANOVAR (F)
      IF(F-F1) 95,95,94
   93 F = 0.
      F1 = 0.
C
   94 CONTINUE
      IF(N5.EQ.0) GO TO 96
      PRINT 106, N1, N2, AVR, SD, F, F1
  106 FORMAT(14X,I3,'  TO ',I3,3X,F10.3,8X,F10.3,5X,F7.3,6X,F7.3)
   96 CONTINUE
      KN = KN + 1
```

MAIN

```
      KOUNT(KN) = N2
C
   95 CONTINUE
      IF (N2.EQ.NT) GO TO 200
      I = I + 1
      IF(F1.GT.F) GO TO 73
      GO TO 75
  200 CONTINUE
      NN(1) = KOUNT(1)
      DO 201 J = 2,KN
  201 NN(J) = KOUNT(J)
      KN1 = KN
      IF ( N5.EQ.1) GO TO 800
      IF(KN1.EQ.K)   N5=1
      K = KN
      NOSE = KN- 1
      KN = 1
      IF(N5)829,193,191
  829 CONTINUE
      STOP
      END
```

FTAB

```
      SUBROUTINE FTAB (F1)
      COMMON X(250,2),NUM(2)
      DIMENSION FT(30)
C
C
      DATA FT /161.0,18.5,10.1,7.71,6.61,
     1          5.99,5.59,5.32,5.12,4.96,
     2          4.84,4.75,4.67,4.60,4.54,
     3          4.49,4.45,4.41,4.38,4.35,
     4          4.32,4.30,4.28,4.26,4.24,
     5          4.17,4.08,4.00,3.92,3.84/
C
C
      ID = NUM(1) + NUM(2) - 2
      A = ID
      IF (ID - 25) 40, 40, 15
   15 IF (ID - 30) 45, 45, 20
   20 IF (ID - 40) 50, 50, 25
   25 IF (ID - 60) 55, 55, 30
   30 IF (ID -120) 60, 60, 35
   35 F1 = FT(29)
      GO TO 65
   40 F1 = FT(ID)
      GO TO 65
   45 F1 = FT(25) +((A -25.)/5.)* (FT(26) - FT(25))
      GO TO 65
   50 F1 = FT(26) +((A -30.)/10.)* (FT(27) - FT(26))
      GO TO 65
   55 F1 = FT(27) +((A -40.)/20.)* (FT(28) - FT(27))
      GO TO 65
   60 F1 = FT(28) +((A -60.)/60.)* (FT(29) - FT(28))
   65 CONTINUE
      RETURN
      END
```

ANOVAR

```
      SUBROUTINE  ANOVAR(F)
      COMMON X(250,2),NUM(2)
      K = 0
      M=0
      SUM=0.
      SS1=0.
      SST1=0.
      DO 200 J=1,2
      SUM1=0.0
      N=0
      LL = NUM(J)
      DO 100 I=1,LL
      IF(X(I,J).EQ.0) GO TO 99
      SUM1= SUM1 + X(I,J)
      SS1 = SS1 + X(I,J)**2
   99 N=N+1
      M=M+1
  100 CONTINUE
      K=K+1
      IF ( SUM1 .EQ. 0.) GO TO 200
      SST1=SST1+((SUM1**2)/N)
      SUM=SUM+SUM1
  200 CONTINUE
      IF (SUM .EQ. 0.) GO TO 201
      C=(SUM**2)/M
      SS=SS1-C
      SST=SST1-C
      SSE=SS-SST
      IF ( SST.EQ.0.0 )  GO TO 201
      IF ( SSE.EQ.0.0 )  GO TO 201
      ITDF=M-1
      IDFBM=K-1
      IDFWS=M-K
      F=(SST*IDFWS)/(SSE*IDFBM)
      IF (F .GT. 0.) GO TO 202
  201 F = 0.
  202 CONTINUE
      RETURN
      END
```

TEXAS HIGHWAY DEPARTMENT

DISTRICT 17 - DESIGN SECTION

THIS PROGRAM WAS RUN - 12-16-70

PROFILE ANALYSIS FOR IH-45

DIST.	COUNTY	CONT.	SECT.	JOB	HIGHWAY	DATE	NO. OF SECT.
17	WALKER	675	5	0	IH-45	06/10/69	4

REFERENCE POINTS	STA.	INPUT DATA
1	+10	0.740
2	+20	0.720
3	+30	0.740
4	+40	0.800
5	+50	0.850
6	+60	0.660
7	+70	0.800
8	+80	0.720
9	+90	0.800
10	1+00	0.720
11	1+10	0.750
12	1+20	1.020
13	1+3	0.790
14	1+4	0.740
15	1+5	0.610
16	1+6	0.660
17	1+7	0.720
18	1+8	0.670
19	1+9	0.630
20	2+00	0.660
21	2+10	0.650
22	2+20	0.580
23	2+30	1.200
24	2+4	0.820
25	2+5	0.740
26	2+6	0.780
27	2+7	0.670
28	2+8	1.050
29	2+90	0.760
30	3+00	0.960

INPUT BREAK PTS. AT 1 5 14 21 30

TEXAS HIGHWAY DEPARTMENT

DISTRICT 17 - DESIGN SECTION

PROFILE ANALYSIS FOR IH-45

THIS PROGRAM WAS RUN - 12-16-70

DIST.	COUNTY	CONT.	SECT.	JOB	HIGHWAY	DATE	NO. OF SECT.
17	WALKER	675	5	0	IH-45	06/10/69	3

AVERAGE AND STANDARD DEVIATION FOR DATA DIVIDED
INTO GROUPS OF SIGNIFICANT DIFFERENCE

BREAK POINTS AT 1 14 21 30

REF. POINTS LIMITS OF SECTIONS	AVERAGE OF SECTIONS	STANDARD DEVIATION OF SECTIONS	F CALC.	F TABLE VALUE
1 TO 14	0.775	0.085	12.134	4.380
15 TO 21	0.657	0.035	5.905	4.600
22 TO 30	0.840	0.195	0.0	0.0

APPENDIX D

COMPUTER PROGRAM TO APPROXIMATE TANGENTIAL STRESS AND DETERMINE THE CUMULATIVE DAMAGE OF AN IN-SERVICE PAVEMENT AND A SAMPLE OUTPUT OF THE PROGRAM

MAIN

```
      REAL*8 GROUP
      COMMON GROUP (13)
      COMMON TS (13)
      COMMON NACT (13)
      DIMENSION IXDATE(2)
      DIMENSION TRO(13)
      DIMENSION KEEP(3)
      DIMENSION X(7)
      PRINT 200
  200 FORMAT (1H1,//////////)
      PRINT 91
   91 FORMAT(37X,25H TEXAS HIGHWAY DEPARTMENT,/)
      PRINT 92
   92 FORMAT(28X,44H HIGHWAY DESIGN DIVISION    RESEARCH SECTION,/)
      PRINT 54
   54 FORMAT(35X,30H SPECIAL ASSIGNMENT 17-69      ,/)
      PRINT 55
   55 FORMAT(31X,38H PROJECT SUPERVISOR   LARRY J. BUTTLER,/)
      PRINT 94
   94 FORMAT(33X,' PROGRAMMER  -     PAUL S. FISHER',/)
      CALL DATE(IXDATE)
      PRINT 95,IXDATE
   95 FORMAT(34X,'THIS PROGRAM WAS RUN - ',2A4,/)
      PRINT 205
  205 FORMAT (1H1)
      PRINT 215
  215 FORMAT (//////////)
      PRINT 10
   10 FORMAT (19X,'ASSUMING A CIRCULAR CURVE TO CALCULATE TANGENTIAL STR
     *ESS',/,19X,'AND CUMULATIVE DAMAGE AT FIVE CONFIDENCE LEVELS',///)
      PRINT 109
  109 FORMAT (19X,'SEN = LOG ( C* (FK /FC-SEFC)**FK )',/,19X,'RD=(NACT)(
     1DD)(DL) /10**(LOG (C*((FC/TS)**FK)- (T*SEN)))',//,19X,'WHERE -',/,
     219X,'SEN=STANDARD ERROR IN ESTIMATING CYCLES TO FAILURE',/,19X,'FK
     3=SLOPE OF FATIGUE CURVE',/,19X,'C=CONSTANT',/,19X,'SEFC=STANDARD E
     4RROR OF TENSILE STRENGTH',/,19X,'DD=DIRECTION DISTRIBUTION',/,19X,
     5'FC=TENSILE STRENGTH OF CONCRETE',/,19X,'TS=TANGENTIAL STRESS',/,1
     69X,'CL=CONFIDENCE LEVEL',/,19X,'NACT=NUMBER OF WHEEL LOAD APPLICAT
     7IONS',/,19X,'T=CONSTANT FOR SPECIFIC CONFIDENCE LEVEL',/,19X,'AG=A
     8XLE GROUP',/,19X,'RD=RESULTANT DAMAGE',/,19X,'RDT=TOTAL RESULTANT
     9DAMAGE',/,19X,'DL=LANE DISTRIBUTION')
      READ  600,(GROUP(I),I=1,13)
  600 FORMAT (10A8)
    6 CONTINUE
      X(1)=2.65
      X(2)=4.5
      X(3)=7.2
      X(4)=8.7
```

MAIN

```
      X(5)=9.6
      X(6)=10.7
      X(7)=12.5
      XC1=4.5
      XC2=10.7
      READ 2 ,V,VID,Y1,Y2,Y3,Y4,J
    2 FORMAT(A4,A3,3X,4F10.3,29X,I1 )
      READ 99, (KEEP(I),I=1,3)
   99 FORMAT  (1X,3I1)
      READ 71,SEFC
   71 FORMAT (6X,F12.4)
      READ 49,(NACT(I) ,I=1,13)
   49 FORMAT (8I10)
      IF (KEEP(3)) 30,30,31
   30 CONTINUE
      PRINT 200
      PRINT 14,V,VID,Y1,Y2,Y3,Y4
   14 FORMAT (13X,A4,A3,3X,4F10.3)
      CK=(((Y2/2)*((XC1**2)+(Y1**2)) - ((Y1/2)* ((XC2 **2)+(Y2**2)))) /
     *((XC1 *Y2)-(XC2 *Y1)))
      CH=(((XC1/2)*((XC2**2)+ (Y2**2)) -((XC2/2) * ((XC1**2)+ (Y1**2)))
     *) / ((XC1 *Y2)- (XC2*Y1)))
      A=CK*CK
      B=CH*CH
      D=A+B
      E=SQRT(D)
      PRINT 11
      PRINT 12
      PRINT 13
   11 FORMAT (/,18X,' SINGLE AXLE',4X,' TAN.',13X,' NUMBER OF W.L. IN')
   12 FORMAT (18X,' WHEEL  LOAD',4X,' STRESS',11X,' BOTH DIRECTIONS')
   13 FORMAT (18X,' KIPS',11X,' PSI')
      DO 3 I=1,6
      T=((SQRT(D-((X(I)-CK)**2))) + CH)
      TS(I)=T
    3 PRINT 4,X(I),T,NACT(I)
    4 FORMAT (13X,F10.2,10X,F10.1,9X,I11)
      Y1=Y1+Y3
      Y2=Y2+Y4
      CK=(((Y2/2)*((XC1**2)+(Y1**2)) - ((Y1/2)* ((XC2 **2)+(Y2**2)))) /
     *((XC1 *Y2)-(XC2 *Y1)))
      CH=(((XC1/2)*((XC2**2)+ (Y2**2)) -((XC2/2) * ((XC1**2)+ (Y1**2)))
     *) / ((XC1 *Y2)- (XC2*Y1)))
      A=CK*CK
      B=CH*CH
      D=A+B
      E=SQRT(D)
      PRINT 19
```

MAIN

```
19 FORMAT (/,18X,' TANDEM AXLE',4X,' TAN.',13X,' NUMBER OF W.L. IN')
   PRINT 12
   PRINT 13
   DO 20 I=1,7
   T=((SQRT(D-((X(I)-CK)**2))) + CH)
   TS(I+6)=T
20 PRINT 9,X(I),T,NACT(I+6)
 9 FORMAT (13X,F10.2,10X,F10.1,9X,I11)
   GO TO 40
31 CONTINUE
   PRINT 200
   PRINT 14,V,VID,Y1,Y2,Y3,Y4
40 CONTINUE
   CALL CALC  (SEFC,KEEP)
   IF(J) 6,5,6
 5 CONTINUE
   STOP
   END
```

CALC

```
      SUBROUTINE CALC   (SEFC,KEEP)
      REAL*8 GROUP
      COMMON GROUP (13)
      COMMON TS (13)
      COMMON NACT (13)
      DIMENSION AG(13)
      DIMENSION TRO(13)
      DIMENSION KEEP(3)
      DIMENSION T(5),        RD(5), RDT(5)
      FC=620.
      FK=34.25
      C=.5274
      DD=.95
      DL=.4
C     IDENTIFICATION
C     FK=SLOPE OF FATIGUE CURVE
C     C=CONSTANT
C     SEFC=STANDARD ERROR OF TENSILE STRENGTH (PSI)
C     DD=DIRECTION DISTRIBUTION
C     FC=TENSILE STRENGTH OF CONCRETE
C     TS=TANGENTIAL STRESS
C     CL=CONFIDENCE LEVEL
C     NACT=NUMBER OF AXLE LOADS IN BOTH DIRECTIONS
C     T=CONSTANT FOR SPECIFIC CONFIDENCE LEVEL
C     AG=AXLE GROUP
C     RD=RESULTANT DAMAGE
C     RDT=TOTAL RESULTANT DAMAGE
C     DD=DIRECTION DISTRIBUTION (%)
C     DL=LANE DISTRIBUTION (%)
C
      DATA AG /2.65, 4.50, 7.20, 8.70, 9.60, 10.70, 5.30, 9.00, 14.40,
     *         17.40, 19.20, 21.40, 25.00/
      T(1)=0.
      T(2)=1.037
      T(3)=1.28
      T(4)=1.645
      T(5)=2.33
C
      IF (KEEP(1)) 41,41,42
   42 CONTINUE
      SEFC= FC - ( FC /(((10**RDXXX) /C)**(1/FK)))
   41 CONTINUE
      READ 555,RDXXX
  555 FORMAT (6X,F9.4)
      READ 666,FK
  666 FORMAT (6X,F9.4)
      IF (KEEP(3)) 30,30,31
   31 CONTINUE
```

CALC

```
      READ 777,(TS(I),I=1,13)
  777 FORMAT(13F6.1)
      GO TO 45
   30 CONTINUE
      READ 888,(TRO(I),I=1,13)
  888 FORMAT (13F6.1)
   45 CONTINUE
C
C
C     KKK=COUNTER
      KKK=1
  100 CONTINUE
      PRINT 51
      PRINT 52
   51 FORMAT (/,18X,' AXLE',2X,' TAN.',18X,' CUMULATIVE DAMAGE AT ',
     *'CONFIDENCE LEVELS')
   52 FORMAT (18X,' GROUP',1X,' STRESS',4X,' 50%',10X,'85%',9X,'90%',9X,
     *'95%',9X,'99%')
      DO 500 KK=1,5
  500 RDT(KK)=0.
      DO 2 I=1,13
      DO 3 J=1,5
      RDXXXX = ( (FC/(FC-SEFC))) **FK
      IF (KEEP(2)) 43,43,44
   44 CONTINUE
      RDXXX = ALOG10  (C*RDXXXX)
   43 CONTINUE
      RDXX= ALOG10 (C *( (FC /TS(I)) ** FK)) - (T (J) * RDXXX)
      RDX  =10 ** RDXX
      RD (J) = (NACT (I) * DD * DL) / RDX
C     CALCULATE RD
C     CALCULATE RESULTING DAMAGES-TOTAL
      RDT(J)=RDT(J)+RD(J)
    3 CONTINUE
      PRINT 20,GROUP(I),TS(I),RD(1),RD(2),RD(3),RD(4),RD(5)
   20 FORMAT (15X,A8,F7.1,2X,5E12.4)
    2 CONTINUE
C     PRINT TOTALS
      PRINT 75,(RDT(J),J=1,5)
   75 FORMAT (23X,' TOTALS =',5E12.4)
      PRINT 908
  908 FORMAT (/)
      PRINT 907,SEFC
  907 FORMAT (20X,'SEFC=',F 9.4)
 1701 FORMAT (20X,'SEN=',F11.5)
      PRINT 1701,RDXXX
      PRINT 1702,FK
 1702 FORMAT (20X,'FK=',F11.4)
```

CALC

```
      PRINT 779, (TS(I),I=1,13)
  779 FORMAT (20X,'TS=',7F6.1,/,25X,6F6.1)
      PRINT 778, (KEEP(I),I=1,3)
  778 FORMAT (6X,3I3)
      KKK=KKK-1
      IF(KKK) 10, 11, 10
   10 CONTINUE
      GO TO 100
   11 CONTINUE
      RETURN
      END
```

ASSUMING A CIRCULAR CURVE TO CALCULATE TANGENTIAL STRESS
AND CUMULATIVE DAMAGE AT FIVE CONFIDENCE LEVELS

```
SEN = LOG ( C* (FK /FC-SEFC)**FK )
RD=(NACT)(DD)(DL) /10**(LOG (C*((FC/TS)**FK)- (T*SEN)))
```

WHERE -
SEN=STANDARD ERROR IN ESTIMATING CYCLES TO FAILURE
FK=SLOPE OF FATIGUE CURVE
C=CONSTANT
SEFC=STANDARD ERROR OF TENSILE STRENGTH
DD=DIRECTION DISTRIBUTION
FC=TENSILE STRENGTH OF CONCRETE
TS=TANGENTIAL STRESS
CL=CONFIDENCE LEVEL
NACT=NUMBER OF WHEEL LOAD APPLICATIONS
T=CONSTANT FOR SPECIFIC CONFIDENCE LEVEL
AG=AXLE GROUP
RD=RESULTANT DAMAGE
RDT=TOTAL RESULTANT DAMAGE
DL=LANE DISTRIBUTION
DX =

3LL6 87.050 187.700 17.550 41.660

SINGLE AXLE WHEEL LOAD KIPS	TAN. STRESS PSI	NUMBER OF W.L. IN BOTH DIRECTIONS
2.65	53.1	595000
4.50	87.0	2322500
7.20	133.1	492750
8.70	157.1	78250
9.60	171.1	28150
10.70	187.7	10300

TANDEM AXLE WHEEL LOAD KIPS	TAN. STRESS PSI	NUMBER OF W.L. IN BOTH DIRECTIONS
2.65	63.2	1021658
4.50	104.5	928000
7.20	161.2	1159750
8.70	191.0	129725
9.60	208.4	28825
10.70	229.3	14273
12.50	262.4	1373

FORCE POINTS= 4.50 AND 10.70

AXLE GROUP	TAN. STRESS	CUMULATIVE DAMAGE AT CONFIDENCE LEVELS 50%	85%	90%	95%	99%
2-6	53.1	0.1216E-30	0.3499E-26	0.3880E-25	0.1440E-23	0.1270E-20
7-11	87.0	0.1045E-22	0.3008E-18	0.3336E-17	0.1238E-15	0.1092E-12
12-16	133.1	0.4594E-17	0.1322E-12	0.1466E-11	0.5441E-10	0.4799E-07
17-18	157.1	0.2145E-15	0.6173E-11	0.6846E-10	0.2541E-08	0.2241E-05
19-20	171.1	0.1421E-14	0.4089E-10	0.4534E-09	0.1683E-07	0.1484E-04
21-22	187.7	0.1258E-13	0.3621E-09	0.4016E-08	0.1490E-06	0.1314E-03
4-13	63.2	0.8073E-28	0.2324E-23	0.2577E-22	0.9562E-21	0.8434E-18
14-25	104.5	0.2177E-20	0.6265E-16	0.6948E-15	0.2578E-13	0.2274E-10
26-32	161.2	0.7672E-14	0.2208E-09	0.2449E-08	0.9087E-07	0.8015E-04
33-36	191.0	0.2839E-12	0.8170E-08	0.9060E-07	0.3362E-05	0.2966E-02
37-40	208.4	0.1258E-11	0.3620E-07	0.4014E-06	0.1490E-04	0.1314E-01
41-44	229.3	0.1638E-10	0.4716E-06	0.5229E-05	0.1941E-03	0.1712E 00
50	262.4	0.1608E-09	0.4628E-05	0.5132E-04	0.1905E-02	0.1680E 01
	TOTALS =	0.1788E-09	0.5145E-05	0.5705E-04	0.2117E-02	0.1868E 01

SEFC= 164.2449
SEN= 4.30000
FK= 34.2500
TS= 53.1 87.0 133.1 157.1 171.1 187.7 63.2
104.5 161.2 191.0 208.4 229.3 262.4

REFERENCES

1. AASHO Interim Guide for the Design of Rigid Pavement Structures, AASHO Committee on Design, April 1962.

2. Alder, H. L., and E. B. Roessler, Introduction to Probability and Statistics, W. H., Freeman and Company, San Francisco, 1964.

3. Brown, James L., Larry J. Buttler, and Hugo E. Orellana, "A Recommended Texas Highway Department Pavement Design System User's Manual, "Report No. 123-2, published jointly by Texas Highway Department; Texas Transportation Institute, Texas A & M University; and Center for Highway Research, The University of Texas at Austin, March 1970.

4. Brown, James L., Larry J. Buttler, and William P. Ezzell, "Survey of Structural Failures in A Continuously Reinforced Concrete Pavements" Texas Highway Department, Special Study No. 1.1, October 1969.

5. Finn, F. N. "Factors involved in the Design of Asphaltic Concrete Surfaces NCHRP Report No. 39, Highway Research Board, Washington, D. C., 1967.

6. Grieb, W. E., and G. Werner, "Comparison of the Splitting Tensile Strength of Concrete with Flexural and Compressive Strengths", Report, Public Roads, Vol. 32, No. 5, December 1962.

7. Hadley, William O., W. Ronald Hudson, and Thomas W. Kennedy, "A Method of Estimating Tensile Properties of Materials Tested In Indirect Tension", Research Report No. 98-7, Center for Highway Research, The University of Texas at Austin, June 1970.

8. Hadley, William O., W. Ronald Hudson, and Thomas W. Kennedy, "An Evaluation of Factors Affecting the Tensile Properties of Asphalt-Treated Materials, "Research Report No. 98-2, Center for Highway Research, The University of Texas at Austin, March 1969.

9. Hadley, William O., W. Ronald Hudson, and Thomas W. Kennedy, "Correlation of Tensile Properties with Stability and Cohesiometer values for Asphalt-Treated Materials", Research Report No. 98-6, Center for Highway Research, The University of Texas at Austin, June 1970.

10. Heathington, K. W. and P. R. Tutt, "Estimating the Distribution of Axle Weights For Selected Parameters", Highway Research Record No. 189, 1967.

11. Hudson W. Ronald, Discontinuous Orthotropic Plates and Pavement Slabs, University of Texas, Dissertation for Doctor of Philosophy Degree, August 1965.

12. Hudson, W. Ronald, and Thomas W. Kennedy, "An Indirect Tensile Test for Stabilized Materials, "Research Report No. 98-1, Center for Highway Research, The University of Texas at Austin, January 1968.

13. Item 360 "Concrete Pavement", Standard Specifications for Road and Bridge Construction, Texas Highway Department, 1962.

14. Lee, Clyde E., Development of Portable Scale for Weighing Vehicles in Motion, Texas Highway Department, Research Report 54-1F, April 1968.

15. McCullough, B. F., A Pavement Overlay Design System Considering Wheel Loads, Temperature Changes, and Performance, University of California, Berkeley, Dissertation for Doctor of Engineering, July 1969.

16. Miller, Samuel Paul, Thomas W. Kennedy, and W. Ronald Hudson, "Evaluation of Factors Affecting the Tensile Properties of Lime-Treated Materials", Research Report No. 98-4, Center for Highway Research, The University of Texas at Austin, March 1970.

17. Pendola, Humberto J., Thomas W. Kennedy, and W. Ronald Hudson, "Evaluation of Factors Affecting the Tensile Properties of Cement-Treated Materials," Research Report No. 98-3, Center for Highway Research, The University of Texas at Austin, September 1969.

18. Scrivner, F. H., and W. M. Moore, "An Electro-Mechanical System for Measuring the Dynamic Deflection of a Road Surface Caused by an Oscillating Load", Research Report 32-4, Texas Highway Department-Texas Transportation Institute Cooperative Research, December 1964.

19. Seed, H. B., F. G. Mitry, C. L. Monismith, and C. K. Chan, "Prediction of Flexible Pavement Deflections from Laboratory Repeated Load Tests", NCHRP Report, No. 35, 1967.

20. "The AASHO Road Test: Pavement Research", Highway Research Board Special Report 61E, 1962.

21. "The AASHO Road Test", Report No. 2, "Materials and Construction", Highway Research Board Special Report 61-B, 1962.

22. "The AASHO Road Test", Report No. 3, "Traffic Operations and Pavement Maintenance", Highway Research Board Special Report 61C, 1962.

23. Treybig, Harvey J., Sensitivity Analysis of the Extended AASHO Rigid Pavement Design Equation, University of Texas, Thesis for Mater of Science in Civil Engineering, August 1969.

24. Tulloch, Walter S., W. Ronald Hudson, and Thomas W. Kennedy, "Evaluation and Prediction of the Tensile Properties of Lime-Treated Materials," Research Report No. 98-5, Center for Highway Research, The University of Texas at Austin, June 1970.

25. Warren, H., and W. L. Eieckmann, "Numerical Computations of Stresses and Strains in a Multiple-Layer Asphalt Pavement System," International Report, unpublished, Chevron Research Corporation, September 1963.

26. Withey, M. O., and G. W. Washa, Materials of Construction, John Wiley and Sons, Inc., New York, 1954.